Vac14 nucleates a protein complex that regulates membrane dynamics *via* the synthesis and turnover of phosphatidylinositol3,5-bisphosphate, PtdIns(3,5)P_2.

神　奈亜子

奈良先端科学技術大学院大学

バイオサイエンス研究科　分子発生生物学講座

(高橋　淑子　教授)

2/13/2009

バイオサイエンス研究科　博士論文要旨

推薦教員	高橋　淑子 教授　（分子発生生物学講座）		
氏名	神　奈亜子	提出	平成２１年１月９日
題目	膜構成リン脂質 $PI(3,5)P_2$ 合成を担う Vac14 タンパク質複合体の解析。		

要旨

細胞膜構成リン脂質、phosphatidylinositol 3,5-bisphosphate, $PtdIns(3,5)P_2$ はエンドソーム膜系において合成され、エンドソーム、リソソーム膜を介したタンパク質をはじめとする物質輸送においてシグナル分子として機能している。出芽酵母において、$PtdIns(3,5)P_2$ の細胞内における存在量は他の phosphoinositide lipids に比べ約２０倍以下であるが、浸透圧変化など外界からの刺激の際には一過的に２０倍以上に上昇し、その後急激に減少することが知られている。$PtdIns(3,5)P_2$ の存在量はリン脂質リン酸化酵素 Fab1 とリン脂質脱リン酸化酵素 Fig4 により制御されている。Fab1 は PtdIns3P を基質としそのイノシトール環の 5 位にリン酸基を加え、Fig4 は $PtdIns(3,5)P_2$ を基質としその 5 位のリン酸基を除去し PtdIns3P へと変換する。　Atg18 は $PtdIns(3,5)P_2$ 合成反応を負に調節すると共に $PtdIns(3,5)P_2$ に結合しそのシグナルを伝える effector として機能する。Vac7 と Vac14 は $PtdIns(3,5)P_2$ 合成反応を正に調節する。興味深い事に、リン脂質脱リン酸化酵素 Fig4 と $PtdIns(3,5)P_2$ 合成反応の正の調節因子である Vac14 は複合体を形成し $PtdIns(3,5)P_2$ 合成反応のみならず $PtdIns(3,5)P_2$ から PtdIns3P への変換反応も制御している。

本研究において、以下の事が明らかとなった。(1)Vac14 はタンパク質間結合ドメインである HEAT repeat を複数個持ち、リン脂質リン酸化酵素 Fab1、リン脂質脱リン酸化酵素 Fig4, 正の調節因子 Vac7,負の調節因子 Atg18 さらに自身と結合することにより巨大なタンパク質複合体を形成し $PtdIns(3,5)P_2$ 合成反応を制御する。(2)この Vac14 を核とした巨大なタンパク質複合体は急激な浸透圧変化における一過的な $PtdIns(3,5)P_2$ 量の上昇及び減少反応をも制御する。(3)この巨大なタンパク質複合体の形成がリン脂質リン酸化酵素 Fab1 と脱リン酸化酵素 Fig4 の活性に必須

であり、この調節機構は出芽酵母のみならず種を超えて保存されている。(4) リン脂質リン酸化酵素 Fab1、リン脂質脱リン酸化酵素 Fig4、Vac14 はタンパク質複合体において核となる三者複合体を形成する。 (5)正の調節因子 Vac7 と負の調節因子 Atg18 は Vac14 の同じ領域に結合する。

本研究により、これまで遺伝学的に同定された PtdIns(3,5)P_2 合成 / 変換機構に関わる因子群が巨大なタンパク質複合体を形成し機能すること、この機構は種を超えて保存されていることが明らかとなった。しかし、PtdIns(3,5)P_2 の細胞内における作用機構については未知な点が多い。遺伝子破壊マウスを用いた研究により PtdIns(3,5)P_2 は神経細胞の機能において重要な役割を担っている事、さらに PtdIns(3,5)P_2 量の異常がヒトの疾病の原因となりうることが示唆されているが、哺乳類における PtdIns(3,5)P_2 の詳細な作用機構については未知である。出芽酵母をモデル生物とし得られた知見を哺乳類へとつなげていく、今後本研究がこれからの出発点となることを信じている。

CONTENTS

ABSTRACT

The signaling lipid phosphatidylinositol 3,5-bisphosphate, PtdIns(3,5)P_2 is generated and functions in the endomembrane system and regulates retrograde traffic to the trans-Golgi network. In yeast, the levels of PtdIns(3,5)P_2 are approximately 20-fold lower than other phosphoinositide lipids. A stimulus of hyperosmotic shock causes a rapid and transient 20-fold elevation in PtdIns(3,5)P_2. This rise and fall in lipid levels occurs in the continued presence of osmolyte, and is tightly regulated both through its synthesis, *via* lipid kinase Fab1p, and turnover *via* lipid phosphatase Fig4p. Atg18p is a negative regulator of Fab1p and an effector of PtdIns(3,5)P_2. Vac7p and Vac14p are activators of Fab1p. Paradoxically a complex of Fig4p and Vac14p comprise a second activation pathway, yet have dual and opposing roles and also turn over of PtdIns(3,5)P_2. Here, we predict that yeast and mammalian Vac14 are composed entirely of HEAT repeats and demonstrate that Vac14 functions as a scaffold for the PtdIns(3,5)P_2 regulatory complex by direct contact with the known regulators of PtdIns(3,5)P_2; Fab1p, Fig4p, Vac7p and Vac14p. Furthermore, formation of the complex is critical for the osmotic-stress induced activation of Fab1p.

Our findings suggest that the tight regulation of PtdIns(3,5)P_2 levels is achieved *via* three mechanisms. First, the lipid kinase and phosphatase reside in the same complex and share Vac14 as an regulator, second, Atg18, a Fab1 inhibitor and Vac7, a Fab1 activator also function within the complex and bind to the same region on Vac14, and third, as shown previously, Fig4p plays dual and opposing roles as an activator of Fab1 and in turnover of PtdIns(3,5)P_2.

The mouse mutant *ingls* (infantile gliosis) which results from a missense mutation in Vac14. Using yeast I show that mutation of this missense residue prevents the association of Vac14

with Fab1, generating a partial complex. These findings demonstrate that the association of Fab1 with the complex is essential in both yeast and mammals.

CHAPTER I

Introduction

Membranes have both structural and regulatory roles.

The cell is separated from outside environment by the plasma membrane (Figure 1). Plasma membranes are important component and absolutely essential for all life. Plasma membranes are not just static structures. Membranes have critical functions in the regulation of spatial and temporal events. For example, membranes harbor receptors, ion channels and scaffolding complexes, and actin regulatory complexes which function to maintain cell growth, cell survival, metabolism and homeostasis. For example, on transporting small molecules such as glucose, sucrose and H_2O or ions such as H^+, Na^+, K^+ and Ca^{2+}, special membrane transport protein complexes associate and function with the plasma membrane. Several stimuli such as growth factors, neurotransmitters and hormones activate specific receptors which in turn transduce stimuli from the outside environment to intracellular pathways.

Moreover, within cell, there are several specialized components, called organelles, which have specific functions for intracellular events. For example, mitochondria generates most of the cell's supply of adenosine triphosphate (ATP). The lysosome degrades excess or damaged organelles and proteins *via* several acid hydrolasese which are stored inside lumen. Each organelle is separately enclosed within its own membranes (Figure 1). Similar to the plasma membranes, the membrane of each organelle includes specific proteins for organelles function. For example, the endoplasmic reticulums (ER) is classified into two types, rough and smooth ER. Ribosomes localize on the rough ER and function in protein-manufacturing. The smooth ER functions in several metabolic processes, including synthesis of lipids and steroids, regulation of intracellular calcium levels and steroid metabolism.

The cell membrane component, Phosphatidylinositol

The plasma membranes and organelle membranes are composed of a lipid bi-layer (Figure 1), which contain multiple types of lipids, including phospholipids. Phospholipids have a glycerol back bone, two fatty acid esters and a phospho-side chain. Membranes are complex and contain >1000 different types of lipids (van Meer, 2005). The dynamic changes in phosphatidylinositol, one type of phospholipids provide spatial and temporal regulations on multiple membranes in eukaryotic cells.

Phosphatidylinositol (PtdIns) is a minor phospholipid component, less than 10% of the total phospholipids, in the cytosolic side of eukaryotic cell membranes. PtdIns is made up of glycerol, fatty acid and the base is replaced by an inositol ring (Figure 2). PtdIns is the substrate for a large number of enzymes. PtdIns can be phosphorylated or de-phosphorylated and converted into other phosphorylated derivatives by a variety of kinases and phosphatases (Vicinanza et al., 2008). The hydroxyl groups 3, 4 and 5 on the inositol ring provide seven different combinations or PtdIns can also be hydrolyzed by phopholipases (Figure 2). This metabolic generation and conversion of PtdIns is crucially required in several temporal signaling pathways. For example, one phosphorylated derivatives, PtdIns(4,5)P_2 is phosphorylated by class I phophoinositide (3) kinase (PI(3)kinase) and converted into PtdIns(3,4,5)P_3 upon cell stimulation by growth factors. PtdIns(3,4,5)P_3 recruits selected proteins including protein serine-threonine kinase, protein tyrosine kinases, exchange factors for GTP-binding proteins and adaptor proteins. These PtdIns(3,4,5)P_3 binding proteins initiate cellular events that control protein synthesis, actin polymerization, cell survival and cell cycle entry (Cantley, 2002). Termination of these signaling pathways occurs *via* dephosphorylation of PtdIns(3,4,5)P_3 by at least two different types of phosphatases. The Src-homology 2 (SH2)-containing phosphatase, SHIP1 and SHIP2 de-phosphorylate the 5 position of the inositol ring and produce PtdIns(3,4)P_2 (Cantley, 2002). PtdIns(4,5)P_2 is cleavaged into two metabolites,

inositol 1,4,5 triphosphate, I (1,4,5)P_3 and diacylglycerol (DAG). These two metabolites propagate and amplify signaling by activation of other proteins or intracellular pathways. The cleavage products of PtdIns(4,5)P_2 are components of two major signaling pathways, that recruit and activate protein kinase C (PKC) to release Ca^{2+} from intracellular stores and vesicles, respectively (Malbon, 2005).

The intracellular vesicular traffic.

Eukaryotic cells have evolved an endo-membrane system which takes up nutrients from the outside and also functions to degrade membrane-bound molecules. These membranes are distinct from those in the biosynthetic-secretory pathway which allows delivering newly synthesized lipids and proteins from the ER to the cell exterior and intracellular compartments. In both pathways, molecular cargos are enclosed in membrane vesicles which continually bud off from one membrane, fuse with another membrane and are finally delivered to their final destination.

In the endocytic pathway (Figure 4), the first step is endocytosis. An invagination of the cell plasma membrane forms a pocket, and pinched off into the cytosolic region to form a membrane vesicle. This step is regulated by several protein complexes. The best-understood example is receptor-mediated endocytosis, which is mediated by several adaptors and clathrin (Owen et al., 2004). Clathrin, large protein assists in the formation of a membrane pit and separation of the vesicl from the plasma membrane by coating the inner membrane surface with adaptor proteins (for example, AP-2, AP180/CALM, espin) which bind specific cargos and clathrin. The adaptor proteins function as mediators between cargos and clathrin. In this step, the GTPase dynamin plays a role pinching off the bud to form a vesicle.

The pinched vesicles travel through the cytosol and fuse with the next membrane compartment, endosomes. Endosomes are, in part, responsible for sorting and transporting

them to lysosomes. Endosomes are internal membrane compartments and classified into two stages, early and late endosomes. Endosomes include a specialized membrane compartment, called multivesiculer bodies (MVB). Functionally early and late endosome are diverse. Functionally, early endosomes are responsible for sorting and transporting cargo materials to late endosome. Late endosomes are responsible for sorting and transporting of cargo materials to the lysosome, that reside a final destination. MVB membranes invaginate into internal vesicles in the lumen of the MVB. Selected cargo are sorted into these internal vesicles. These cargoes are delivered into the lumen of the lysosome by fusion the membrane between the late endosome / MVB and the lysosome. Some protein complexes have been identified that regulate endosomal membrane trafficking and proteins sorting. For example, EEA1 and Rab5 (GTPase) specifically localize and function in membrane fusion on the early endosome (Simonsen et al., 1998). Membrane fusion is regulated by proteins including SNAREs (soluble *N*-ethylmaleimidesensitive fusion protein attachment protein receptor) (Martens and McMahon, 2008). SNAREs can be divided into two categories: vesicle or v-SNAREs , which are localized on the membranes of donor vesicle and target or t-SNAREs, which are localized on the membranes of target compartments and regulate the membrane fusion steps through v- and t-SNAREs complexes association.

In the biosynthetic-secretory pathway (Figure 5), proteins which are newly synthesized on the ER are translocated into the lumen and a subset are packaged into vesicles which are targeted to the *cis* Golgi. In the Golgi post-translation, these proteins undergo modification. After the proteins arrive at the *trans* Golgi network (TGN), these proteins are sorted and packaged into vesicles that are targeted to cell exterior by exocytosis or targeted to other intracellular compartments. One example of vesicle transport in the biosynthetic-secretory pathway is the CPY (Carboxypeptidase Y) pathway (Banta et al., 1988). In yeast, some proteins including CPY, CPS (intgral membrane protein carboxy peptidase S), PrA and PrB

(proteases A, B) are synthesized as precursor proteins on the ER and sorted to the vacuole *via* Golgi apparatus and endosomal membrane compartments and then maturated in the vacuole where they function as hydrolases. Vesicles are continually bud from one membrane and fuse with another membrane and are finally delivered to their final destination.

Interestingly, there is semi cross-talk between endocytic and biosynthetic-secretory pathways. They share a subset of the membrane tafficking machinery (Gundelfinger et al., 2003). Also each vesicle targeting pathway has a related retrograde pathway (for example, from the lysosome to TGN) (Bryant et al., 1998). Vesicle transport mediates the spatial and temporal regulation of multiple intracellular processes.

The spatial distribution of PtdIns and phosphoinositides and their effector proteins.

PtdIn and its phosphorylated derivatives spatially and temporally regulate a wide variety of cellular functions (Di Paolo and De Camilli, 2006). PtdIns and its phosphorylated phosphoinositides lipids are found at the plasma membrane and on intracellular membranes (Vicinanza et al., 2008). PtdIns(4,5)P_2 and PtdIns(3,4,5)P_3 are concentrated at plasma membrane. PtdIns(3,4)P_2 is mostly found at the plasma membrane and in early endocytic compartment. PtdIns(4)P is enriched at the Golgi complex, but is also present at the plasma membrane. PtdIns(3)P is concentrated in early endosomes and PtdIns(3,5)P2 is likely concentrated on both early and late compartments of the endosomal pathway. Note that the spatial restriction of specific phosphoinositides are determined by the concerted action of phosphoinositide lipid kinases and phosphatases. The localization of these lipid kinase and phosphatase determines the localization of their product. For example, PtdIns(4)P is synthesized from the phosphorylation of PtdIns by PtdIns 4-kinases. Some PtdIns 4-kinases localize specifically to the Golgi apparatus and maintain Golgi structure and function. These

enzymes play a role in vesicle transport to the lysosome and the plasma membrane (De Matteis and D'Angelo, 2007).

PtdIns and phosphoinositides function by recruiting a complex of down stream effector proteins that bind to distinct phophoinositides and promote diverse membrane functions. These effector proteins are classified according its lipid binding modules. Examples include PH (pleckstrin himology), FYVE (Fab1, YOTB, Vac1, EEA1), PX (Phox-homolohgy), ENTH (epsin N-terminal homology), ANTH (AP180 N-terminal homology), C1 (conserved region-1 from protein kinase C), BAR (Bin, amphiphysin and Rvs), and GRAM (glucosyltransferase, Rab-like GTPase and myotubularins domains) (Vicinanza et al., 2008). For example, FYVE domains specifically recognize PtdIns(3)P and effectors such as EEA1 which has a FYVE domain recruited to the membrane region where and when PtdIns(3)P is generated (Stenmark et al., 1996). PH domains recognize PtdIns(3,4,5)P3. In the PI(3)K pathway, upon stimulation of the target cell by insulin and other growth factors, PI(3)K synthesizes PtdIns(3,4,5)P3 from PtdIns(4,5)P2 on the plasma membrane, serine/threonine protein kinase PDK and Akt are recruited *via* its PH domains and then cooperate in the activation of signaling pathways, such as TOR pathway (Cantley, 2002). Thus, phosphoinositides act as signaling molecules and provide a phosphoinositide code that plays a role in organelle identity and function (Di Paolo and De Camilli, 2006).

PtdIns(3,5)P_2,

PtdIns(3,5)P_2, phosphatidylinositol3,5-bisphosphate, is a very low abundance phosphoinositide which is found in yeast, mammalians and plants. PtdIns(3,5)P_2 is 0.1 % or less of the total PtdIns (Dove et al., 1997). PtdIns(3,5)P_2 functions in surround endosomal and lysosomal/vacuole trafficking pathways and likely function in vacuole homeostasis. In yeast, low levels of PtdIns(3,5)P_2 leads to several vacuole related defects (described the details in

below). In mammalian cells, low levels of PtdIns(3,5)P_2 result in the formation of large, water-filled vacuoles and a defect in endosome to TGN retrograde traffic (Rutherford et al., 2006); (Zhang et al., 2007). Mice with a defect in the production of PtdIns(3,5)P_2 exhibit massive neurodegeneration (Zhang et al., 2007); (Chow et al., 2007).

The levels of PtdIns(3,5)P_2 are tightly regulated through both its synthesis and turnover. Changes in the cellular environment such as hyperosmotic stress cause the levels of PtdIns(3,5)P_2 to dramatically increase (Dove et al., 1997). This increase is rapid and transient. Upon treatment yeast cells with high salt media as a hyperosmotic condition, within 5 min, there is a 20-fold increase in PtdIns(3,5)P_2 levels, yet by 30 min, PtdIns(3,5)P_2 returns to basal levels even in the continued presence of hyperosmotic conditions (Duex et al., 2006a). Also in plant and animal cells, PtdIns(3,5)P_2 concentration increases up to 2-6 fold in hyperosmotic conditions (Meijer, 1999; Sbrissa and Shisheva, 2005). These dynamic changes strongly suggest that the levels of PtdIns(3,5)P_2 are tightly regulated and may play a key role in the first response to the environmental changes.

Fab1, the phosphatidylinositol 3-phosphate 5-kinase

In yeast, a single phosphatidylinositol 3-phosphate 5-kinase, Fab1p synthesizes PtdIns(3,5)P_2 from PtdIns(3)P (Cooke et al., 1998). The name Fab1p comes from one of the phenotype of a *fab1Δ* knock-out, forms annucleate and binucleate cell. Based on its sequence, Fab1p was initially isolated and proposed to function as phosphatidylinositol 4-phosphate 5-kinase in *S. cerevisiae* (Yamamoto et al., 1995). Fab1p was discovered before PtdIns(3,5)P_2. Several lines of evidence demonstrate that Fab1p act as a phosphatidylinositol 3-phosphate 5-kinase. In *fab1Δ* cells or mutant cells which have mutation sites in its kinase domain such as D2134R, PtdIns(3,5)P_2 is undetectable at basal condition (Gary et al 1998). Moreover, *in vitro*, Fab1p has PtdIns(3)P 5-kinase activity (Cooke et al., 1998; Sbrissa et al., 1999). Fab1p

regulates several vacuole function and vacuolar proteins sorting to inside of vacuolar lumen *via* endosomal membrane trafficking machinery, through the synthesis of PtdIns(3,5)P_2.

(1) PtdIns(3,5)P_2 function in the maintenance of vacuole structure.

Wild-type cell have small and multi-lobed vacuoles, while *fab1Δ* cells or kinase dead *fab1D2134R* mutant cell have a glossly enlarged vacuole (Gary et al., 1998; Yamamoto et al., 1995). This suggests membrane fission from endosomal compartments is impaired in the absence of lPtdIns(3,5)P_2.

(2) PtdIns(3,5)P_2 function in the maintenace of vacuole acidification.

In wild-type cell, the yeast vacuole lumen is approximately pH6.0. In contrast, vacuoles in *fab1Δ* cells are pH7.0 or higher (Yamamoto et al., 1995). The acidic environment in lysosome/vacuole is important for optimal activation of several vacuolar hydrases, which are stored inside of the vacuole lumen and activated in acidic conditions. Also vacuole acidification is required in the dissociation of ligand-receptor complex during receptor recycling such as mammalian recycling of the Man-6-P receptors to the trans-Golgi (Forgac, 1998).

(3) PtdIns(3,5)P_2 function in the membrane trafficking and proteins sorting in the endomembrane system.

In the CPY pathway, some proteins such as CPS and Phm5 are ubiquitinated by the Ubc/Tul1 ubiquitin ligase complex and then sorted into the vacuole lumen *via* MVBs (Reggiori and Pelham, 2002). In *fab1Δ* cells and mutant cells, there is a significant delay in the maturation of processed proteins in the CPY pathway (Gary et al., 1998); sorting into the vacuole lumen was impaired (Odorizzi et al., 1998). Also in *S. pombe*, Ste3, a-factor receptor, is sorted from the plasma membrane into the vacuole for degradation of Ste3 in absence of a-factor. In *ste12Δ (fab1Δ)* cells, sorting of Ste3 into the vacuole lumen was impaired (Shaw et al., 2003). These data suggest that Fab1p regulates multiple vacuolar functions. The defect in

the membrane trafficking/proteins sorting in the endosomal systems might also be the underlying cause of several other defects, including impaired vacuole inheritance (Bonangelino et al., 1997) and defects in vacuole-to-endosome retrograde transport (Bryant et al., 1998).

S. cerevisae Fab1 is a large protein of 2,278 amino acids and contains three known domains, FYVE, CCT and the kinase domain (Figure 6). The N-terminal FYVE domain binds with a substrate PtdIns(3)P. The CCT domain interacts with other proteins (Botelho et al., 2008). The C-terminal region is the kinase domain and catalyzes the conversion of PtdIns(3)P to PtdIns(3,5)P_2. In yeast Fab1 kinase activity is modulated by regulatory proteins, including Fig4p, Vac14p, Vac7p and Atg18p.

The PtdIns(3,5)P2 5'-phosphatase, Fig4p.

Fig4p is the PtdIns(3,5)P_2 5'-posphatase that turns over PtdIns(3,5)P_2 *via* removal of its 5'-phosphate (Rudge et al., 2004). A *fig4* mutant was isolated from a screen for mutants that were able to bypass the high temperature sensitive growth defect of *vac7Δ cells*. Fig4p is one of four proteins that contains a polyphosphoinositide phosphatase domain called the Sac1 domain (Guo et al., 1999; Figure 6). *In vitro*, the Sac1 domains from Sac1, Sj12/Inp52 and Sj13/Inp53 are able to de-phosphorylate PtdIns(3,5)P_2, PtdIns(3)P, PtdIns(4)P (Guo et al., 1999). Fig4p was shown to have activity as a PtdIns(3,5)P_2 5'-phosphatase *in vitro* and *in vivo* (Rudge et al., 2004). Fig4p localizes to the limiting membrane of the vacuole and formes a complex with another regulator of Fab1 kinase, Vac14p (Rudge et al., 2004). Paradoxically Fig4p has dual and opposing roles. Fig4p is also required for the activation of Fab1 kinase activity and Fig4p absolutely requires Vac14p for both functions (Duex et al., 2006b).

Vac14p is a positive regulator of Fab1 kinase activity.

In yeast, VAC14 (for Vacuole Inheritance defect) or SVP2 (for Swollen Vacuole Phenotype) gene was isolated from distinct two screens (Wang et al., 1996); (Dove et al., 2002). Each gene encoded the same ORF, YLR386w/VAC14. Like *fab1Δ* cells, *vac14Δ* cells showed an enlarged vacuole morphology and failed to acidify the vacuole correctly (Bonangelino et al., 2002). Moreover v*ac14Δ* cells were defective in proteins sorting from the TGN to the vacuole lumen *via* MVB (Dove et al., 2002) and were impaired in the synthesis of PtdIns(3,5)P_2 at both basal and hyperosmotic stress (Bonangelino et al., 2002). Interestingly, yeast two hybrid studies suggest that Vac14p associates with proteins which are involved in phosphoinositide metabolism and membrane trafficking, including Fig4p, Nyv1p (Vacuolar SNARE) (Dove et al., 2002). Also Vac14p was predicted to contain some HEAT repeat motifs, which are protein-protein interaction modules (Dove et al., 2002).

Vac7p and Atg18p function as a positive and negative regulators of Fab1 kinase, respectively.

Vac7p was isolated as a protein that regulates vacuole inheritance (VAC gene). *vac7Δ* mutants also have an abnormal enlarged vacuole morphology (Bonangelino et al., 1997). The Fig4p/Vac14p complex functions during hyperosmotic stress in dual and opposing pathways, the synthesis and turnover of PtdIns(3,5)P_2. Interestingly, Vac7p can act as positive regulator of Fab1 kinase activity independent of the Fig4p/Vac14p complex during hyperosmotic stress (Duex et al., 2006b). Vac7p contains a transmembrane domain at its carboxy terminus (Figure 6), but its mechanisms for activation of Fab1 kinase is unknown.

ATG18 was isolated as a SVP1 in the same screen that identified SVP2/VAC14 (Dove et al., 2002). *atg18Δ* has an enlarged vacuole phenotype similar to *fab1Δ* cells, Swollen Vacuole Phenotype. Atg18 binds PtdIns(3,5)P_2 with high affinity and specificity and is required for the recycling of the vacuole membrane between the vacuole and Golgi (Dove et

al., 2004). Surprisingly, in *atg18Δ* cells, the levels of PtdIns(3,5)P_2 under basal conditions are elevated (Dove et al., 2004). These data suggest that Atg18 functions both as a negative regulator of Fab1 kinase activity and is also an effector protein which regulates retrograde membrane trafficking from the vacuole to the Golgi. Interestingly in the *atg18* mutant (285RR286 to 285GG286) which ia impaired in binding with PtdIns(3,5)P2, the mutant *ag18* could function as a inhibitor of Fab1p when the mutant is forced to the vacuole membrane (Efe et al., 2007). These data suggest that Atg18p functions as a inhibitor of Fab1 kinase activity *via* interaction with the vacuole membrane.

The roles and regulation of PtdIns(3,5)P_2 in higher organism

The machinery for the regulation of PtdIns(3,5)P_2 levels is conserved through out eukaryotes. The orthologues of Fab1p, Fig4p and Vac14p are found in the eukaryotic genomes including fungi, plants, insects, nematodes, vertebrates and mammals (Michel et al., 2006).

Mammalian Fab1 is also referred to as PIKfyve (FYVE finger-containing-phosphoinositide kinase) in mouse and PIP5K3 (phosphotidylinositol-3-phosphate 5-kinase, typeIII) in human. Mammalian Fig4 is also referred to as Sac3, Vac14 as ArPIKfyve (associated regulator of PIKfyve). Fab1/PIKfyve, Fig4/Sac3 and Vac14/ArPIKfyve form a complex in mammals (Sbrissa et al., 2007) which is the same as the Fab1p/Fig4p/Vac14p in yeast (described below).

In mammals, PtdIns(3,5)P_2 may be involved in insulin signaling. Upon insulin stimulation, the Glucose Transporter –4 (GLUT4), which normally localizes on vesicle in the cytosol, translocates to the plasma membrane and functions in glucose uptake. Fab1/PIKfyve regulates GLUT-4 translocation (Shisheva, 2008).

Aims on this study.

Our lab has focused our research efforts on the regulation and functions of the synthesis and turnover of PtdIns(3,5)P_2. Previous work suggested that Fab1p is a phosphatidylinositol 3-phosphate 5-kinase, and regulates the levels of PtdIns(3,5)P_2, which functions in several intracellular events, including membrane trafficking, proteins sorting *via* the endosome system and vacuole/lysosome functions. Also Fab1 kinase activity is regulated by several regulators, including Vac14p, Fig4p, Vac7p as positive regulators and Atg18p as a negative regulator, moreoever that PtdIns(3,5)P_2 may function as a signaling lipid which responds to acute environmental stimuli. The mechanisms of how PtdIns(3,5)P_2 levels are regulated by Fab1 kinase and its modulators, is still unknown, especially at the molecular level. My graduate research was focused on how PtdIns(3,5)P_2 levels are regulated at the molecular level.

Chapter II

Fab1 resides in a large protein complex in yeast.

Fab1 kinase activity is regulated by multiple regulators, including Fig4p, Vac14p, Vac7p and Atg18 (Bonangelino et al., 1997; Bonangelino et al., 2002; Dove et al., 2002; Dove et al., 2004; Gary et al., 2002; Rudge et al., 2004). In an approach to understand how Fab1 kinase activity is regulated by, we tested whether Fab1p colocalizes with each of its known regulators; Fig4p, Vac14p, Vac7p and Atg18p. A chromosomal integrant of Fab1p with the RFP variant *tandem-Tomato* (tdTomato) at its C-terminus was generated along with chromosomal integrants of each protein with a C-terminal tag of 3xGFP or the YFP variant, *Venus*. The corresponding tagged versions of Fab1p, Fig4p, Vac14p and Atg18p were functional. However, Vac7p-Venus could not be detected (data not shown). We inserted Venus between residue 84 and 85 of Vac7p. This construct (p-central-Venus-Vac7p) was functional. Colocalization of Fab1p with Atg18p (Efe et al., 2007), Fig4p, Vac14p, and Vac7p was observed (Figure. 7A), suggesting that Fab1p and its regulators form a complex.

To test whether Fab1p resides in a complex, we analyzed detergent solubilized cell lysates using a 10-50% glycerol gradient and found that Fab1p was distributed into two peaks (Figure. 7B). The first peak, fraction 3, contained monomeric Fab1p; predicted molecular weight 257 kDa. The second peak, fractions 6-8, contained Fab1p in a complex that is much greater than the 670 kDa standard (fractions 4-5). The predicted molecular weights of Vac7p, Fig4p, and Vac14p, are 128 kDa, 101 kDa, and 99 kDa, respectively. Notably, significant amounts of these proteins comigrated with the higher molecular weight Fab1p complex, Vac7p in fractions 6-7, Fig4p in fractions 6-8, and Vac14p in fractions 5-8. Moreover while most of the Atg18p (predicted molecular weight 55 kDa) behaved as a monomer (fractions 1-2), some Atg18p co-migrated with the Fab1 complex (fractions 5-7). Atg18p functions not only in PtdIns(3,5)P_2 levels regulation but also in aoutophagy. We expected that most of the

monomeric Atg18p functions in autophagy. However, below we show that Atg18p is a part of Fab1 kinase complex but the interaction may be transient. These results strongly suggest that Fab1p is part of a large complex that contains Fig4p, Vac7p, Vac14p and Atg18p.

Vac14p interacts with known regulators of PtdIns(3,5)P_2 levels.

Vac14p regulates PtdIns(3,5)P_2 levels (Dove et al., 2002) and functions with Fig4p in the synthesis and turnover of PtdIns(3,5)P_2 (Duex et al., 2006b). An earlier analysis suggested that Vac14p contains at least one and possibly three HEAT repeats (Dove et al., 2004). HEAT repeats are composed of two anti-parallel helices (helix A and B) connected with a short loop (Andrade et al., 2000; Groves et al., 1999) often appear in series. The sequences of HEAT repeats are degenerate. Moreover bona fide repeats are often not detected by motif detection programs. The analysis of full length Vac14 proteisn from 17 diverse using improved algorithms for detection of protein motifs including pfam (http://pfam.sanger.ac.uk/), REP (http://www.embl-heidelberg.de~andrade/papers/rep/search.html) and several alignments, identified 17 HEAT repeats in human Vac14; all 17 align with predicted HEAT repeats in yeast. Vac14p is predicted to have a minimum of nine HEAT repeats and may have as many as twenty-one HEAT repeats (Thesis / Yanling Zhang 2008, Figure 8A). HEAT repeat motifs are found in some proteins including Huntingtin, elogation factor 3, A subunit of protein phosphates 2A, TOR1 and serve a surface for protein-protein interactions. The prediction that Vac14 protein may be composed entirely of HEAT repeats suggested that the Vac14 protein acts as a scaffold and may bind proteins that regulate PtdIns(3,5)P_2 levels.

Since Fab1p and Vac7p are large proteins, truncated peptides of Fab1p and Vac7p were constructed to use in a yeast two hybrid study of protein-protein interaction. Fab1 peptide 538-1085 and Vac7 peptide 394-918 interact with yeast Vac14p in the yeast two-hybrid test (Figure 9A). Vac14p also interacts with full-length constructs of Fig4p and Atg18p (Figure

9A), and with itself (Figure 9A). Furthermore co-immunoprecipitation experiments showed that Vac14p coprecipitated with itself, Fab1p, Fig4p and Vac7p. Using the tagged proteins, Vac14p-HA and Vac14p-V5, I found that immunoprecipitation with anti-HA antibody coprecipitated Vac14p-V5 (Figure 9B). Furthermore, Fab1p containing a C-terminal Tandem Affinity Purification (TAP) tag (Fab1-TAP) coprecipitated Vac14p-V5 (Figure 9C). Immunoprecipitation of Vac14p-V5 coprecipitates Fig4p-Myc (Figure 9D). In addition, Fab1p-TAP coprecipitates Fig4p-Myc (Figure 9E). Immunoprecipitation of Vac14p-Venus also coprecipitated Vac7p (Figure 9F).

Unfortunately, Vac14p did not coprecipitate Atg18p. In a yeast two hybrid test, the interaction between Vac14p and Atg18p was weak. We predict that the interaction between Vac14p and Atg18p is transient or weak. Thus I turned to *in vitro* binding experiments using purified proteins from *E.coli*, I separately expressed and purified MBP-HIS-full length Atg18p and GST-full length Vac14p and found the Vac14p and Atg18p interact *in vitro* (Figure 9G).

To test whether Vac14p colocalizes with Fab1p, Fig4p, Vac7p and Atg18p *in vivo*, we generated a chromosomal integrant of a Vac14 fusion construct containing the fluorescent tag RFP-mCherry. Consistent with the yeast two-hybrid test, the immunoprecipitation and *in vitro* pulldown experiments, Vac14p-mCherry co-localized with Fab1p, Fig4p, Vac7p and Atg18p (Figure 9H). These results are consistent with the model that Vac14p nucleates a large complex containing Fab1p, Fig4p, Vac7p, Vac14p and Atg18p (Figure 9I).

Fab1p, Vac14p and Fig4p form a ternary complex.

Fab1p did not interact with Fig4p in yeast two hybrid test. However, Fab1p-TAP coprecipitated with Fig4p. Fab1p-TAP coprecipitated with Vac14p. Vac14p coprecipitated with Fig4p. Vac14p interacted with Fab1p and Fig4p in a yeast hybrid test. These data suggest that Fab1p, Vac14p and Fig4p form a ternary complex (Figure 10A). Moreover, in absence of

Vac14p neither Fig4p (Rudge et al., 2004) nor Fab1p (Figure 10B) localize to the vacuole membrane. Similarly in the absence of Fab1p, Fig4p and Vac14p no longer localize to the vacuole membrane (Rudge et al., 2004). Likewise, Fab1p (Figure 10B) and Vac14p (Rudge et al., 2004) no longer localize to the vacuole membrane in the absence of Fig4p. These observations suggest that the ternary complex of Fab1p, Vac14p and Fig4p must form in order for each protein to localize correctly to the vacuole membrane. Moreover it appears that all three proteins need to be present to form a complex. In absence of either Fig4p or Vac14p, a pulldown of Fab1p-TAP did not pulldown Vac14p or Fig4p, respectively (Figure 10C and D).

We were unable to determine whether the Fab1p/Vac14p/Fig4p tripartite complex is required for Fab1 kinase activity. We performed *in vitro* kinase assays using Fab1p-TAP, isolated from WT, *vac14Δ* or *fig4Δ* cells and saw no difference in the levels of Fab1 kinase activity (Figure 11A and B). However, only 3-4% of Vac14p or Fig4p were pulled down with Fab1p-TAP (data not shown). Thus we need to determine conditions that preserve the ternary complex *in vitro* in order to test its role in the regulation of Fab1 kinase activity.

Vac7p is not required for the formation or localization of the Fab1p/Fig4p/Vac14p tripartite complex.

Fab1p-TAP did not pull-down Vac7p and we did not observed the interaction between Fab1p and Vac7p in yeast two hybrid test (data not shown). Vac7p is a main positive regulator of Fab1p and the only member of the complex with a transmembrane domain (Bonangelino et al., 1997). We tested whether Vac7p links the Fab1 kinase complex to vacuole membranes. However, in the absence of Vac7p, the localization of Vac14p, Fig4p (Rudge et al., 2004) and

Fab1p (Figure 12A) were normal. Moreover in the absence of Vac7p, Fab1p coprecipitated with Vac14p and Fig4p (Figure 12B and C). In addition, in the absence of Vac7p, Fig4p coprecipitated with Vac14p (Figure 12D). These results indicate that Vac7p regulates Fab1 kinase activity, but does not regulate the formation and localization of Fab1p/Vac14p/Fig4p ternary complex.

The activation of Fab1 requires its association with the Vac14 complex.

In 1995, Yamamoto et al., isolated one fab1 mutant, *fab1-2* (Yamamoto et al., 1995). The *fab1-2* mutant showed enlarged vacuoles at the nonpermissive temperature (Figure 13A). We sequenced the mutant *fab1-2*, and identified a single missense mutation, G864E, in the CCT domain (Figure 13B). The CCT domain of Fab1 shares homology with the GroEL and the CCT (chaperonin-containing TCP-1) family of Hsp60 chaperones. Chaperones function in protein folding *via* binding unfolded or refolded proteins. The fab1-2 protein is stable *in vivo* (Figure 13C) and retains normal kinase activity *in vitro* (Figure 13D and E). These data suggest that the CCT domain of Fab1p could be involved in protein-protein interactions and forming the Fab1 complex is required for its kinase activity. Indeed, the G864E mutation is located within Fab1 peptide 538-1085, which interacts with Vac14p in a yeast two hybrid test (Figure 13F). The G864E mutation disrupted the interaction with Vac14p in yeast two hybrid test (Figure 13F). Thus, we tested the biological effect of this mutation on the interaction between Fab1p and Vac14p *in vivo*. Although wild-type Fab1p coprecipitated with Vac14p, mutant fab1-2 protein did not (Figure 13G). Thus the G864E mutation disrupts interaction of Fab1p with Vac14p *in vivo*. Moreover, the fab1-2 mutant protein did not coprecipitate with Fig4p (Figure 13H). This further supports the model that interaction of Fab1p with Fig4p is dependent on interaction of Vac14p with Fab1p and Fig4p (Figure 10A and C). These co-

precipitation results are similar to those observed for fab1-T1017I, another point mutation within the CCT domain (Botelho et al., 2008).

The fab1-2 mutant protein fails to localize to the vacuole membrane (Figure 13I). Localization of Vac14p-Venus and Fig4p-3xGFP to the vacuole membrane is impaired in the presence of fab1-2 (Figure 13I). These observations further support the hypothesis that formation of the Fab1p/Fig4p/Vac14p ternary complex is required for correct localization of each component.

To determine the importance of formation of the ternary complex for the hyperosmotic stress-induced activation of Fab1 kinase, we test PtdIns(3,5)P_2 levels in response to osmotic stress in the *fab1-2* mutant. In the wild-type strain, the basal PtdIns(3,5)P_2 level of 0.05% of total PI lipid increases 20-fold to 1.15% within 10 minutes after the start of hyperosmotic stress, then falls to 0.32% at 20 minutes and 0.11% at 30 minutes (Figure 13J and Table 2). In the *fab1-2* mutant, the basal level of 0.033% increased only 2-fold to 0.076% after 10 minutes. The data support the conclusion that association with the complex is required for activation of Fab1 kinase and for physiological regulation of PtdIns(3,5)P_2 levels.

Vac7p and Atg18p function through interaction with Vac14p.

Vac7p is a major activator of yeast Fab1p, and basal levels of PtdIns(3,5)P_2 are significantly reduced in a *vac7Δ* mutant, resulting in an enlarged vacuole (Bonangelino et al., 1997). To understand how Vac7p is involved in the synthesis and turnover of PtdIns(3,5)P_2 in Fab1 kinase complex, we screened for gain-of-function mutations of *VAC14* that could rescue the low levels of PtdIns(3,5)P_2 and enlarged vacuolar size in *vac7Δ* cells. Random PCR mutagenesis of *VAC14* was performed and the mutants were transformed into a *vac14Δ, vac7Δ* strain. Mutants that restored growth at 37°C and partially corrected the enlarged vacuoles were isolated. We obtained seven *vac14* mutants and classified them according to

the strength of their ability to bypass *vac7Δ* vacuole morphology defect (Figure 14). When the strongest of these mutants, *vac14-2*, was expressed in a *vac14Δ* strain, vacuole size was smaller than in wild-type cells (Figure 15A), suggesting that PtdIns(3,5)P_2 is elevated in this mutant similar to what occurs in *fab1-14*. The *fab1-14* mutant was isolated from the screen for gain-of-function mutations of *FAB1* (Duex et al., 2006b). In *fab1-14* mutant, the vacuole size was smaller than in wild-type and the PtdIns(3,5)P_2 levels were elevated at both basal and hyper osmotic shock. Indeed, direct measurement demonstrated a two-fold elevation of the basal level of PtdIns(3,5)P_2 in the *vac14-2* mutant (Figure 15B and Table 2). However, surprisingly, when the *vac14-2* mutant was treated with hyperosmotic stress, the levels of PtdIns(3,5)P_2 increased only 1.7 fold, compared with an 8-fold increase in the wildtype strain (Figure 15B and Table 2). There is no change in the steady-state level of vac14-2 protein compared to wild-type (Figure 15C). The abnormal regulation of PtdIns(3,5)P_2 thus appears to be caused by altered function of the vac14-2 protein.

In a yeast two-hybrid test, *vac14-2* is specifically defective in interaction with Vac7p and Atg18p (Figure 15D). Interaction of vac14-2 with Vac14p, Fig4p and Fab1p is normal and formation of the ternary complex is unaffected. The vac14-2 protein also coprecipitated Fab1p to the same extent as wild-type Vac14p (Figure 15D).

vac14-2 contains four mutations: H56Y, R61K, Q101R and L329I (Figure 15F). Three of these mutations, H56, R61 and Q101, are located in HEAT repeat loops 2 and 3. These residues exhibit evolutionary conservation. Tested singly in a yeast two-hybrid test, each mutation perturbed the interaction of Vac14p with Vac7p and Atg18p, without disrupting interaction with its other binding partners (data not shown). Thus all three residues are important for Vac14p interaction with Vac7p and Atg18p. L329 alone had no affect on the interaction of Vac14p with its known binding partners (data not shown). These results indicate that HEAT repeats 2 and 3 directly contact Vac7p and Atg18p, but do not contact Fab1p.

The elevation in basal levels of PtdIns(3,5)P_2 in the *vac14-2* mutant is consistent with the model that negative regulation of Fab1 kinase activity by Atg18p requires binding of Atg18p to Vac14p (Figure 15G). We expected that a mutation in Vac14p that interrupts its ability to interact with Atg18p also results in PtdIns(3,5)P_2 levels that are consistent with a partial release of Atg18p inhibition of Fab1 kinase.

That the *vac14-2* mutant is defective in the elevation of PtdIns(3,5)P_2 levels in response to osmotic stress supports the model that Vac7p, a positive regulator of Fab1 kinase, acts through binding to Vac14p (Figure 15H).

The Fig4p binding site on Vac14p is distinct from the Fab1p, Vac7p and Atg18 binding sites

Fab1p and Vac7p bind near the N-terminus of Vac14p. Using the predicted HEAT motifs of Vac14p, we divided the protein into several overlapping constructs (Figure 16A). HEAT repeats 1-10 interact with Fab1p and Vac7p but not with Fig4p. HEAT repeats 10-21 of Vac14p interact only with Fig4p. Moreover, when HEAT repeats 1-10 or 10-21 were expressed *in vivo*, only HEAT repeats 10-21 coprecipitated with Fig4p, not with Fab1p (Figure 16B and C). These results suggest that Fab1p and Vac7p bind to the N-terminal half, while Fig4p binds to a distinct site at the C-terminal half of Vac14p. Atg18p binds full-length Vac14p but does not bind either truncation. However, based on the vac14-2 mutant, we predict that contact points for Atg18p include the intra-repeat loops of HEAT repeat 2 and HEAT repeat 3. Fab1p did not coprecipitate HEAT repeats 1-10 *in vivo* (Figure 16C). This data suggests that HEAT repeats 1-10 are not sufficient for the interaction between Fab1p and HEAT repeats 1-10 of Vac14p.

The formation of Fab1 kinase complex which VAC14 nucleates is essential for the acute interconversion of PI3P and PtdIns(3,5)P_2 in yeast and mouse.

The *ingls* (infantile gliosis) mutant mouse arose at the Jackson Laboratory in 1991 (Bronson, 2003). It was reported that the *ingls* is linked to Chromosome 8 between the microsatellite markers *D8Mit33* and *D8Mit200* and it is non-recombinant with *D8Mit271*. The *ingls* mouse survives after birth, but during the first weeks of life always develops diffuse astrocytic hypertrophy and hyperplasia in brain and spinal cord. Most also develop hydrocephaly and a few develop status spongiosis, resulting in death by 4 weeks of age.

In latest paper, Jin and Chow et al, 2008, we showed that *ingls* postnatal phenotypes are caused by defective Vac14 function. The *ingls* has the nucleotide substitution c.467T>G (amino acid substitution L156R) in exon 4 of *VAC14* gene and the mouse showed many similarities with the phenotypes of Vac14 or Fig4 null mice (Chow et al., 2007; Zhang et al., 2007). To confirm the ability of the *ingls* allele to complement the recessive lethality of the null allele $Vac14^{\Box\text{-}geo}$, heterozygous *ingls* (*ingls*/+) mice were crossed with Vac14 null heterozygotes ($Vac14^{+/\Box\text{-}geo}$). *ingls*/ $Vac14^{\Box\text{-}geo}$ heterozygotes were born in the predicted Mendelian ratio of 25%, but did not survive to weaning and showed phenotypic similarity between $Vac14^{\Box\text{-}geo\ /\Box\text{-}geo}$ and *ingls*/ $Vac14^{\Box\text{-}geo}$ (Jin et al., 2008; Zhang et al., 2007). These data suggest Vac14-L156R as the *ingls* mutation.

L156R located in the predicted HEAT repeat 4 of human Vac14. Sedimentation and co-immunoprecipitation analysis demonstrated that mammalian Vac14, Fab1 and Fig4 associate with each other (Sbrissa et al., 2007). As described above, Vac14p nucleates a Fab1 kinase complex (Figure 9). We performed a yeast two hybrid test and found that human Vac14 interacts with Fab1 and Fig4 (Figure 17A). The ingls/ Vac14-L156R mutant protein was stable, but we found reduced levels of PtdIns(3,5)P_2 and vacuolization of cultured *ingls* fibroblasts (Jin et al., 2008), suggesting that the $Vac14^{L156R}$ allele retains partial function.

Indeed, ingls /vac14-L156R specifically disrupts the interaction between Vac14 and Fab1 but retains interaction with Fab1 and Fig4 in a yeast two hybrid test (Figure 17A). In yeast, Vac14 interacts with itself (Dove et al., 2002; Figure 9). In a yeast two hybrid test, human Vac14 interact with itself and the vac14-L156R mutation is unaffected in Vac14-Vac14 self interaction (Figure 17A). These data suggest that disruption of the interaction between Fab1 and Vac14 is the molecular consequence of the *ingls* phenotype.

To further test the molecular consequences of the *ingls*/Vac14-L156R mutation, we turned to the equivalent yeast mutant, *vac14-L149R*. Similar to the mouse Vac14-ingls, the vac14-L149R mutant protein was stable (Figure 17B). *vac14Δ* cell has grossly enlarged vacuole compared to wild-type cells, which have small and multi-lobed vacuoles. When vac14-L149R was expressed in *vac14Δ* cells, the vacuole morphology was intermediate between wild-type and the *vac14Δ* mutant (Figure 17C). These data suggest that vac14-L149R has a partial loss of function.

In a yeast two-hybrid test, vac14p-L149R was defective in binding Fab1p, Vac7p and Atg18p, while retaining normal interaction with Fig4p and with itself (Figure 17D). vac14p-L149R also failed to coprecipitate with Fab1p-TAP (Figure 17E). In the presence of vac14p-L149R, Fab1p did not localize to the vacuole membrane (Figure 17F). L149R is located in HEAT repeat 4 of yeast Vac14 (Figure 17G). Thus, HEAT repeat 4 is critical for the interaction between Vac14p and Fab1p and is required for the intracellular localization of Fab1p.

In contrast, vac14p-L149R did coprecipitate with Fig4p and with itself (Figure 17H and I), indicating that the Fig4p and Vac14p interaction domains are located in a different region of Vac14p from the L149 mutation. (Indeed, we described that Fig4p interacted and coprecipitated with the C-terminus Vac14p in yeast two hybrid test and immunoprecipitation experiment, respectively.)

To examine the effect of loss of Fab1p from the PtdIns(3,5)P_2 regulatory complex, we examined the *in vivo* levels of PI(3,5)P_2. Under basal conditions, PtdIns(3,5)P_2 comprises approximately 0.04% of total PI lipid in the *vac14*□ strain expressing wildtype *VAC14* from a plasmid. When cells are exposed to hyperosmotic stress, PtdIns(3,5)P_2 increases 10-fold to approximately 0.5% of total PI lipid within 10 minutes, then falls to 0.3% at 20 minutes, and to 0.09% at 30 minutes (Figure 17J and Table 2). (The 10-fold increase in this wild-type strain compared with a more typical 20-fold increase may be a consequence of the expression of *VAC14* from a plasmid rather than from its chromosomal location.) In the *vac14Δ* strain expressing *vac14-L149R*, PtdIns(3,5)P_2 comprises 0.03% of the PI lipid under basal conditions and increases only 2-fold to 0.06% after 10 minutes of hyperosmotic stress. Thus, dissociation of Fab1p from the complex *via* loss of interaction with Vac14p results in defective activation of Fab1 lipid kinase activity in response to hyperosmotic shock. That the modest increase in PI(3,5)P_2 is sustained for at least 30 min, suggests that regulation of Fig4p lipid phosphatase activity may also be impaired by the loss of association of Fab1p and Vac14p. Vac14p is required for the function of Fig4p (Duex et al., 2006b). We expected that the association between Fig4p and Fab1 kinase complex is required for Fig4 phosphatase activity.

CHAPTER III

Discussion and Future direction

Test how Fab1 kinase activity is regulated by its regulators *in vitro*.

In this study, we demonstrated that Fab1 and its known regulators form a large protein complex and regulate the both synthesis and turnover of PtdIns(3,5)P_2. Surprisingly, lipid phosphatase Fig4p resides in same complex. Some previous researches showed that Fig4p form a complex with Vac14p (Duex et al., 2006b; Rudge et al., 2004) and functions in the both synthesis and turnover of PtdIns(3,5)P_2 (Rudge et al., 2004). We found that Fig4p is required for forming a ternary core complex including Fab1p and Vac14p and the forming of a ternary complex is required for Fab1 kinase activity. In absence of Fig4p, Fab1p could not localize on the vacuole membrane and not associate with Vac14p. We demonstrated that Fig4p may also contribute to Fab1p activation via stabilization of the regulatory complex in latest paper (Jin et al., 2008). In mammalian, PIKfyve/Fab1, Sac3/Fig4 and ArPIKfyve/Vac14 form a complex and ArPIKfyve/Vac14 is required for the efficient formation of this complex (Sbrissa et al., 2007). It is likely that there are significant similarities in the formation and function of the complex that include Fab1p and its regulators, in yeast and mammalian. However, it remains unclear how the known regulators of Fab1p act in the synthesis and turnover of PtdIns(3,5)P_2. An effective approach to address this question would be to perform a purely *in vitro* Fab1 kinase reaction using purified proteins from *E.coli*. I performed *in vitro* kinase assays using purified Fab1p from yeast (Figure 11), but could not see any significant differences in isolated Fab1p kinase activities between wild type and *fig4Δ* cells or *vac14Δ* cells. Because of the low efficiency in coprecipitation of Vac14p or Fig4p, we could not examine how Fig4p and Vac14p are involved in the regulation of Fab1 kinase activity (Figure 11).

There are a number of steps associated with establishing an *in vitro* Fab1 kinase reation with only recombinant proteins. One is a how to purify Fab1p. We tried to express full length Fab1p in *E.coli*, but did not succeed (data not shown). We will attempt to purify Fab1p from yeast and from baculovirus infected insect cells, because the molecular weight of Fab1p is around 260kD. It is difficult to express full-length Fab1p in *E.coli*. The other difficulty is the amount of Fab1 proteins. Indeed, we could not detect purified Fab1p in silver staining and coomassie staining, in small scale pull-down experiment using yeast cells (data not shown). Using a larger number of yeast cells and Tandem affinity purification (TAP) method (Rigaut et al., 1999). I purified a greater amount of Fab1p protein, and could detect it by silver staining (Figure 12). For the next step, I will calculate the minimum amount of Fab1p required for *in vitro* kinase assay and establish a method for large scale purification of the Fab1p protein.

In addition, I need to develop methods to purify the other regulators. I have successfully expressed and purified full-length Vac14p, Fig4p and Atg18p from *E.coli* (Figure 18). The next problem is to determine how to check whether these proteins can function correctly. One approach is to perform functional assays. For example, I will test whether purified Vac14p interacts with its known binding partners. I found that purified Atg18p and Vac14p bind *in vitro* (Figure 9). In case of Fig4p, I will also test its phosphatase activity *in vitro.* An assay has already been published (Rudge et al., 2004).

Vac7p and Atg18p compete with each other to bind Vac14p.

In the *vac14-2* mutant, the hyperosmotic-stress induced elevation in PtdIns(3,5)P_2 was impaired. In addition, the negative regulation of Fab1 kinase activity under basal condition was also partially impaired (Figure 15B). The vac14-2 mutant did not interact with Atg18p and Vac7p in yeast two hybrid test (Figure 15D). In the vac14-2 mutant has three

mutation sites in HEAT repeat 2; H56Y, R61K and in HEAT repeat 3; Q101R (Figure 15F). It is likely that HEAT repeat 2 and 3 on Vac14p are direct interaction domains for Atg18p and Vac7p. However, it is still unclear how Atg18p and Vac7p function through Vac14p.

An effective approach to determine how Vac7p and Atg18p function is competition experiments. In first preliminary experiment, I found that Vac7p and Atg18p compete with each other in the regulation of vacuole morphology. A wild-type cell has small multi-lobed vacuoles (Figure 13A, 15A and 17C). In contrast, *vac7Δ* or *atg18Δ* cells have one enlarge vacuole (Bonangelino et al., 1997; Dove et al., 2004). We classified the vacuole morphology of *atg18Δ* cell into 3 types; (1) small multi-lobed vacuole, (2) single and unlobed vacuole and (3) enlarged and single vacuole with small structure (Figure 19). Almost wild-type cells had type (1) vacuoles (data not shown). However, *atg18Δ* cells had ~70% type (2) and ~20% type (1) vacuoles (Figure 19A and B). When Vac7p was over-expressed in *ag18Δ* cells, the population of type (2) was decreased; ~30% and the population of type (1) was increased; ~55%. This data suggested that Vac7p suppressed the single and unlobed vacuole morphology of *atg18Δ* cells. Nortably, in wild-type cells, when both Vac7p and Atg18p were over-expressed, the cells had the same vacuole morphology as over-expression of Vac7p alone. We classified the vacuole morphology of each cells into 3 types; (1) small and multi-lobed vacuole, (2) single and unlobed vacuole and (3) multi-lobed and fragmented vacuole. Almost wild-type cells had type (1) vacuoles. When Vac7p was over-expressed in wild-type cell, cells had ~95% type (1) and ~5% type (3) vacuoles. When Atg18p was over-expressed in wild-type cell, cells had ~50% type (1) and ~50% type (2) vacuoles. When Vac7p and Atg18p were over-expressed in wild-type cell, the cells had the same vacuole morphology as over-expression of Vac7p alone (Figure 19 C and D). Moreover, Atg18p did not suppressed single and enlarged vacuole morphology of *vac7Δ* cells (Figure 19F). These data suggest that Vac7p and Atg18p compete with each other in the regulation of vacuole size and morphology and

that Atg18p functions a upstream of Vac7p for regulation of vacuole morphology. In second preliminary experiment, I plan to check PtdIns(3,5)P_2 levels using the same yeast strains and transformants described above, and test the relationship between the synthesis/turnover of PtdIns(3,5)P_2 and vacuole morphology. I*n vitro* competition experiments will also be used whether Vac7p and Atg18p compete with each other for access to Vac14p. in an assay , I detected binding between purified recombinant Vac14p and Atg18p generated in *E.coli*. I am currently testing recombinant peptides of Vac7p that express well. The same peptide of Vac7p which we used for yeast two hybrid tests would be a candidate region. Once a Vac7p peptide is identified, I plan to perform competition experiments, such as FCPIA and use wild-type Vac14p and vac14-2 mutant, to test the model, that Vac7p and Atg18p compete through binding to Vac14p to regulate Fab1 kinase activity (Figure 15).

Determine Fab1p and its regulators undergo post-translated modification before or after osmotic shock.

During hyper osmotic stress, PtdIns(3,5)P_2 levels rapidly increase within 1 min, achieve a maximum point within 5 min and rapidly return to basal levels (Duex et al., 2006a). These observations suggest that Fab1 kinase activity is tightly regulated by a rapid signaling pathway, that likely includes protein modifications. In preliminary experiments, I found that the protein expression levels of Fab1p, Vac14p, Fig4p, Vac7p and Atg18p were not changed (Figure 20A,B,C,D and E). Notably I found that Fab1p is phosphorylated before and after hyper osmotic stress (Figure 20F and G). Moreover, it is possible that during hyperosmotic stress Fab1p is modified by other modifications as well (Figure 20F and G).

Mass spectrometry can be useful for determination of the precise modification sites of Fab1p. Above part, sufficient levels of Fab1p can be purified from yeast to detect by silver staining (Figure 18). Moreover, we found that yeast could be treated TCA. Fab1p-TAP could

be subsequently resuspended using a pull-down experiment (data not shown). This suggests that the determination of modification sites of Fab1p, and its known regulators including Vac14p, Vac7p Fig4p and Atg18p, would be possible before and after hyper osmotic stress. Subsequent site-directed mutagenesis and investigation using those mutants can be used to analyze the biological meaning of the modification of Fab1p / its regulators and how Fab1 kinase activity is regulated within cells, and *via* apposing stimuli.

Determine upstream pathways of Fab1 kinase complex.

The increase in PtdIns(3,5)P_2 levels in response to hyperosmotic stress is rapid and transient. Within 5 min, there is a 20-fold increase in PtdIns(3,5)P_2 levels, yet by 30 min, PtdIns(3,5)P_2 returns to basal levels even in the continued presence of hyperosmotic conditions (Duex et al., 2006). Fab1 kinase activity is tightly regulated by mechanisms that include formation of a protein complex as well as post-translational modification. At thus point the upstream pathways that function the activation and inactivation of Fab1 kinase activity by outside stimuli are unknown. I initiated a screen to identify the candidate genes which regulate Fab1 kinase activity (data not shown). I visually examined over 100 knock out yeast cells which each are missing a single non-essential protein kinase gene. Mutant yeasts, which are defective in the synthesis and turnover of PtdIns(3,5)P_2, show either enlarged or small vacuole morphology, respectively. Kinase deletion mutants which have abnormal vacuole morphology under basal conditions and / or in response to hyperosmotic stress will be tested further for their potential role in the regulation of Fab1p, Fig4p or their regulators.

The crystal structure of Vac14p.

The lipid kinase Fab1p and the lipid phosphatase Fig4p bind Vac14p. Thus, the lipid kinase and phosphatase likely share access to the same pools of PtdIns(3)P and PtdIns(3,5)P_2.

Fab1p and Fig4p bind distinct site on Vac14p. We propose that Vac14p assumes a conformation that brings Fab1p into close proximity to Fig4p (Figure 21). The Fab1p lipid kinase and Fig4p lipid phosphatase reside in the same complex and bind to opposite ends of Vac14p. A conformational change in Vac14p could simultaneously affect the activities of the kinase and phosphatase in opposite directions. In addition, the complex contains both an activator and an inhibitor of Fab1p, Vac7p and Atg18p respectively. They bind to the same region of Vac14p, HEAT repeats 2 and 3, and likely bind close to Fab1p. A conformation change in Vac14p could result in opposite effects on binding of the two proteins, amplifying the effect of either one alone on Fab1p activity. Thus, the structure of the protein complex may be key to the rapid modulation of PtdIns(3,5)P_2 levels *in vivo.* Therefore, we have initiated studies of structure of individual members of the complex. In preliminary test, we succeeded the purification of full-length recombinant Vac14p generated in *E.coli*. Future work can focus on determination of condition for crysalization of recombinant Vac14p.

MATERIALS AND METHODS

Strains, media, and expression vectors

The strains used in this study are listed in Table 1. Strains were grown at 24 °C in either YEPD or SC minimal media. For plasmid expression, the pRS400 series of vectors were used (Christianson et al., 1992).

FM4-64 labeling of yeast vacuoles

Approximately 0.1 OD_{600} units of cells were collected and resuspended in 250 ml YEPD media. To this solution, 3 □l of FM4-64 (2mg/ml dissolved in DMSO, Molecular Probes) was added. This mixture was incubated at 24 °C for 30min. Cells were washed twice with the YEPD media, resupended with the appropriate media and allowed to chase for 3hours. Fluorescence and differential interference contrast (DIC) images generated with a Deltavision system (Applied Precision, WA). Images processed using Adobe Photoshop.

Inositol extraction

Cells were labeled with [3H]-inositol, total cellular phosphatidylinositol extracted, deacylated and measured as described previously (Duex et al., 2006a).

Immunoprecipitation in yeast cells

10 OD log phase cells were lysed in lysis buffer; 50 mM Tris pH 7.5, 120 mM NaCl, 10 mM EDTA, 1 mM EGTA, 5 mM 2-glycerophosphate, 1 mM PMSF, 10 mM benzamidine, 1 mg/ml leupeptin, 5 mg/ml aprotonin. Extracts spun at 500g to sediment unbroken cells. Octyl-glucoside (Sigma) added to the supernatant to a final concentration of 0.5%. Subsequent manipulations performed at 4 °C. Resulting extracts incubated for 30 min and spun at 13,000g,

10 min. For the precipitation of Vac14p-HA,V5 or GFP and Fig4p-3XGFP, Anti-HA (COVANCE), anti-GFP (Roche Applied Science) or anti-V5 (Invitrogen) were added to the supernatant and incubated 1 h. Protein A immobilized on Sepharose beads (Sigma) was added and incubated for 1 h. For the precipitation of Fab1p-TAP, Fig4p-TAP or Vac14p-TAP, IgG conjugated with Sepharose beads (GE health care) was added and incubated for 1h. Protein complexes bound to the beads were washed 7 times with lysis buffer containing 0.5% octyl-glucoside, the eluted in sample buffer (50 mM Tris, pH6.8, 2% SDS, 5% □mercaptoethanol, 10% glycerol, 0.01% BPB) at 80 °C, 5 min. SDS-PAGE and western blot analysis were used to detect.

Yeast two hybrid analysis

Full length *VAC14* or truncated Vac14 was subcloned into the multi cloning site of pGAD (Gal4-Actibation Domain) or pGBD (Gal4-Binding Domain). Full length or truncated Vac14 fragment subcloned into pGBD or pGAD. Yeast *FAB1* encoding amino acids 538-1085, human FAB1 encoding amino acids was subcloned into the EcoRI-BglII site of pGBD. *VAC7* encoding amino acids 394-918 was subcloned into SmaI-SalI site of pGBD. Full length *ATG18* was subcloned into the EcoRI-SalI site of pGBD. Full length *FIG4* was subcloned into the BamHI-PstI site of pGBD. Plasmids were cotransformed into the yeast strain PJ69-4A, transformants were plated onto SC-LEU-TRP, replica-plated onto SC-LEU-TRP, SC-LEU-TRP-ADE-HIS+3AT or SC-LEU-TRP-ADE-HIS and grown for 4-10 days, 24 ºC. The yeast strain PJ69-4A and the pGAD and pGBD vectors have been described (James et al., 1996).

Glycerol Gradients

12 ml 10-50% glycerol gradients were prepared in the lysis buffer (see above) with 0.5 % octyl-glucoside. S13 lysates were prepared from 20 OD cells as described above, loaded on

the top and spun at 31,000 rpm, 18 h, 4 ºC. Fractions (1 ml) were precipitated with TCA, and 1/10 of the sample separated by SDS-PAGE.

In vitro kinase assay

in vitro kinase assay adapted from (Okada et al., 1996). Fab1p-TAP protein from 5 OD cells bound to IgG beads, was used for one reaction. Assays performed with 10 µl beads, a liposome mixture 34.7 µl including 0.02 mg phosphatidylethanolamine (Sigma) and 0.006 mg PI3P (Echelon), in a final volume of 65 µl of 25 mM HEPES pH 7.4, 120 mM NaCl, 1.5 mM $MgCl_2$, 5 mM 2-glycerophosphate and 1 mM DTT. Samples incubated at 30°C for the times indicated. Kinase reactions terminated by the addition of 243 □l Me-OH/$CHCl_3$ (2:1). Lipids were extracted with 58 µl 2.4 M HCl, 245 µl $CHCl_3$, and the lipid phase extracted a second time with 239 µl 1M HCl/methanol/chloroform (47:48:3). Reaction products were analyzed on K6 silica Gel 60A 20 x 20 cm glass-backed TLC plates (Whatman Inc) chromatographed with the solvent (chloroform/acetone/methanol/acetic acid/H_2O; 70:20:50:20:20). Labeled phosphoinositides were visualized by autoradiography.

^{32}P labeled lipid standards

^{32}P labeled PtdIns(3)P and PtdIns(3,5)P_2 generated as described (Rameh et al., 1995). PtdIns and PtdIns(5)P were phosphorylated using phosphoinositide 3-kinase p110/ human (Sigma). A liposome mixture, 20 µl, including 0.018 mg PE and 0.002 mg PtdIns or 0.002 mg PtdIns(5)P (Echelon) in 30 mM HEPES pH 7.0, 1 mM EGTA, ATP mixture 9 µl (0.5 mM ATP, 0.13 M $MgCl_2$, 0.04 M HEPES pH 7.0), and 1□l [^{32}P]ATP (GE Healthcare), final volume of 100 µl in 20 mM HEPES pH 7.0. After 30 min at 30°C, kinase reactions were terminated and products were analyzed by TLC.

REFERENCES

Andrade, M.A., Ponting, C.P., Gibson, T.J., and Bork, P. (2000). Homology-based method for identification of protein repeats using statistical significance estimates. Journal of molecular biology *298*, 521-537.

Banta, L.M., Robinson, J.S., Klionsky, D.J., and Emr, S.D. (1988). Organelle assembly in yeast: characterization of yeast mutants defective in vacuolar biogenesis and protein sorting. The Journal of cell biology *107*, 1369-1383.

Bonangelino, C.J., Catlett, N.L., and Weisman, L.S. (1997). Vac7p, a novel vacuolar protein, is required for normal vacuole inheritance and morphology. Molecular and cellular biology *17*, 6847-6858.

Bonangelino, C.J., Nau, J.J., Duex, J.E., Brinkman, M., Wurmser, A.E., Gary, J.D., Emr, S.D., and Weisman, L.S. (2002). Osmotic stress-induced increase of phosphatidylinositol 3,5-bisphosphate requires Vac14p, an activator of the lipid kinase Fab1p. The Journal of cell biology *156*, 1015-1028.

Botelho, R.J., Efe, J.A., Teis, D., and Emr, S.D. (2008). Assembly of a Fab1 phosphoinositide kinase signaling complex requires the Fig4 phosphoinositide phosphatase. Molecular biology of the cell *19*, 4273-4286.

Bronson, R. (2003). Infant gliosis (ingls) a new spontaneous mutation in the mouse. MGI Direct Data Submission http://mousemutantjaxorg/gliosis_paperhtml.

Bryant, N.J., Piper, R.C., Weisman, L.S., and Stevens, T.H. (1998). Retrograde traffic out of the yeast vacuole to the TGN occurs via the prevacuolar/endosomal compartment. The Journal of cell biology *142*, 651-663.

Cantley, L.C. (2002). The phosphoinositide 3-kinase pathway. Science (New York, NY *296*, 1655-1657.

Chow, C.Y., Zhang, Y., Dowling, J.J., Jin, N., Adamska, M., Shiga, K., Szigeti, K., Shy, M.E., Li, J., Zhang, X.*, et al.* (2007). Mutation of FIG4 causes neurodegeneration in the pale tremor mouse and patients with CMT4J. Nature *448*, 68-72.

Christianson, T.W., Sikorski, R.S., Dante, M., Shero, J.H., and Hieter, P. (1992). Multifunctional yeast high-copy-number shuttle vectors. Gene *110*, 119-122.

Cooke, F.T., Dove, S.K., McEwen, R.K., Painter, G., Holmes, A.B., Hall, M.N., Michell, R.H., and Parker, P.J. (1998). The stress-activated phosphatidylinositol 3-phosphate 5-kinase Fab1p is essential for vacuole function in S. cerevisiae. Curr Biol *8*, 1219-1222.

De Matteis, M.A., and D'Angelo, G. (2007). The role of the phosphoinositides at the Golgi complex. Biochemical Society symposium, 107-116.

Di Paolo, G., and De Camilli, P. (2006). Phosphoinositides in cell regulation and membrane dynamics. Nature *443*, 651-657.

Dove, S.K., Cooke, F.T., Douglas, M.R., Sayers, L.G., Parker, P.J., and Michell, R.H. (1997). Osmotic stress activates phosphatidylinositol-3,5-bisphosphate synthesis. Nature *390*, 187-192.

Dove, S.K., McEwen, R.K., Mayes, A., Hughes, D.C., Beggs, J.D., and Michell, R.H. (2002). Vac14 controls PtdIns(3,5)P(2) synthesis and Fab1-dependent protein trafficking to the multivesicular body. Curr Biol *12*, 885-893.

Dove, S.K., Piper, R.C., McEwen, R.K., Yu, J.W., King, M.C., Hughes, D.C., Thuring, J., Holmes, A.B., Cooke, F.T., Michell, R.H.*, et al.* (2004). Svp1p defines a family of phosphatidylinositol 3,5-bisphosphate effectors. The EMBO journal *23*, 1922-1933.

Duex, J.E., Nau, J.J., Kauffman, E.J., and Weisman, L.S. (2006a). Phosphoinositide 5-phosphatase Fig 4p is required for both acute rise and subsequent fall in stress-induced phosphatidylinositol 3,5-bisphosphate levels. Eukaryotic cell *5*, 723-731.

Duex, J.E., Tang, F., and Weisman, L.S. (2006b). The Vac14p-Fig4p complex acts independently of Vac7p and couples PI3,5P2 synthesis and turnover. The Journal of cell biology *172*, 693-704.

Efe, J.A., Botelho, R.J., and Emr, S.D. (2007). Atg18 regulates organelle morphology and Fab1 kinase activity independent of its membrane recruitment by phosphatidylinositol 3,5-bisphosphate. Molecular biology of the cell *18*, 4232-4244.

Forgac, M. (1998). Structure, function and regulation of the vacuolar (H+)-ATPases. FEBS letters *440*, 258-263.

Gary, J.D., Sato, T.K., Stefan, C.J., Bonangelino, C.J., Weisman, L.S., and Emr, S.D. (2002). Regulation of Fab1 phosphatidylinositol 3-phosphate 5-kinase pathway by Vac7 protein and Fig4, a polyphosphoinositide phosphatase family member. Molecular biology of the cell *13*, 1238-1251.

Gary, J.D., Wurmser, A.E., Bonangelino, C.J., Weisman, L.S., and Emr, S.D. (1998). Fab1p is essential for PtdIns(3)P 5-kinase activity and the maintenance of vacuolar size and membrane homeostasis. The Journal of cell biology *143*, 65-79.

Groves, M.R., Hanlon, N., Turowski, P., Hemmings, B.A., and Barford, D. (1999). The structure of the protein phosphatase 2A PR65/A subunit reveals the conformation of its 15 tandemly repeated HEAT motifs. Cell *96*, 99-110.

Gundelfinger, E.D., Kessels, M.M., and Qualmann, B. (2003). Temporal and spatial coordination of exocytosis and endocytosis. Nature reviews *4*, 127-139.

Guo, S., Stolz, L.E., Lemrow, S.M., and York, J.D. (1999). SAC1-like domains of yeast SAC1, INP52, and INP53 and of human synaptojanin encode polyphosphoinositide phosphatases. The Journal of biological chemistry *274*, 12990-12995.

James, P., Halladay, J., and Craig, E.A. (1996). Genomic libraries and a host strain designed for highly efficient two-hybrid selection in yeast. Genetics *144*, 1425-1436.

Jin, N., Chow, C.Y., Liu, L., Zolov, S.N., Bronson, R., Davisson, M., Petersen, J.L., Zhang, Y., Park, S., Duex, J.E.*, et al.* (2008). VAC14 nucleates a protein complex essential for the acute interconversion of PI3P and PI(3,5)P(2) in yeast and mouse. The EMBO journal.

Malbon, C.C. (2005). G proteins in development. Nature reviews *6*, 689-701.

Martens, S., and McMahon, H.T. (2008). Mechanisms of membrane fusion: disparate players and common principles. Nature reviews *9*, 543-556.

Meijer, H.J.G. (1999). Hyperosmotic stress induces rapid synthesis of phosphatidyl-D-inositol 3,5-bisphosphate in plant cells. Planta *208*, 294-298.

Odorizzi, G., Babst, M., and Emr, S.D. (1998). Fab1p PtdIns(3)P 5-kinase function essential for protein sorting in the multivesicular body. Cell *95*, 847-858.

Okada, T., Hazeki, O., Ui, M., and Katada, T. (1996). Synergistic activation of PtdIns 3-kinase by tyrosine-phosphorylated peptide and beta gamma-subunits of GTP-binding proteins. The Biochemical journal *317 (Pt 2)*, 475-480.

Owen, D.J., Collins, B.M., and Evans, P.R. (2004). Adaptors for clathrin coats: structure and function. Annual review of cell and developmental biology *20*, 153-191.

Rameh, L.E., Chen, C.S., and Cantley, L.C. (1995). Phosphatidylinositol (3,4,5)P3 interacts with SH2 domains and modulates PI 3-kinase association with tyrosine-phosphorylated proteins. Cell *83*, 821-830.

Reggiori, F., and Pelham, H.R. (2002). A transmembrane ubiquitin ligase required to sort membrane proteins into multivesicular bodies. Nature cell biology *4*, 117-123.

Rigaut, G., Shevchenko, A., Rutz, B., Wilm, M., Mann, M., and Seraphin, B. (1999). A generic protein purification method for protein complex characterization and proteome exploration. Nature biotechnology *17*, 1030-1032.

Rudge, S.A., Anderson, D.M., and Emr, S.D. (2004). Vacuole size control: regulation of PtdIns(3,5)P2 levels by the vacuole-associated Vac14-Fig4 complex, a PtdIns(3,5)P2-specific phosphatase. Molecular biology of the cell *15*, 24-36.

Rutherford, A.C., Traer, C., Wassmer, T., Pattni, K., Bujny, M.V., Carlton, J.G., Stenmark, H., and Cullen, P.J. (2006). The mammalian phosphatidylinositol 3-phosphate 5-kinase (PIKfyve) regulates endosome-to-TGN retrograde transport. Journal of cell science *119*, 3944-3957.

Sbrissa, D., Ikonomov, O.C., Fu, Z., Ijuin, T., Gruenberg, J., Takenawa, T., and Shisheva, A. (2007). Core protein machinery for mammalian phosphatidylinositol 3,5-bisphosphate synthesis and turnover that regulates the progression of endosomal transport. Novel Sac phosphatase joins the ArPIKfyve-PIKfyve complex. The Journal of biological chemistry *282*, 23878-23891.

Sbrissa, D., Ikonomov, O.C., and Shisheva, A. (1999). PIKfyve, a mammalian ortholog of yeast Fab1p lipid kinase, synthesizes 5-phosphoinositides. Effect of insulin. The Journal of biological chemistry *274*, 21589-21597.

Sbrissa, D., and Shisheva, A. (2005). Acquisition of unprecedented phosphatidylinositol 3,5-bisphosphate rise in hyperosmotically stressed 3T3-L1 adipocytes, mediated by ArPIKfyve-PIKfyve pathway. The Journal of biological chemistry *280*, 7883-7889.

Shaw, J.D., Hama, H., Sohrabi, F., DeWald, D.B., and Wendland, B. (2003). PtdIns(3,5)P2 is required for delivery of endocytic cargo into the multivesicular body. Traffic (Copenhagen, Denmark) *4*, 479-490.

Shisheva, A. (2008). Phosphoinositides in insulin action on GLUT4 dynamics: not just PtdIns(3,4,5)P3. American journal of physiology *295*, E536-544.

Simonsen, A., Lippe, R., Christoforidis, S., Gaullier, J.M., Brech, A., Callaghan, J., Toh, B.H., Murphy, C., Zerial, M., and Stenmark, H. (1998). EEA1 links PI(3)K function to Rab5 regulation of endosome fusion. Nature *394*, 494-498.

Stenmark, H., Aasland, R., Toh, B.H., and D'Arrigo, A. (1996). Endosomal localization of the autoantigen EEA1 is mediated by a zinc-binding FYVE finger. The Journal of biological chemistry *271*, 24048-24054.

van Meer, G. (2005). Cellular lipidomics. The EMBO journal *24*, 3159-3165.

Vicinanza, M., D'Angelo, G., Di Campli, A., and De Matteis, M.A. (2008). Function and dysfunction of the PI system in membrane trafficking. The EMBO journal *27*, 2457-2470.

Wang, Y.X., Zhao, H., Harding, T.M., Gomes de Mesquita, D.S., Woldringh, C.L., Klionsky, D.J., Munn, A.L., and Weisman, L.S. (1996). Multiple classes of yeast mutants are defective in vacuole partitioning yet target vacuole proteins correctly. Molecular biology of the cell *7*, 1375-1389.

Yamamoto, A., DeWald, D.B., Boronenkov, I.V., Anderson, R.A., Emr, S.D., and Koshland, D. (1995). Novel PI(4)P 5-kinase homologue, Fab1p, essential for normal vacuole function and morphology in yeast. Molecular biology of the cell *6*, 525-539.

Zhang, Y., Zolov, S.N., Chow, C.Y., Slutsky, S.G., Richardson, S.C., Piper, R.C., Yang, B., Nau, J.J., Westrick, R.J., Morrison, S.J*., et al.* (2007). Loss of Vac14, a regulator of the signaling lipid phosphatidylinositol 3,5-bisphosphate, results in neurodegeneration in mice. Proceedings of the National Academy of Sciences of the United States of America *104*, 17518-17523.

ACKNOWLEDGMENTS

I first and foremost thank my husband Yui Jin for support throughout this entire endeavor and being very patient with me as the years passed.

I also gratefully recognize my grandmother Ayako Morita and my parents Hideo Morita and Kikue Morita for their support.

I also want to thank Lois Weisman and current and former members of her laboratory who contributed to my success. Most significantly among these members are Emily Kauffman, Sujin Park and Jason Petersen. Especially, Jason guided and taught me basic technique and knowledge of yeast cell biology and discussed about my project from the beginning of my project.

謝辞

本研究を行うにあたり、また、奈良先端科学技術大学院大学前期博士課程の２年間を過ごすにあたり、非常に多くの方々に支えていただきました。

2005 年より研究室のメンバーとして、University of Michigan /Weisman 研究室に迎えてくださり、このようなすばらしい研究テーマを与えてくださった Lois Weisman 博士に心から感謝いたします。

Weisman 研究室のメンバーには慣れない環境での研究生活を支えていただきました。特に、基礎的な実験技術ならず事務的なことまで様々なことを教え支えてくれた Emily Kauffman、つたない英語の私に辛抱強く付き合いサイエンスのことだけでなく日々の生活についてディスカッションしてくれた Sujin Park 博士、私とは異なる視線でいつも冷静な意見をくれた Yanling Zhang 博士に感謝します。渡米直後、英語による意思疎通がままならない私に酵母の基本的な実験技術について懇切丁寧に教えてくれた Jason Petersen 博士には深く感謝します。

旧安田研究室では安田國雄先生をはじめとした諸先生方の研究者としての姿勢を間近で見ることにより私の目指す研究写像を作る土台ができました。安田國雄先生にはサイエンスとは既知の概念を取払い新しいものを見つけていくものだということを教えていただきました。今後諸先生方から学んだことを糧に研究に邁進していきたいと思います。

旧安田研究室の先輩方には心より感謝します。特に修士時代に日々実験技術を含め厳しく指導してくださった前川真吾博士、越智陽城博士には、この博士号取得の際にもご尽力いただきました。心から感謝いたします。今後は両博士の心をときめかすような研究ができるように研究に励んでいきたいと思います。

分子発生生物学講座高橋研究室の諸先生方ならびに学生の方々には心から感謝致します。

高橋淑子教授には修士号ならびに論文博士号取得のため多大なご助力をいただきました。厚く御礼申し上げます。

最後に、興味の赴くまま突き進んできた私を支えてくれた森田家、神家両家族に心から感謝します。特に公私ともに私の研究生活を支えてくれた神唯博士には心より感謝致します。

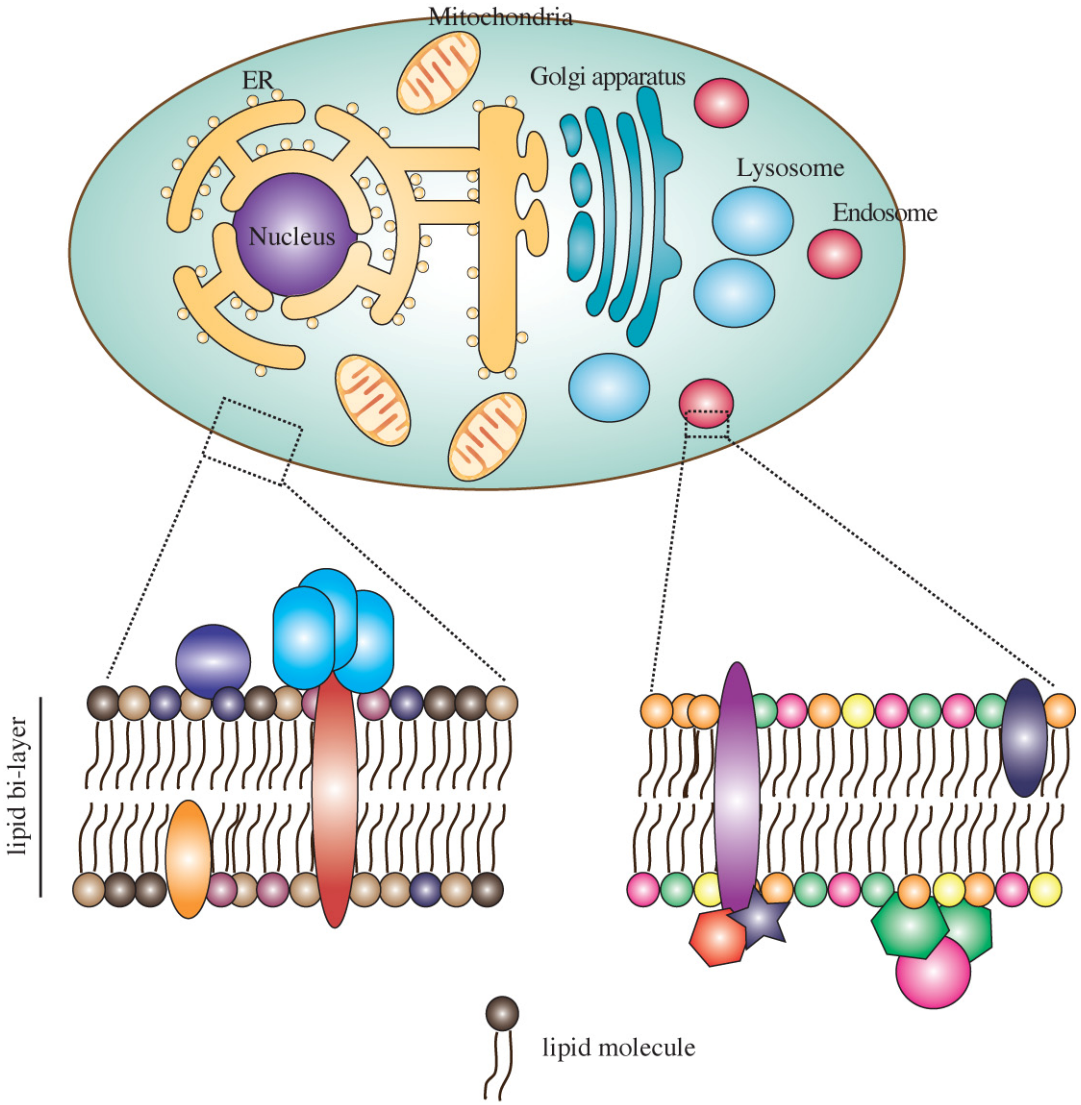

Figure 1. Cells and organelles are enclosed by membranes.
Membranes are made up of a lipid-bi-layer.
There are several lipid isomers, and also many proteins associates with the membrnaes.
Their distributions are distinct. Thus, lipids and membrane-assciated proteins are identified a specificity of the each organelle and plasma membrane.

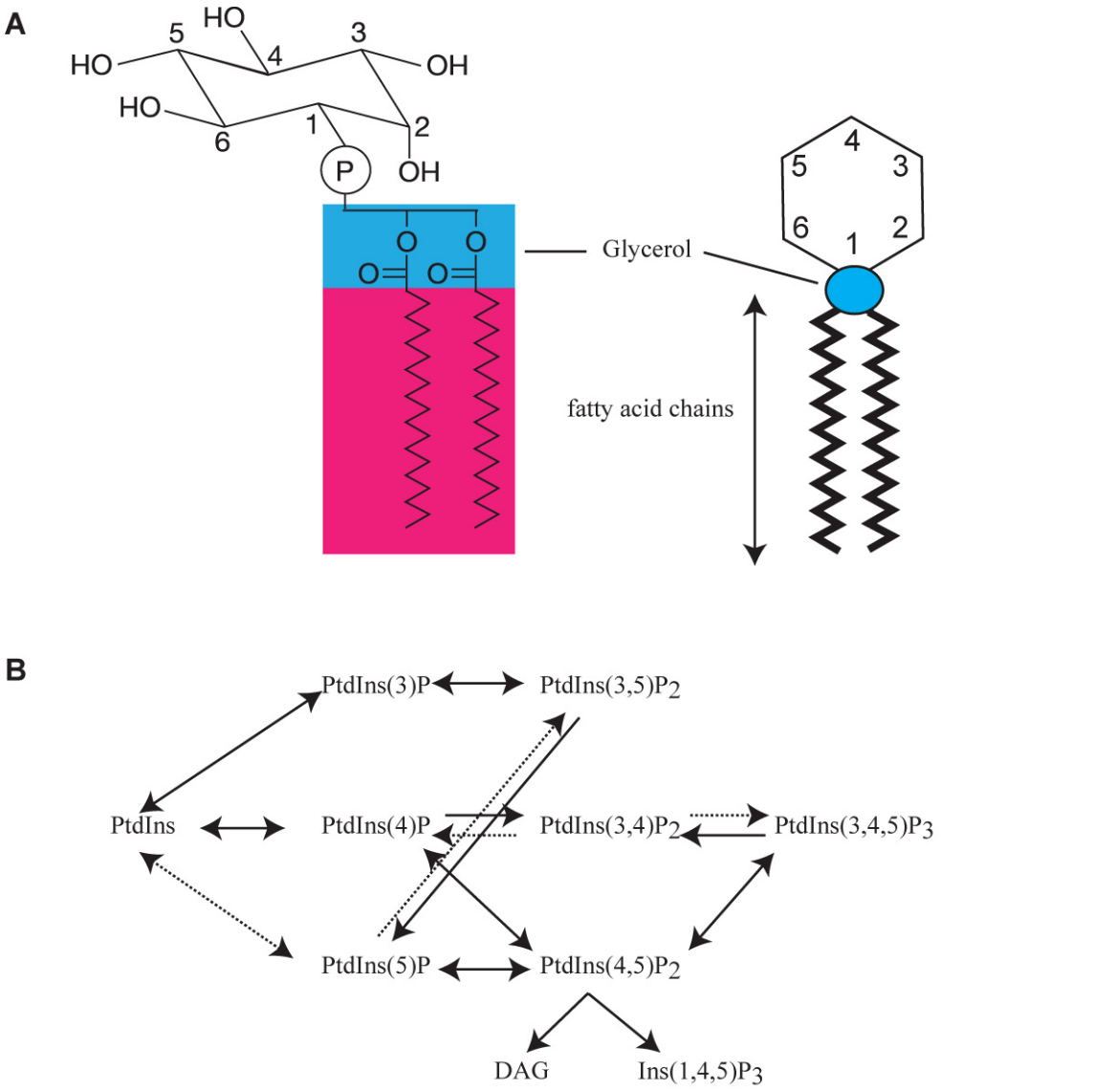

Figure 2. Phosphatidylinositol and its phosphorylated derivatives.
(A) The structure of Phosohatidylinositol (PtdIns). PtdIns is made up of glycerol (bule shading), fattiy acid (pink shading) and a hexahydric alchohol, called as inositol ring.
(B) Metabolic reactions ledaing to the generation of seven phosphoinositides derivatives from PtdIns. Reactions omdocated with dotted arrows have been shwon in vitro.
Diacylglycerol (DAG) and inositol 1,4,5 triphosphate ($Ins(1,4,5)P_3$ are metabolites by hydrolation of $PtdIns(4,5)P_2$.

A

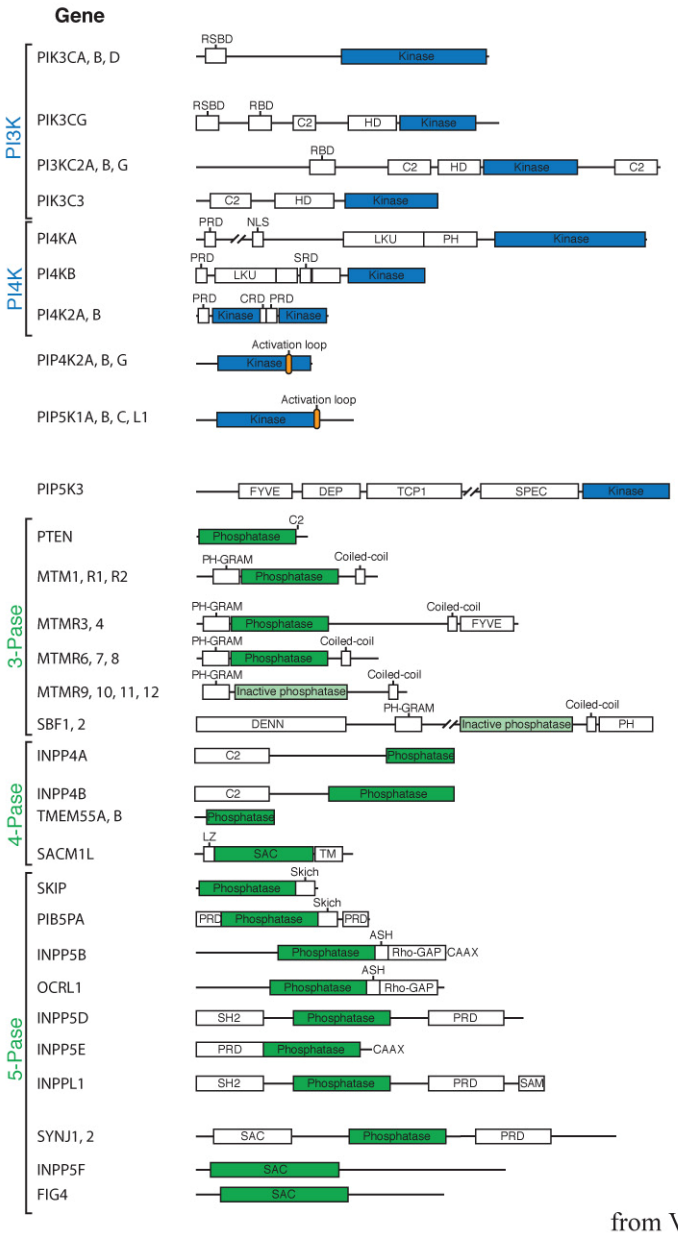

from Vicinanza et al., 2008

Figure 3. A variety of kinases or phosphatases convert PtdIns into other derivatives.
(A) Listing of different isoforms of PIKs and PI phosphatases.
(B) Schematic representation of the PI metabolic cycle with PIKs and the PI phosphatases,

B

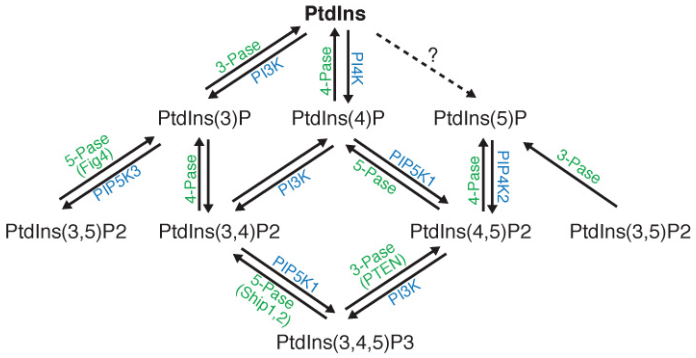
PtdIns
3-Pase
PI3K
4-Pase
PI4K
?
PtdIns(3)P
PtdIns(4)P
PtdIns(5)P
5-Pase (Fig4)
PIP5K3
4-Pase
PI3K
PIP5K1
5-Pase
4-Pase
PIP4K2
3-Pase
PtdIns(3,5)P2
PtdIns(3,4)P2
PtdIns(4,5)P2
PtdIns(3,5)P2
PIP5K1
5-Pase (Ship1,2)
3-Pase (PTEN)
PI3K
PtdIns(3,4,5)P3

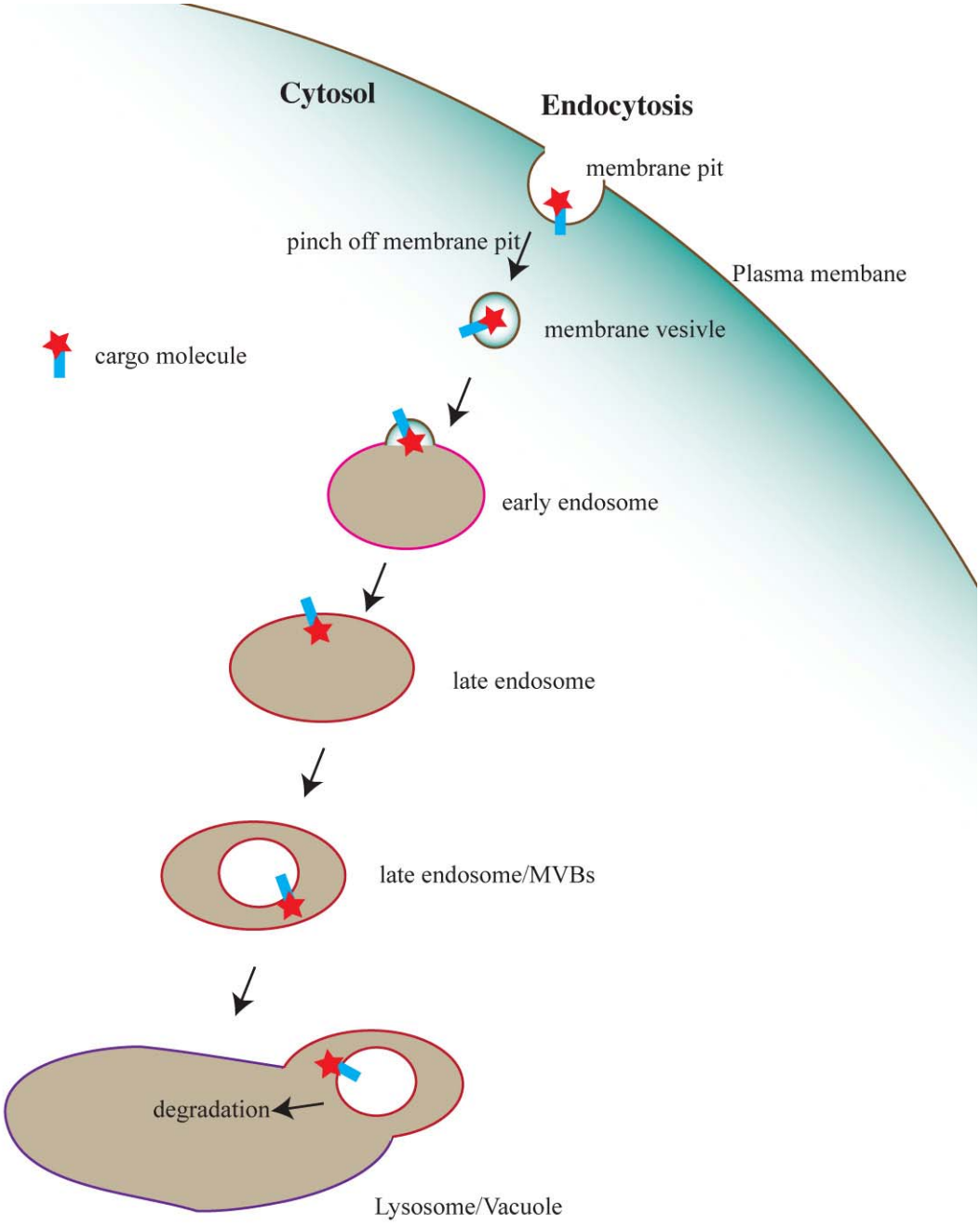

Figure 4. The endocytic pathway.

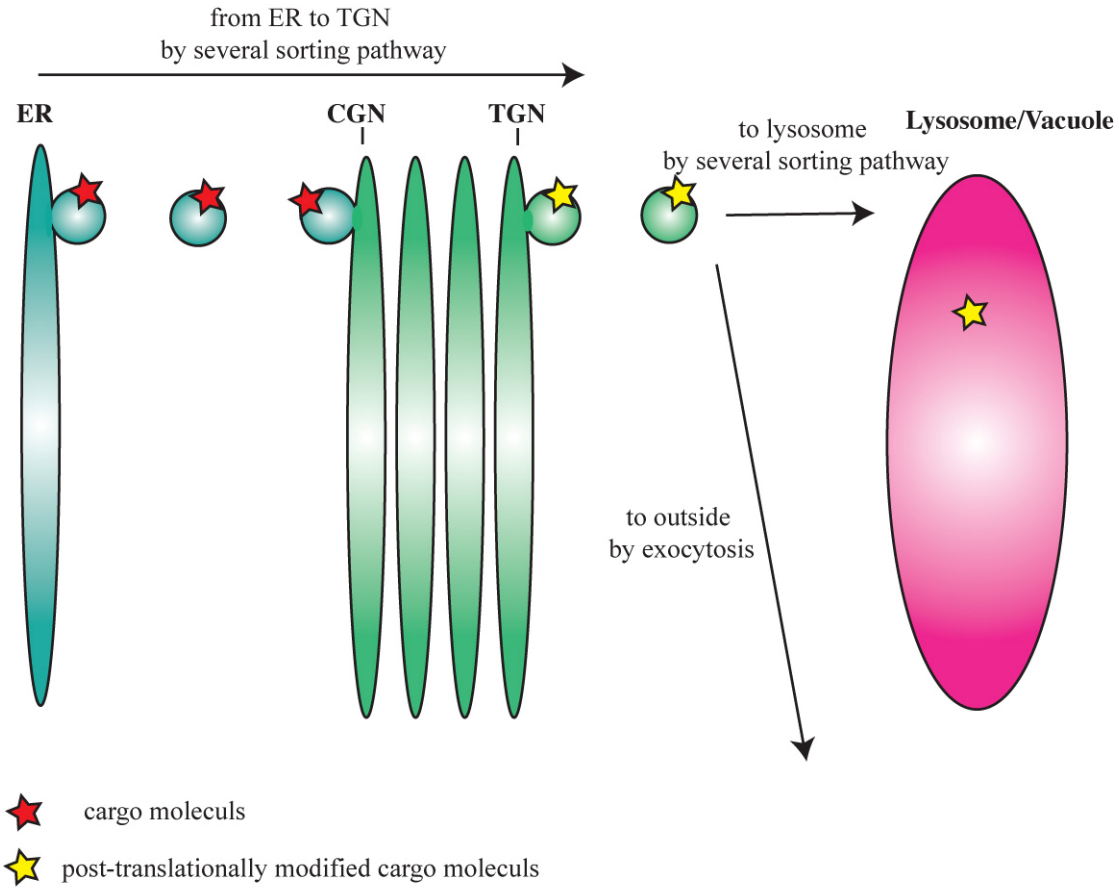

Figure 5. The biosynthetic-secretory pathway

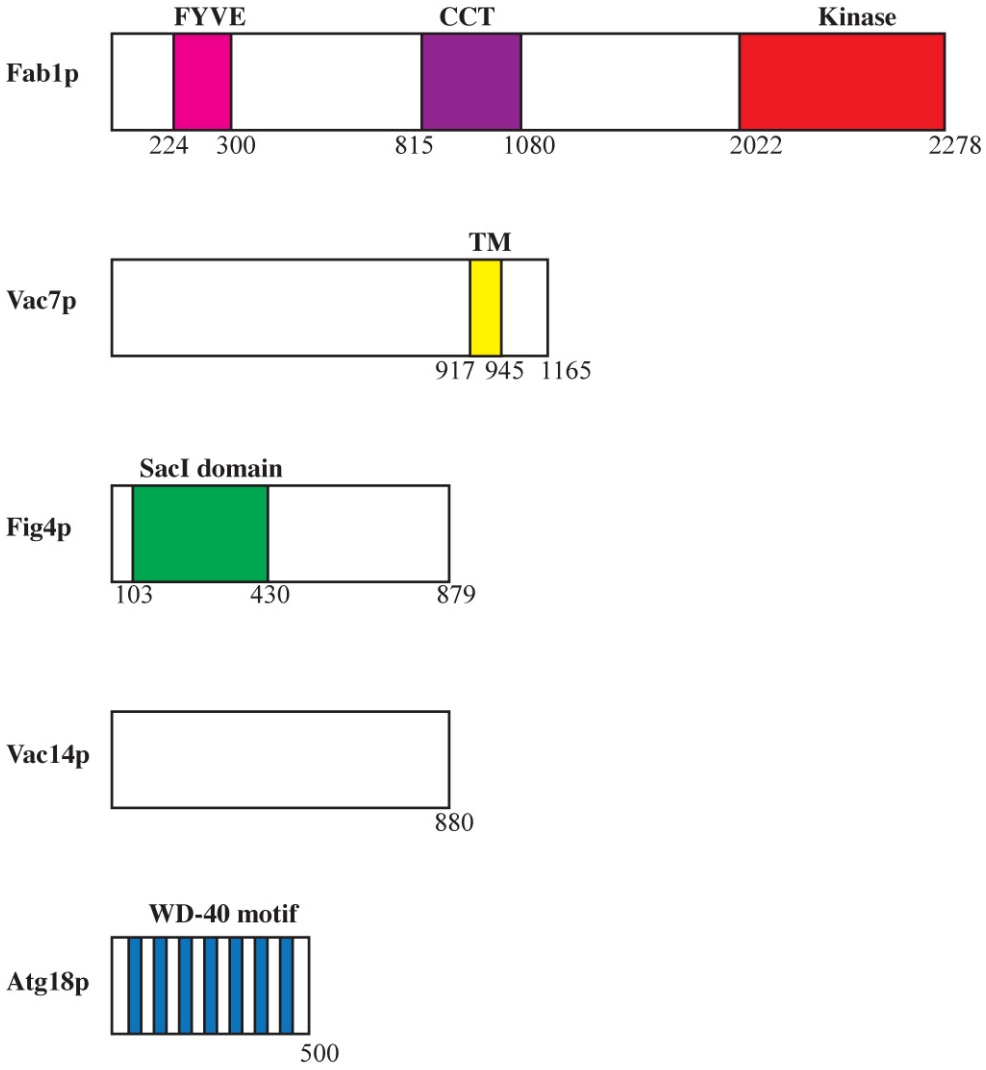

Figure 6.Schematic diagram of Fab1p and its regulators.

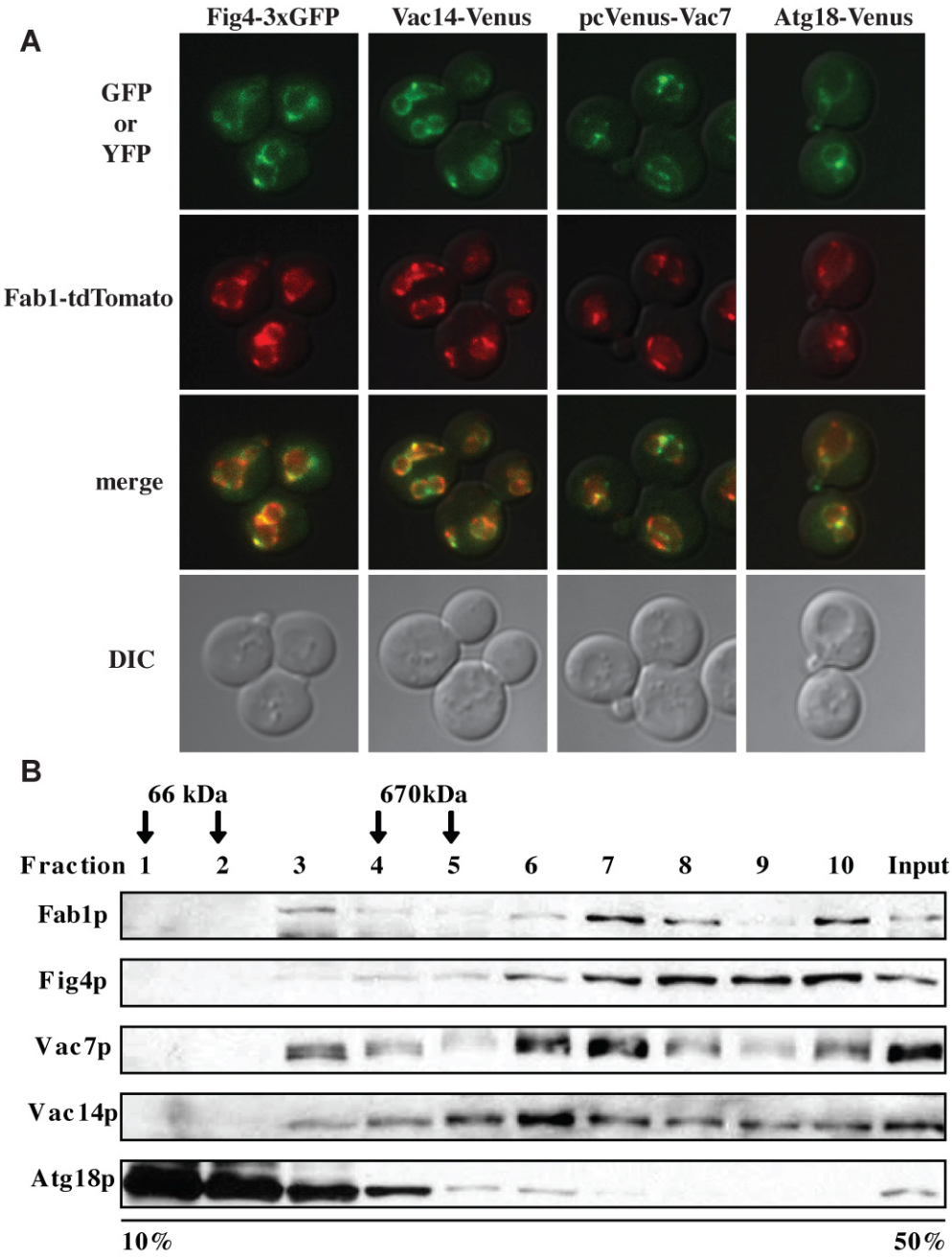

Figure 7. Fab1 and its regulators reside in a large protein complex.
(A) Cells expressing Fab1p-tdTomato / Fig4p-3XGFP, Vac14p-Venus or Atg18p-Venus were used. *Fab1p-tdTomato* / *vac7*Δ cell expressing pRS416-central-Venus-Vac7(cVenus-Vac7) was used.
(B) Analysis on glycerol gradients (10-50%) indicate that Fab1p and regulators form a complex > 670 kDa. Molecular weight markers; bovine serum albumin, 66 kDa, and thyroglobulin, 670 kDa, run in an adjacent tube. Representative profile of two independent gradients. *vac14*Δ / *fig4*Δ / *ATG18-Venus* cells expressing pRS413-VAC14-V5 and pRS415-FIG4-Myc were used.

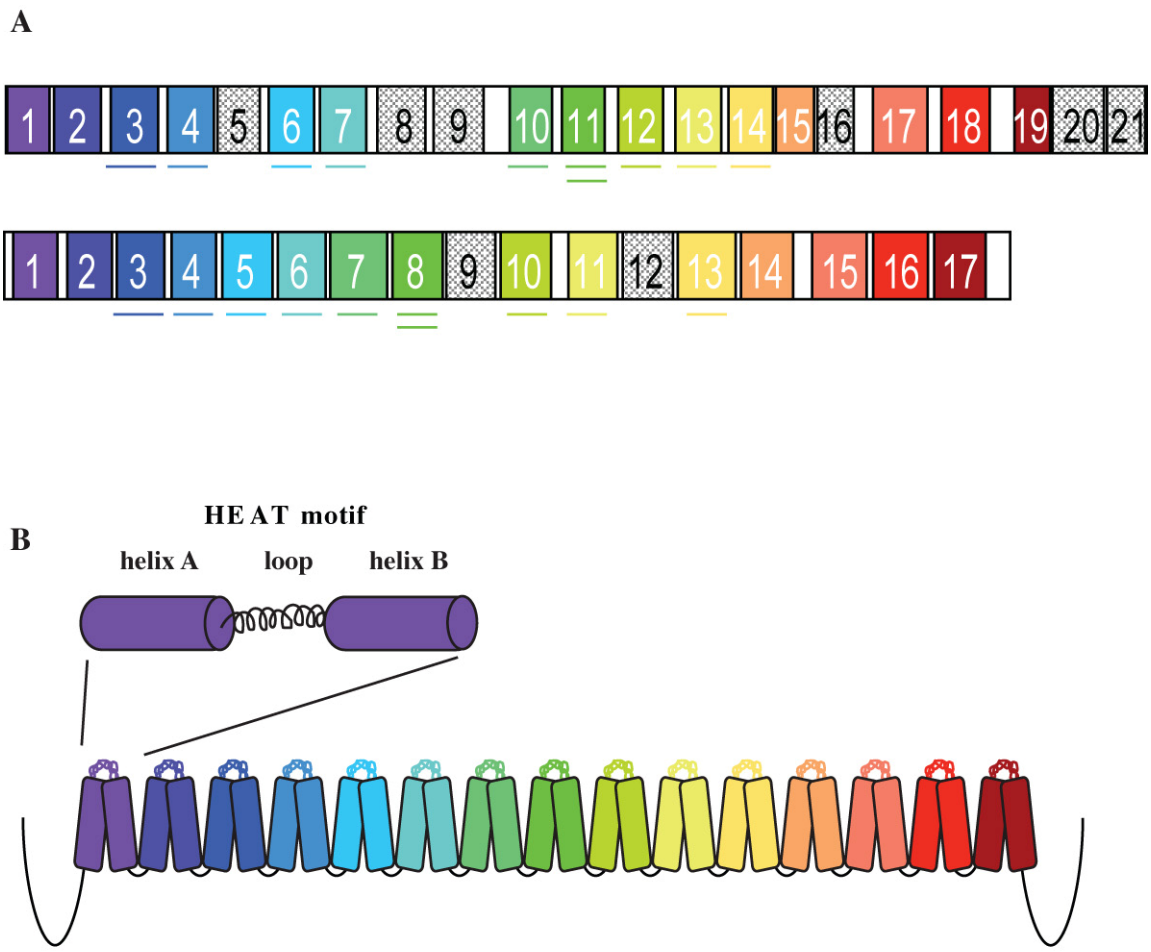

Figure 8. Vac14 is composed entirely of HEAT repeats.
(A) Vac14 contains twenty-one and seventeen HEAT repeats in S. cerevisiae (top) and mammalian Vac14 (bottom), respectively. Identical colors indicate homologous repeats between S. cerevisiae and mammalian Vac14. Underlines; HEAT repeats identified by REP with a confidence threshold better than at Pθ<1e-6.
(B) HEAT repeats are composed of two anti-parallel helics (helix A and B) connected with a short loop. The helix A and helix B interact each other. The loop connects two helices.

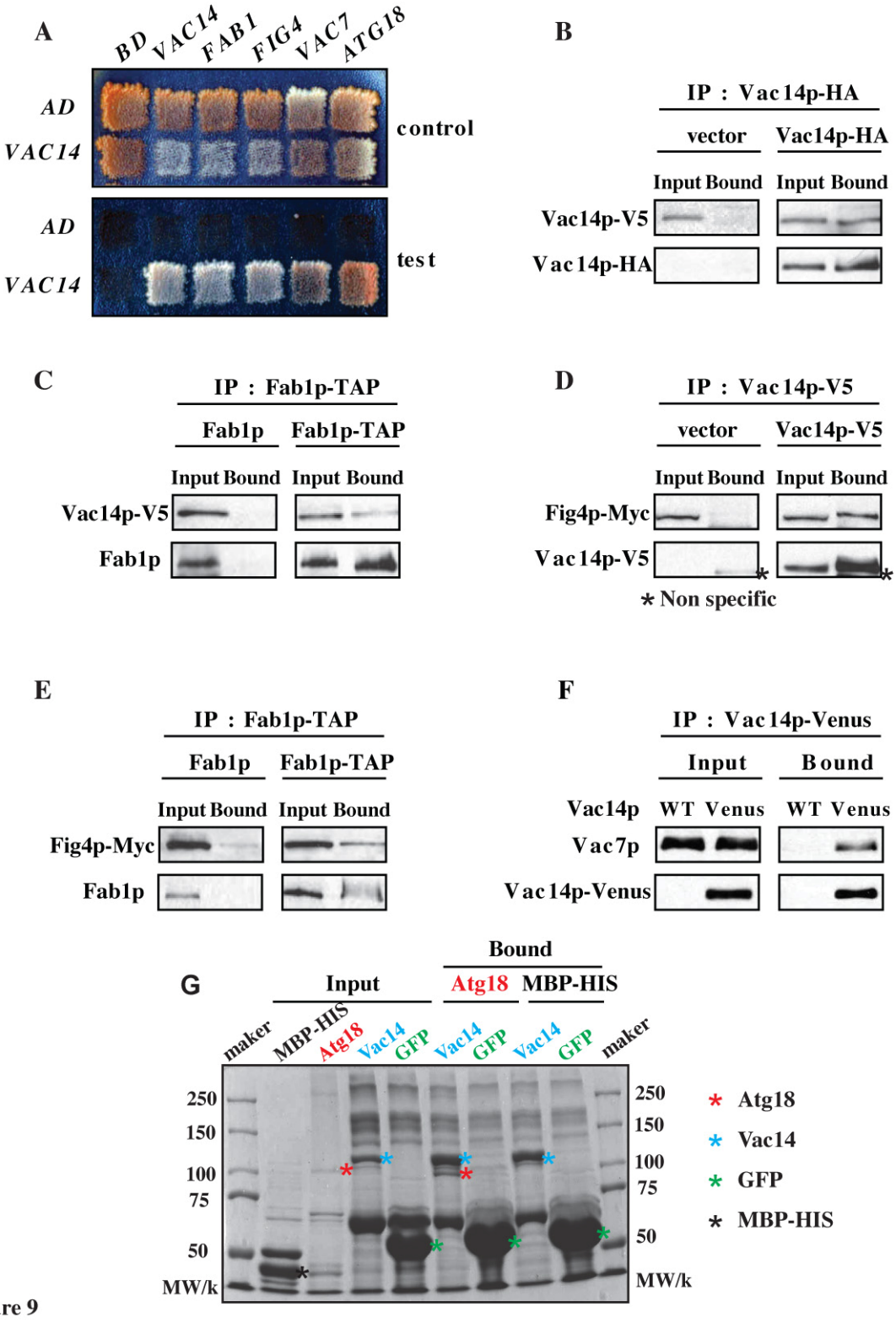
A
BD
VAC14
FAB1
FIG4
VAC7
ATG18
AD
VAC14
control
AD
VAC14
test
B
IP : Vac14p-HA
vector
Vac14p-HA
Input Bound
Input Bound
Vac14p-V5
Vac14p-HA
C
IP : Fab1p-TAP
Fab1p
Fab1p-TAP
Input Bound
Input Bound
Vac14p-V5
Fab1p
D
IP : Vac14p-V5
vector
Vac14p-V5
Input Bound
Input Bound
Fig4p-Myc
Vac14p-V5
* Non specific
E
IP : Fab1p-TAP
Fab1p
Fab1p-TAP
Input Bound
Input Bound
Fig4p-Myc
Fab1p
F
IP : Vac14p-Venus
Input
Bound
Vac14p
WT Venus
WT Venus
Vac7p
Vac14p-Venus
G
Bound
Input
Atg18
MBP-HIS
maker
MBP-HIS
Atg18
Vac14
GFP
Vac14
GFP
Vac14
GFP
maker
250
150
100
75
50
MW/k
250
150
100
75
50
MW/k
* Atg18
* Vac14
* GFP
* MBP-HIS

Figure 9

H

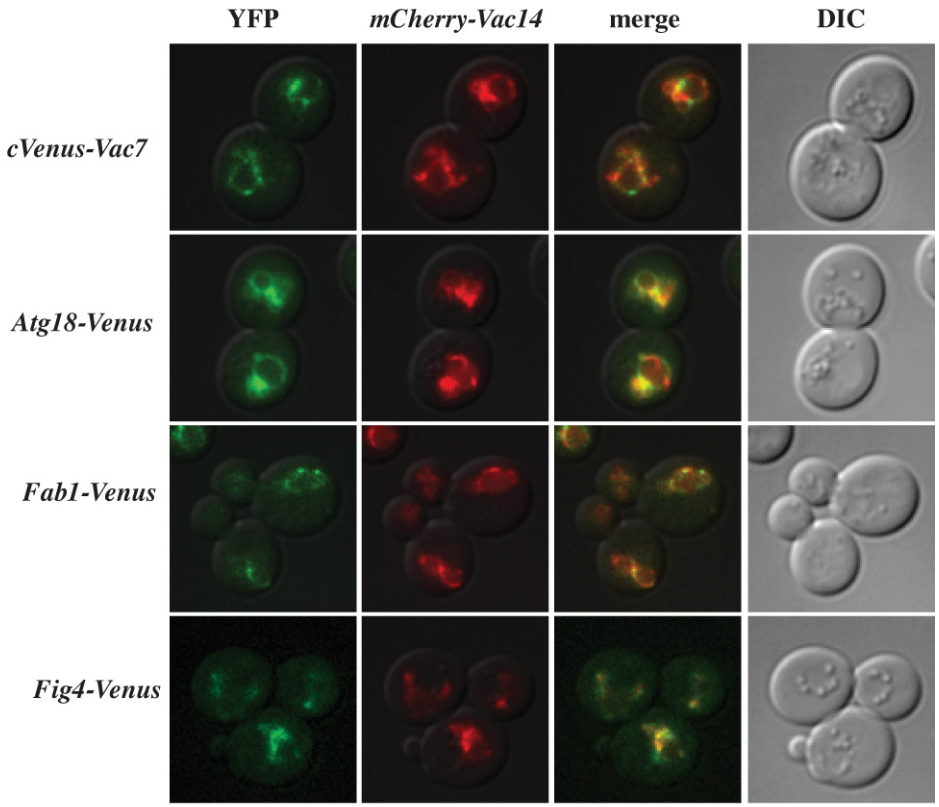
YFP
mCherry-Vac14
merge
DIC
cVenus-Vac7
Atg18-Venus
Fab1-Venus
Fig4-Venus

I

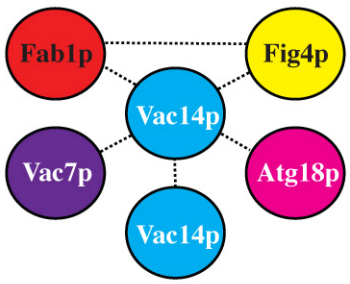
Fab1p
Fig4p
Vac14p
Vac7p
Atg18p
Vac14p

Figure 9

Figure 9. Vac14 interacts with the known regulators of $PI3,5P_2$.
(A) Yeast two-hybrid test of Vac14 with either Fab1p, Fig4p, Vac7p, Atg18p or Vac14p.
Full-length Vac14p was fused with the GAL4-activation domain (AD). Residues 538-1085 of Fab1, full-length Fig4, residue 394-918 of Vac7 or full-length Atg18 was fused with the GAL4-binding domain (BD). Plasmids were cotransformed into the yeast cells and transformants were plated onto the SC-LEU-TRP plate and replica-plated onto SC-LEU-TRP (control) or SC-LEU-TRP-ADE-HIS+3AT plate (test).
Plates incubated 24ºC, 7 days. Growth on the test plate indicates protein-protein interaction.
(B) Vac14p-HA coprecipitated Vac14p-V5. *vac14*Δ cells expressing pRS413/pRS416-VAC14-V5 or pRS413-VAC14-HA/pRS416-VAC14-V5 were used. (C) Fab1p-TAP coprecipitated Vac14p-V5.
*vac14*Δ cells or *vac14*Δ/*FAB1-TAP* cells expressed pRS413-VAC14-V5 were used.
(D) Vac14p-V5 coprecipitated Fig4-Myc. *vac14*Δ/*fig4*Δ cells expressed pRS415-FIG4-Myc/pRS413 or pRS415-FIG4-Myc/pRS413-VAC14-V5 were used. (E) Fab1p-TAP coprecipitated Fig4p-Myc.
*fig4*Δ cells or *fig4*Δ/*FAB1-TAP* cells espressed pRS415-FIG4-Myc were used.
(F) Vac14p-Venus coprecipitated Vac7p. Wild-type or *VAC14-Venus* cells were used.
(G) GST-Vac14p coprecipitated MBP-HIS-Atg18p.
Vac14p and Atg18 were expressed in *E.coli* separately and lysed. The beads bound GST-Vac14p was prepared, add the lysate of MBP-HIS-Atg18p and incubated. Each samples was loaded onto SDS-PAGE gel and detected by coomassie staining. Red asterisk; MBP-HIS-Atg18, Blue asterisk; GST-Vac14,
Green asterisk; GST-GFP, Black asterisk; MBP-HIS. (H) Vac14 colocalizes with its intraction partners.
VAC14-mCherry / *ATG18-Venus, FAB1-Venus or FIG4-Venus* cells were used.
VAC14-mCherry / *vac7*Δ cells expressed pRS416-central-Venus-VAC7 were used.
(I) Schematic of the interaction between Fab1 and its regulators.

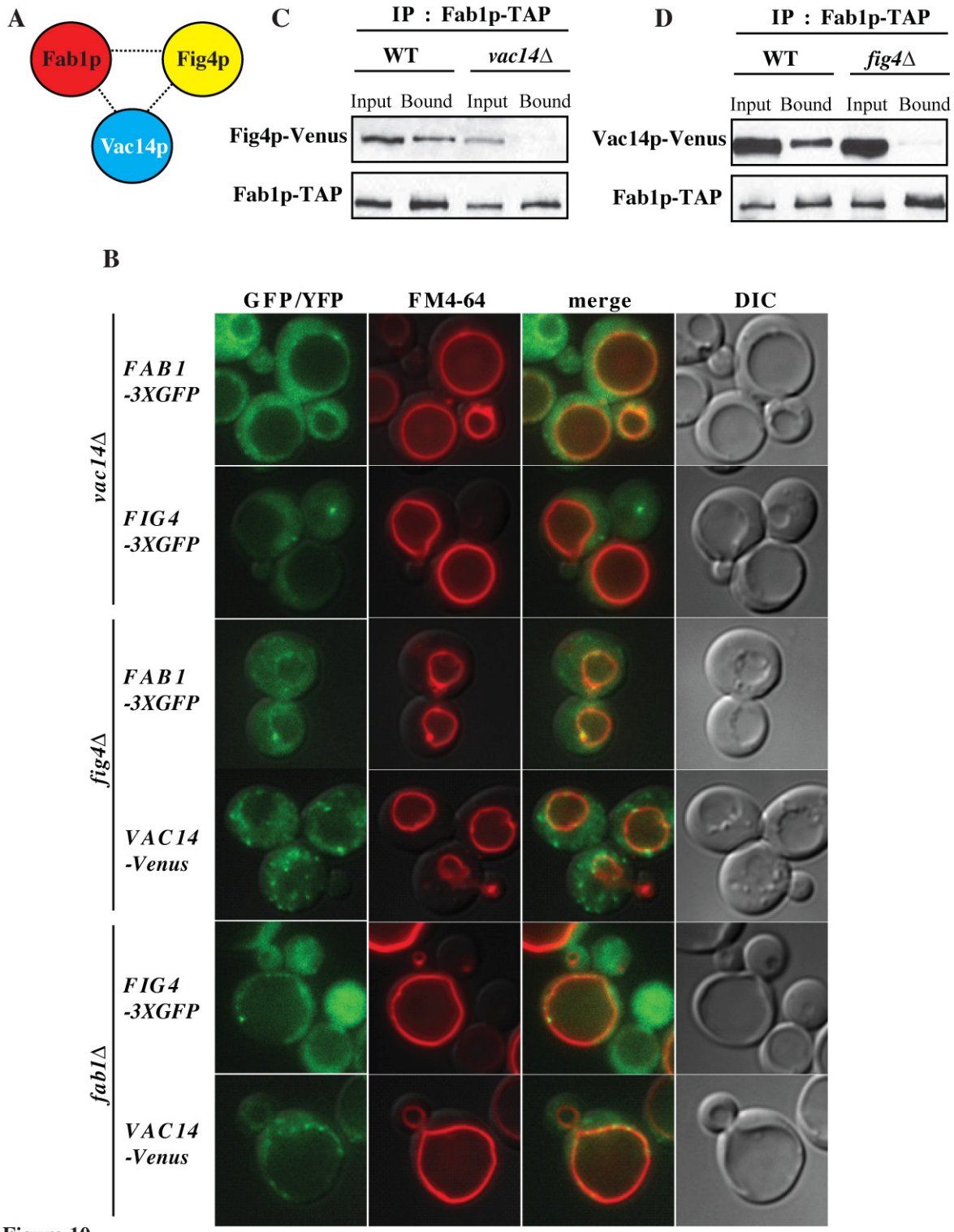
A
Fab1p
Fig4p
Vac14p
C
IP : Fab1p-TAP
WT
vac14Δ
Input Bound Input Bound
Fig4p-Venus
Fab1p-TAP
D
IP : Fab1p-TAP
WT
fig4Δ
Input Bound Input Bound
Vac14p-Venus
Fab1p-TAP
B
GFP/YFP
FM4-64
merge
DIC
vac14Δ
FAB1 -3XGFP
FIG4 -3XGFP
fig4Δ
FAB1 -3XGFP
VAC14 -Venus
fab1Δ
FIG4 -3XGFP
VAC14 -Venus

Figure 10

Figure 10. Fab1p, Fig4p and Vac14p form a ternary complex.
(A) Schematic of the interaction within a ternary complex.
(B) The localization of Fab1p, Fig4p and Vac14p to the vacuole membrane requires the presence of all three proteins. Cells labeled with FM4-64 (red) to visualize the vacuole membrane. Wildtype cells with FAB1-3xGFP, FIG4-3xGFP, or VAC14-Venus integrated at the proper chromosomal locus were used.
FAB1-3xGFP or *FIG4-3xGFP*/ *vac14*Δ cells, *FAB1-3xGFP* or *VAC14-Venus*/ *fig4*Δ cells and *FIG4-3xGFP* or *VAC14-Venus* / *fab1*Δ cells were used.
(C) In absence of Vac14p, Fab1p did not coprecipitate Fig4p. *FAB1-TAP* / *FIG4-Venus* or *FAB1-TAP* / *FIG4-Venus*/ *vac14*Δ cells were used.
(D) In absence of Fig4p, Fab1p did not coprecipitate Vac14p. *FAB1-TAP* / *FIG4-Venus* or *FAB1-TAP* / *FIG4-Venus*/ *fig4*Δ cells were used.

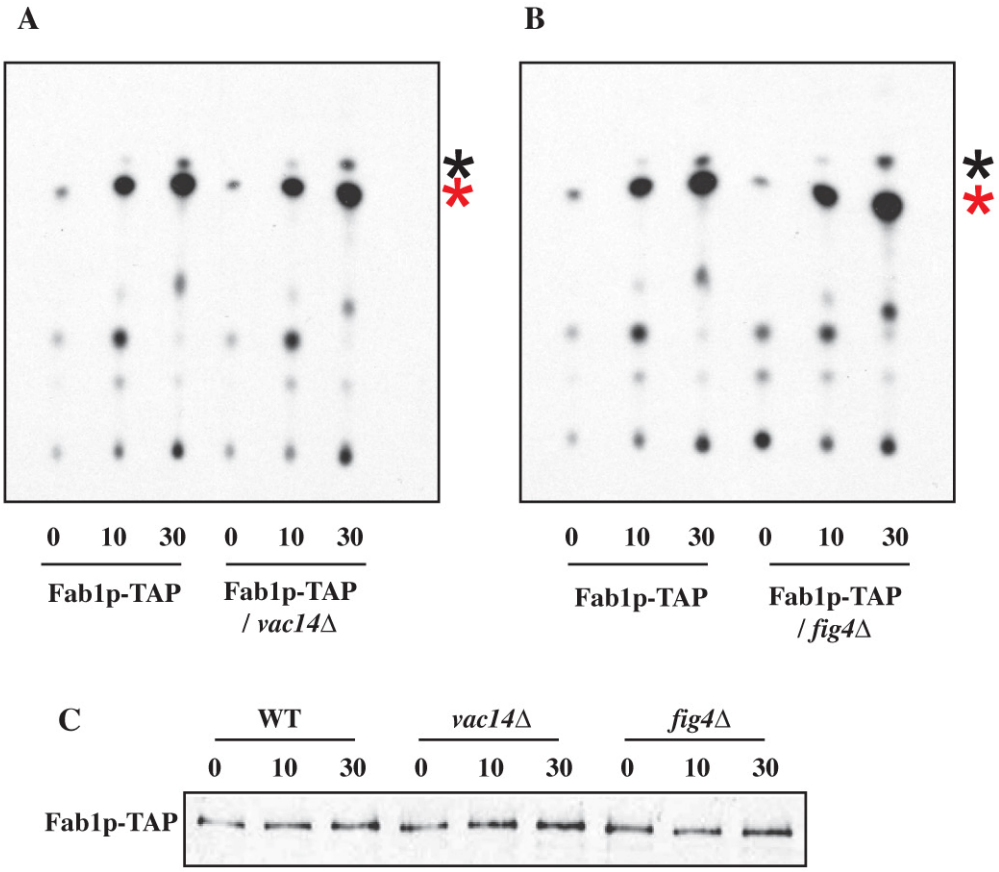

Figure 11. Fab1p-TAP isolated from wild-type, *vac14*Δ and *fig4*Δ cells exhibits the same level of lipid kinase activity.

(A)-(B) Autoradiograph of a thin-layer chromatogram of the products of the in vitro kinase assay, using IgG beads bound Fab1p-TAP from wild-type, *vac14*Δ or *fig4*Δ cells.
The asterisks indicate the migration of 32P-labeled PI3,5P_2 (red) and PI3P (black) standards.
(C) Western blot of Fab1p-TAP pulled down for each reaction.

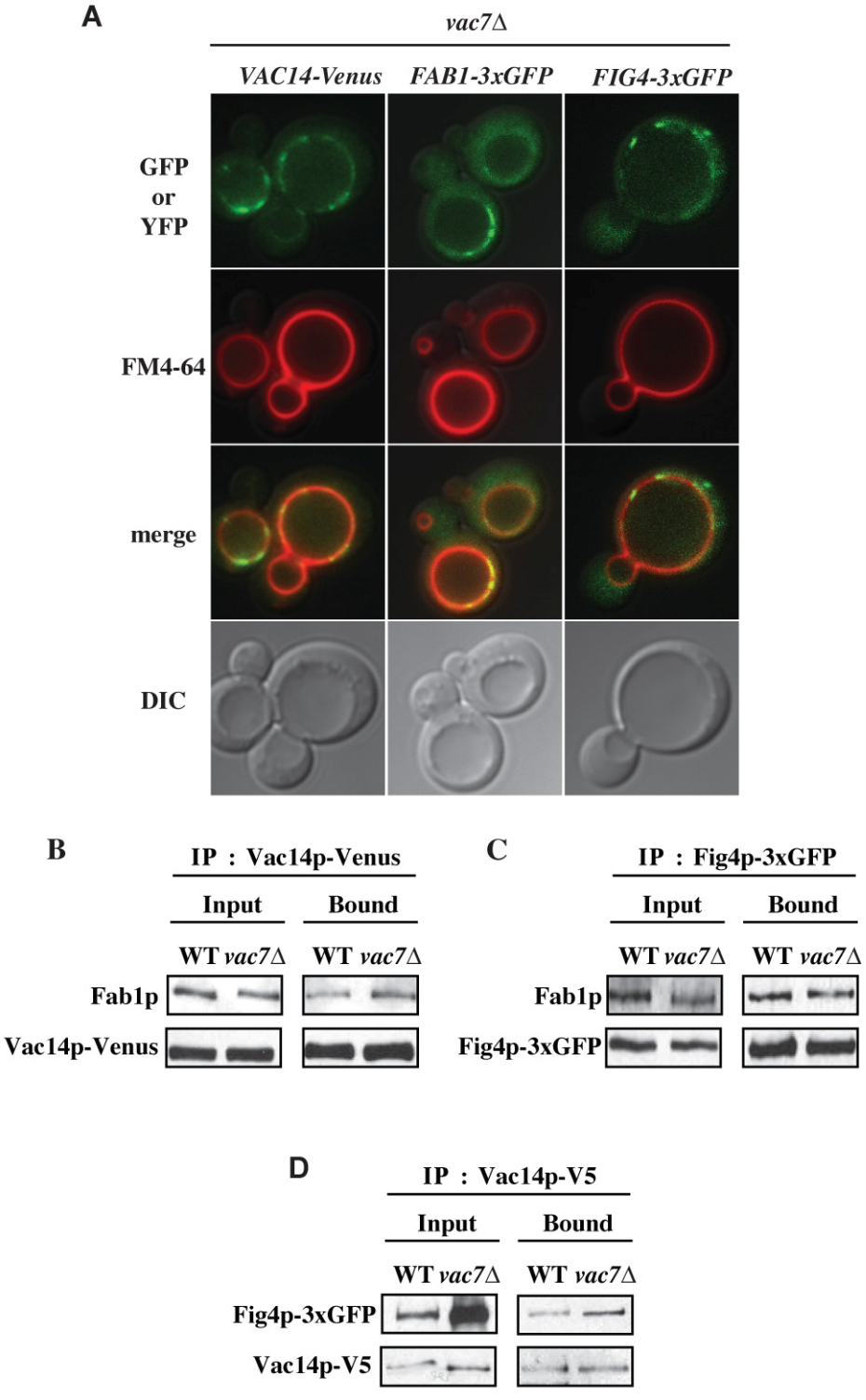
A
vac7Δ
VAC14-Venus
FAB1-3xGFP
FIG4-3xGFP
GFP or YFP
FM4-64
merge
DIC
B
IP : Vac14p-Venus
Input
Bound
WT vac7Δ
WT vac7Δ
Fab1p
Vac14p-Venus
C
IP : Fig4p-3xGFP
Input
Bound
WT vac7Δ
WT vac7Δ
Fab1p
Fig4p-3xGFP
D
IP : Vac14p-V5
Input
Bound
WT vac7Δ
WT vac7Δ
Fig4p-3xGFP
Vac14p-V5

Figure 12

Figure 12. Vac7p regulates Fab1 kinase activity, but not the localization and formation of the ternary complex of Fab1p, Vac14p and Fig4p.
(A) Vac14p, Fig4p and Fab1p localize on the vacuole membrane in absence of Vac7p.
VAC14-Venus/*vac7*Δ, *FIG4-3xGFP*/*vac7*Δ or *FAB1-3xGFP*/*vac7*Δ cells were labeled with FM4-64 (red) for visualizing the vacuole membrane.
(B)-(D) A ternary complex forms in absence of Vac7p.
(B) Fab1p coprecipitated with Vac14p in absence of Vac7p. *VAC14-Venus* or *VAC14-Venus* /*vac7*Δ cells were used. (C) Fab1p coprecipitated with Fig4p.
FIG4-3xGFP or *FIG4-3XGFP* / *vac7*Δ cells were used. (D) Fig4p coprecipitated with Vac14p.
FIG4-3XGFP / *vac14*Δ or *FIG4-3XGFP* / *vac14*Δ / *vac7*Δ cells expressed pRS413-VAC14-V5 were used.

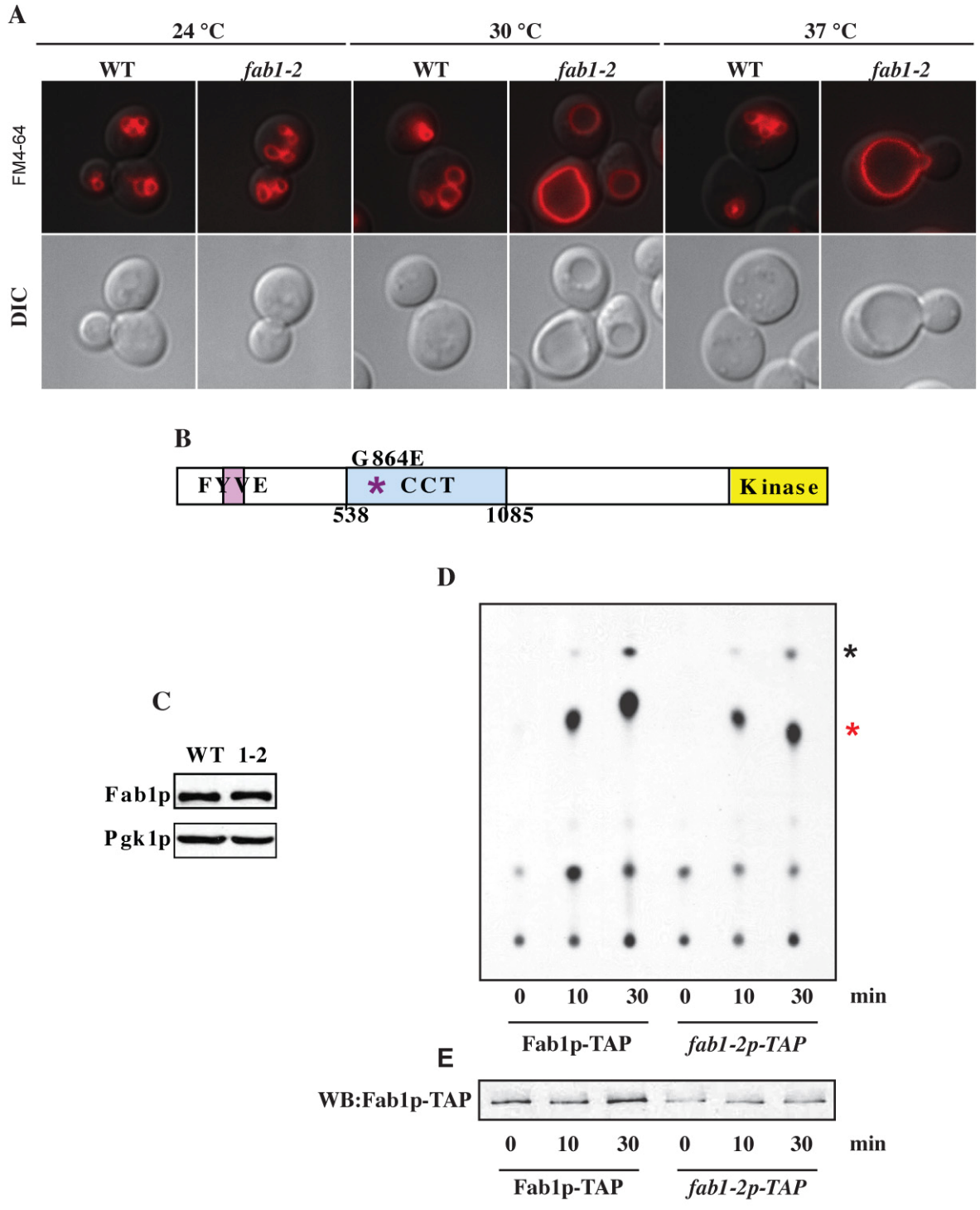
A
24 °C
30 °C
37 °C
WT
fab1-2
WT
fab1-2
WT
fab1-2
FM4-64
DIC
B
G864E
FYVE
CCT
Kinase
538
1085
C
WT 1-2
Fab1p
Pgk1p
D
*
*
0 10 30 0 10 30 min
Fab1p-TAP
fab1-2p-TAP
E
WB:Fab1p-TAP
0 10 30 0 10 30 min
Fab1p-TAP
fab1-2p-TAP

Figure 13

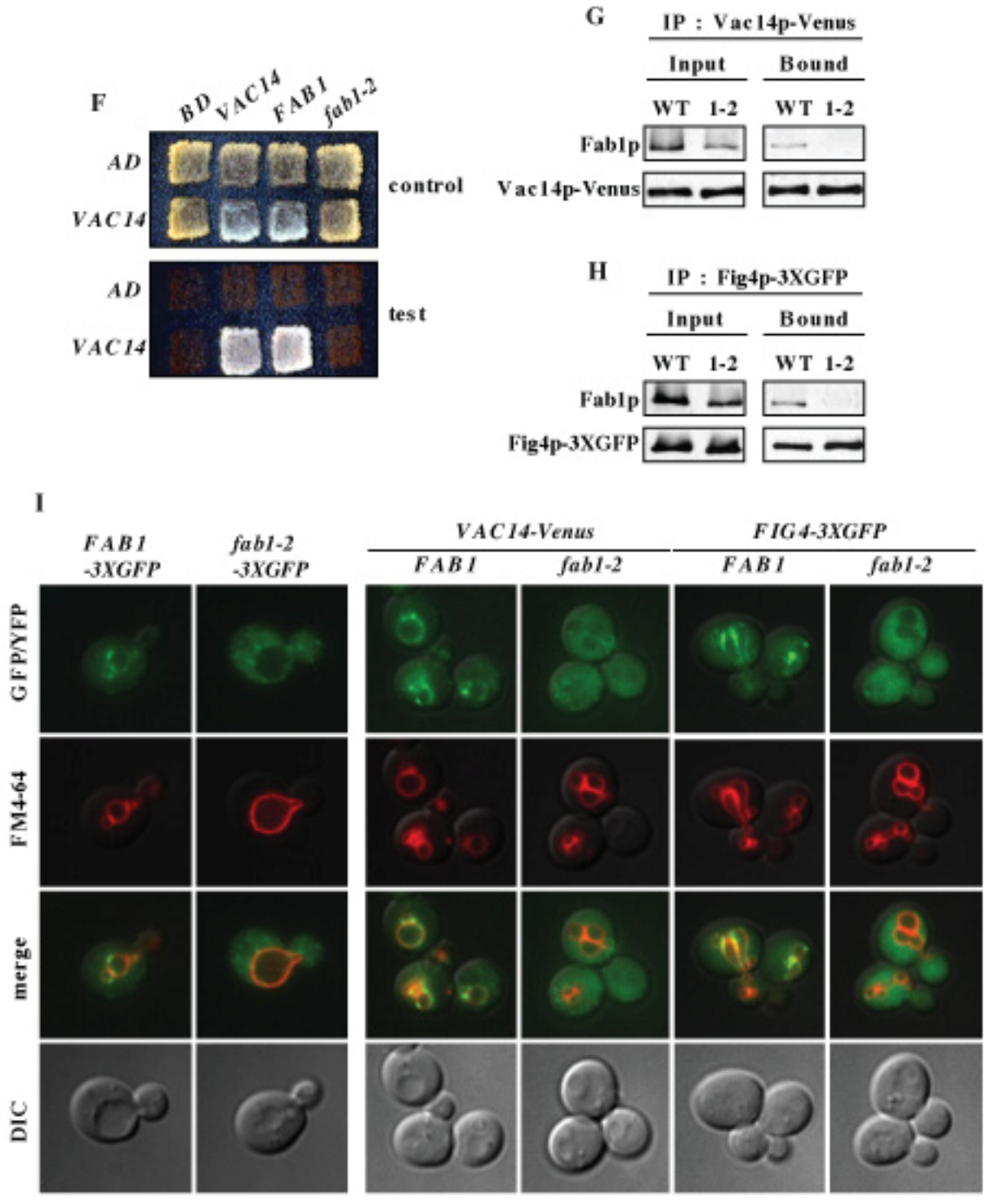
F
BD
VAC14
FAB1
fab1-2
AD
VAC14
control
AD
VAC14
test
G
IP : Vac14p-Venus
Input
Bound
WT 1-2 WT 1-2
Fab1p
Vac14p-Venus
H
IP : Fig4p-3XGFP
Input
Bound
WT 1-2 WT 1-2
Fab1p
Fig4p-3XGFP
I
FAB1 -3XGFP
fab1-2 -3XGFP
VAC14-Venus
FAB1
fab1-2
FIG4-3XGFP
FAB1
fab1-2
GFP/YFP
FM4-64
merge
DIC

Figure 13

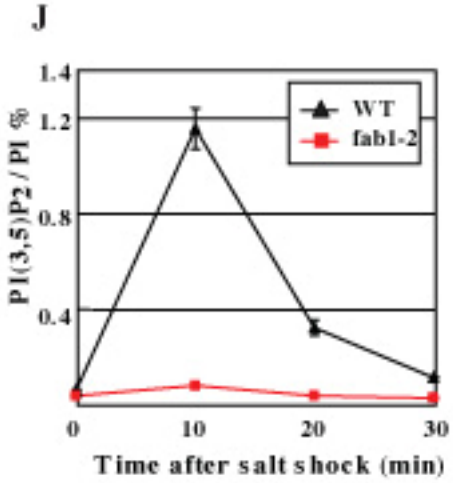

Figure 13. Formation of a ternary complex of Fab1p, Fig4p and Vac14p is essential for Fab1p kinase activity *in vivo*.

(A) *fab1-2* has enlarged vacuoles at nonpermissive temperature. *fab1*Δ cells expressing pRS416-FAB1 or pRS416-fab1-2 were labeled with FM4-64. The images were taken at 24°C, 30°C or 37°C.

(B) Schematic of the *fab1-2* allele ; purple asterisk, the G864 mutation.

(C) fab1-2 protein is present at wild type levels. Cell lysates were analyzed by western analysis from *fab1*Δ cells expressing pRS416-FAB1 or pRS416-fab1-2. Equal proteins are loaded. Pgk1p was used as a lodaing control.

(D) When measured in vitro, isolated fab1-2 protein has same kinase activity as Fab1p. Autoradiograph of a thin-layer chromatogram of the products of the in vitro kinase assay. The red asterisk indicates the migration of 32P-labeled PI(3,5)P_2standards. The black asterisk indicates the migration of standard 32P-labeled PI3P.

(E) Western blot of Fab1-TAPp or fab1-2-TAP protein pulled down for each reaction in (D).

(F) *VAC14* interactes with *FAB1*, but not *fab1-2*. Yeast two hybrid test of *FAB1* or *fab1-2* interaction with *VAC14*. Full-length *VAC14* was fused with Ga14-AD. *FAB1* or *fab1-2*, amino acids 538-1085, was fused with Gal4-BD. Upper panel, SC-LEU-TRP (control); lower panel SC-LEU-TRP-ADE-HIS+3AT (test). Plates were incubated at 24C, 4 days.

(G)-(H) fab1-2 does not form a ternary complex with Vac14p and Fig4p.

(G) Vac14p-Venus does not coprecipitate fab1-2. *fab1*Δ / *VAC14-Venus* cells expressing pRS416-FAB1 or pRS416-fab1-2 were used.

(H) Fig4p-3xGFP does not coprecipitate fab1-2. *fab1*Δ / *FIG4-3xGFP* cells expressing pRS416-FAB1 or pRS416-fab1-2 were used.

(I)) fab1-2, Vac14p and Fig4p in a fab1-2 mutant do not localize to the vacuole membrane. pRS416-FAB1-3xGFP or pRS416-fab1-2 -3xGFP was expressed in *fab1*Δ, or *fab1*Δ / *VAC14-Venus*, or *fab1*Δ / *FIG4-3xGFP*. Cells were labeled with FM4-64 (red).

(J) The fab1-2 mutant does not transiently elevate its levels of PI(3,5)P_2 in response to hyperosmotic stress. *fab1*Δ cells expressing pRS416-*FAB1* or pRS416-*fab1-2* measured. Error bars; SD (n=3).

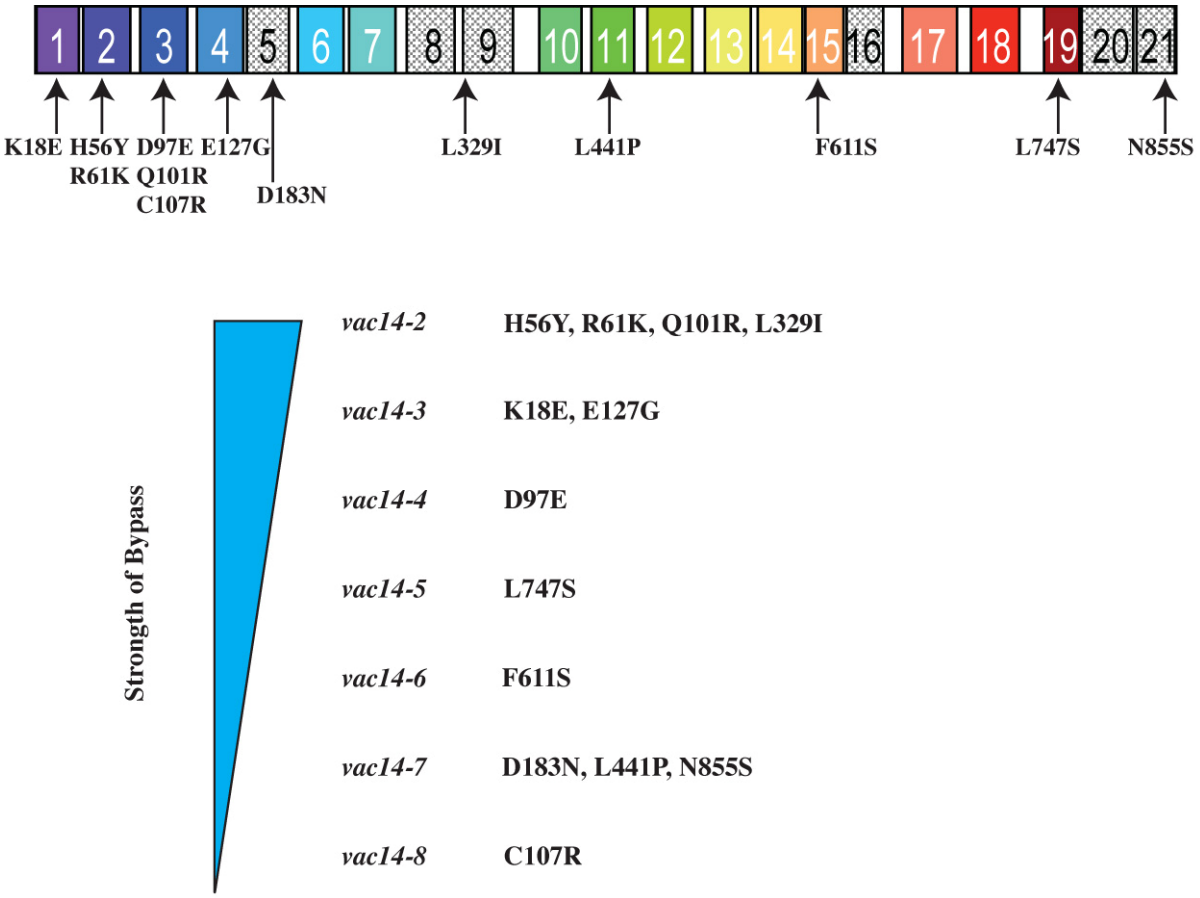

Figure 14. The screen of *vac14* mutants.
Schematic of *vac14* mutants, classfied according to the strength of bypass ability of *vac7*Δ vacuole morphoogy.

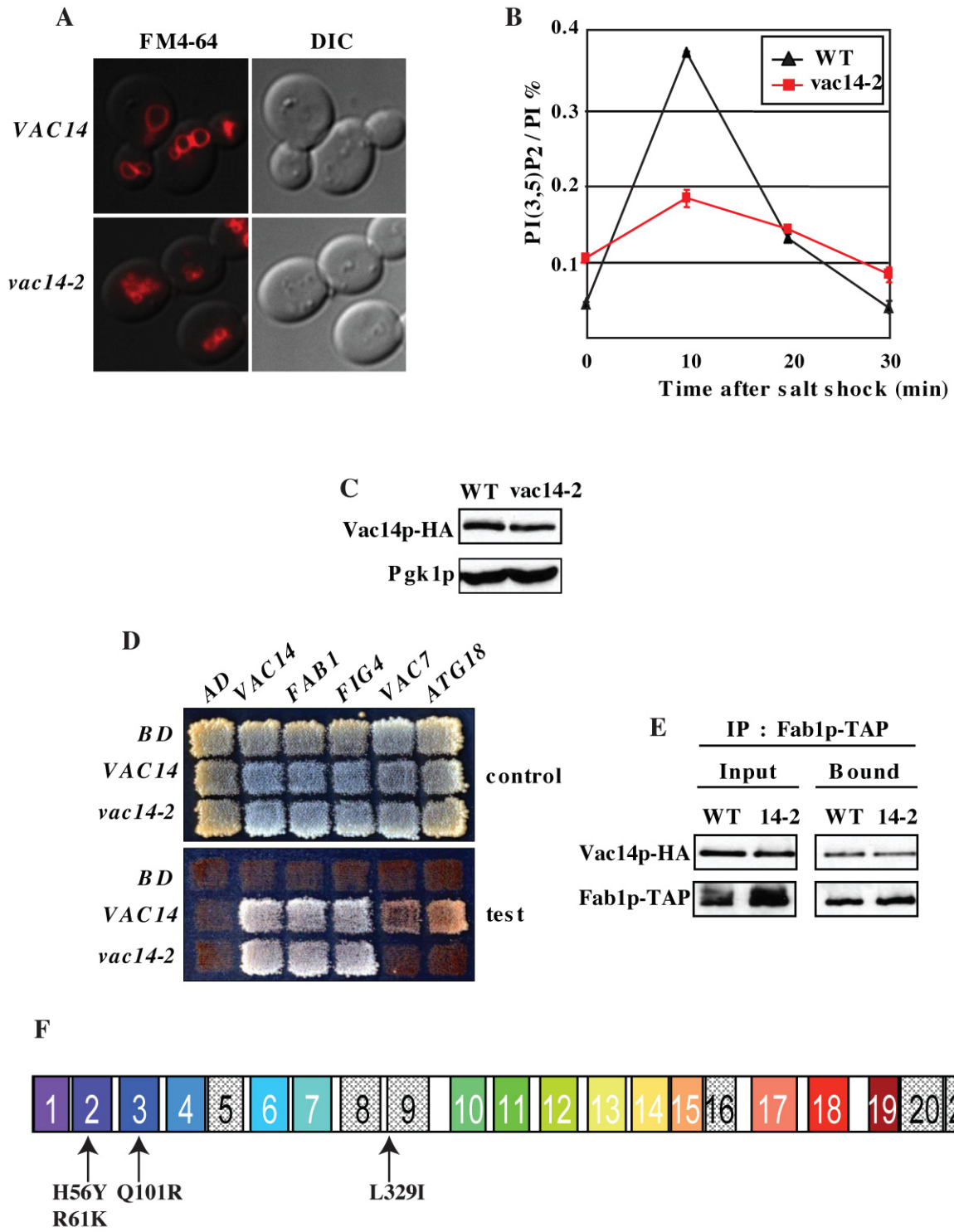
A
FM4-64
DIC
VAC14
vac14-2
B
WT
vac14-2
PI(3,5)P2 / PI %
0.4
0.3
0.2
0.1
0
10
20
30
Time after salt shock (min)
C
WT vac14-2
Vac14p-HA
Pgk1p
D
AD
VAC14
FAB1
FIG4
VAC7
ATG18
BD
VAC14
vac14-2
control
BD
VAC14
vac14-2
test
E
IP : Fab1p-TAP
Input
Bound
WT 14-2 WT 14-2
Vac14p-HA
Fab1p-TAP
F
1 2 3 4 5 6 7 8 9 10 11 12 13 14 15 16 17 18 19 20 21
H56Y Q101R
R61K
L329I

Figure 15

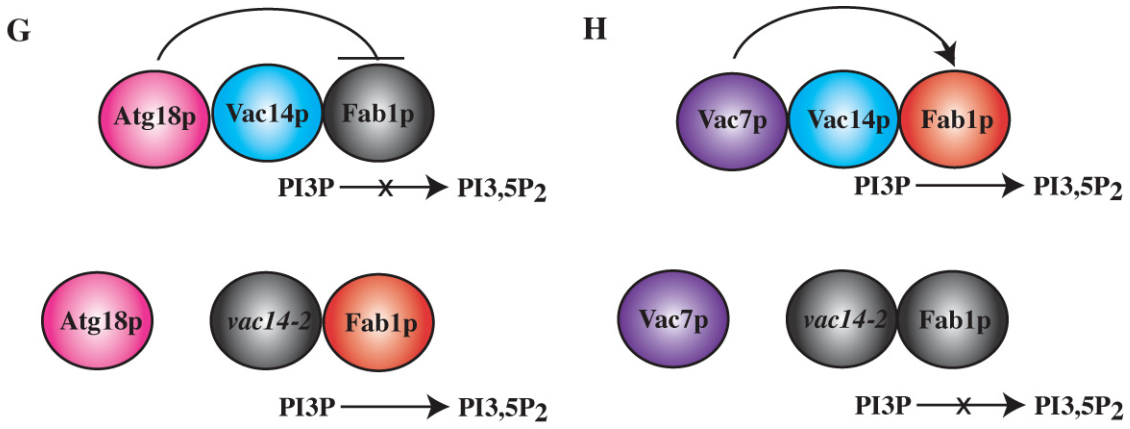

Figure 15. Vac7p and Atg18p function through Vac14p.
(A) *vac14-2* has smaller vacuoles than wild type. *vac14*Δ cells expressing pRS416-*VAC14* or pRS416-*vac14-2* were labeled with FM4-64 (red). (B) *vac14-2* exhibited higher basal levels of $PI3,5P_2$, but did not show elevation of the lipid or its tunrover of $PI3,5P_2$ during osmotic stress. *vac14*Δ cells expressing pRS416-*VAC14* or pRS416-*vac14-2* were mesured. Error bars; SD (n=3).
(C) vac14-2 protein is present at wild type levels. Cell lysates were analyzed by western from *vac14*Δ cells expressing pRS416-*VAC14* or pRS416-*vac14-2*. Pgk1p was used as a loading control.
(D) vac14-2 is defective in binding Vac7p and Atg18p.
Yeast two hybrid test between *VAC14* or *vac14-2*, fused with Gal4-AD, and *FAB1, FIG4, VAC7,* itself and *ATG18*, fused with Gal4-BD.
Upper panel, SC-LEU-TRP (control); lower panel, SC-LEU-TRP-ADE-HIS+3AT (test).
Plates were incubated at 24C, 7days.
(E) Fab1p-coprecipitated with vac14-2.
*vac14*Δ / *FAB1-TAP* cells expressing pRS416-*VAC14* or pRS416-*vac14-2* were used.
(F) Schematic of vac14-2 mutant. Each arrow show a mutation site.
(G) The model that negative regulation of Fab1 by Atg18 requires binding of Atg18 to Vac14.
In *vac14-2* mutant, a partial release of Atg18 inhibition of Fab1 results in higher levels of $PI3,5P_2$.
(H) The model that positive regulation of Fab1 by Vac7p requires binding of Vac7 and Vac14.
In osomotic stress, Vac7p acts through binding to Vac14p.

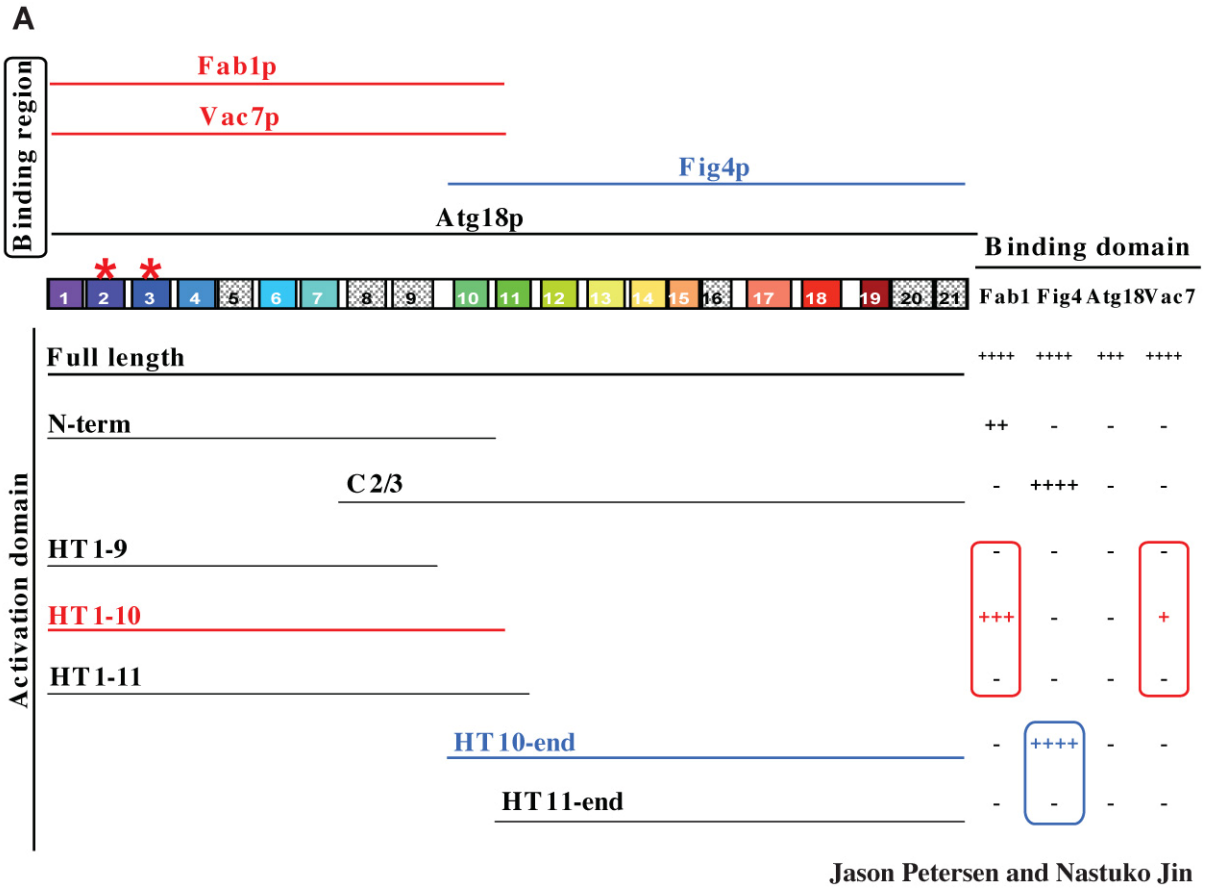

Figure 16. The Fig4p interaction site on Vac14p is distinct from Fab1p, Vac7p and Atg18p binding sites.
(A) Lines above the schematic indicate the minimal region of Vac14p required for binding with each protein. Full length *VAC14* or truncated *VAC14* was fused with Gal4-AD. *FAB1* encoding amino acids 538-1085, *VAC7* encoding amino acids 394-918, full-length *ATG18* or *FIG4* was fused with the Gal4-BD.
Lines below the schematic indicate the regions of Vac14p tested.
Red asteriks show the mutaion sites of *vac14-2* mutant, H56Y, R61K and Q101R.

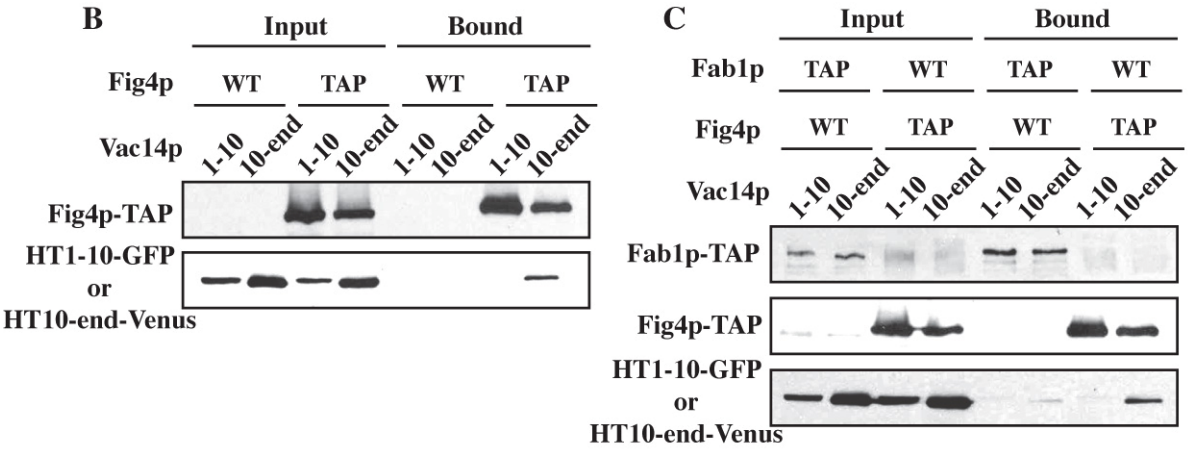

Figure 16. The Fig4p interaction site on Vac14p is distinct from the Fab1p, Vac7p and Atg18p binding sites.

(B)-(C) The C-terminus Vac14p interacts with Fig4p, but not with Fab1p *in vivo*.

(B) Fig4p-TAP coprecipitated Vac14 HEAT repeats 10-end, but not with HEAT repeats 1-10.

Wild type or *FIG4-TAP* cells expressed pVT-*VAC14 HT1-10-GFP* or pVT-*VAC14 HT 10-end-Venus* were used.

(C) Fab1p-TAP did not coprecipitate Vac14 HEAT repeats 1-10 *in vivo*.

Wild type or *FAB1-TAP* cells expressed pVT-*VAC14 HT1-10-GFP* or pVT-*VAC14 HT 10-end-Venus* were used.

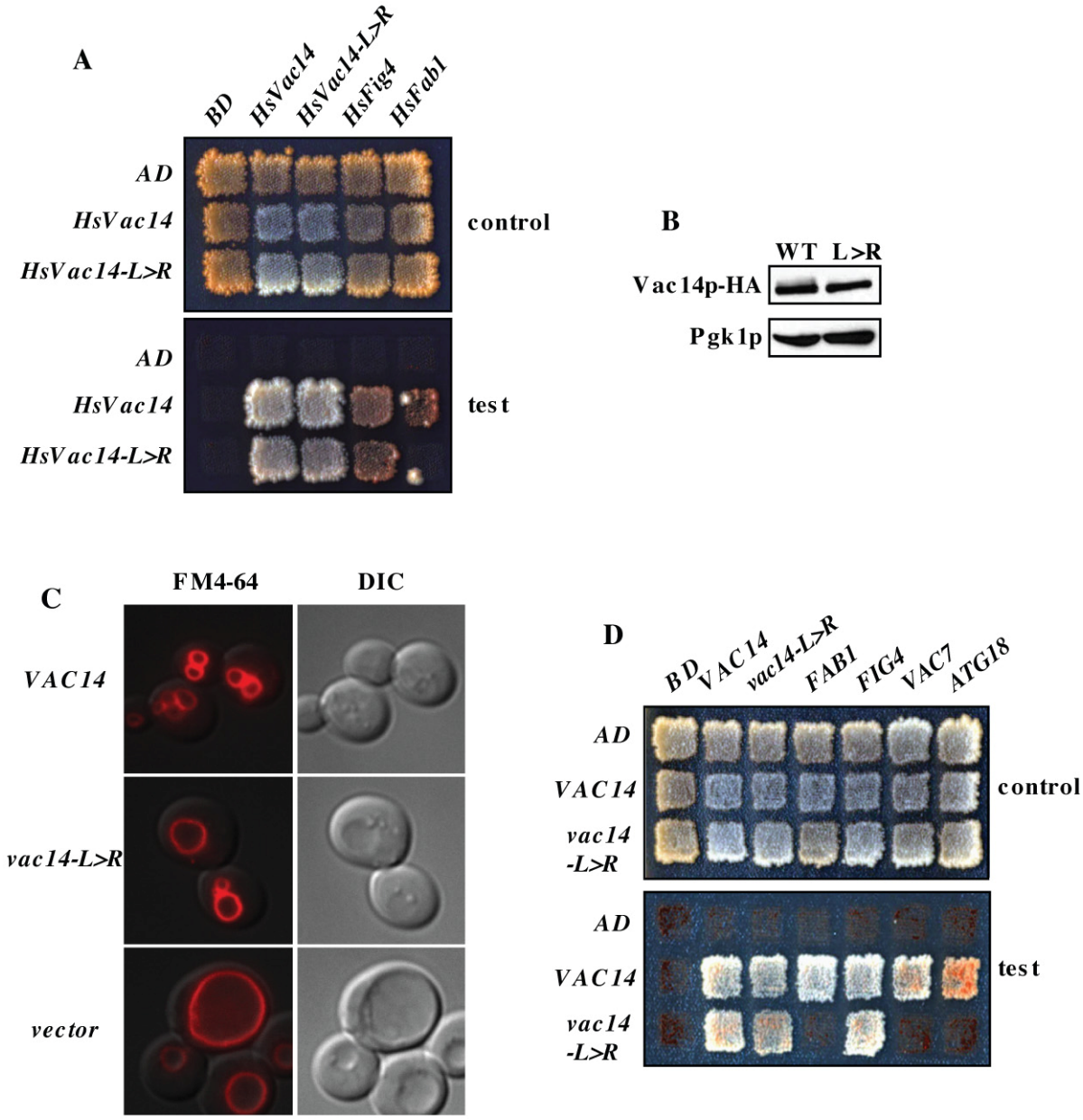
A
BD
HsVac14
HsVac14-L>R
HsFig4
HsFab1
AD
HsVac14
HsVac14-L>R
control
AD
HsVac14
HsVac14-L>R
test
B
WT L>R
Vac14p-HA
Pgk1p
C
FM4-64
DIC
VAC14
vac14-L>R
vector
D
BD
VAC14
vac14-L>R
FAB1
FIG4
VAC7
ATG18
AD
VAC14
vac14 -L>R
control
AD
VAC14
vac14 -L>R
test
E
IP : Fab1p-TAP
Input
Bound
Fab1p WT TAP TAP WT TAP TAP
Vac14p WT WT L>R WT WT L>R
Vac14p-HA
Fab1p

Figure 17

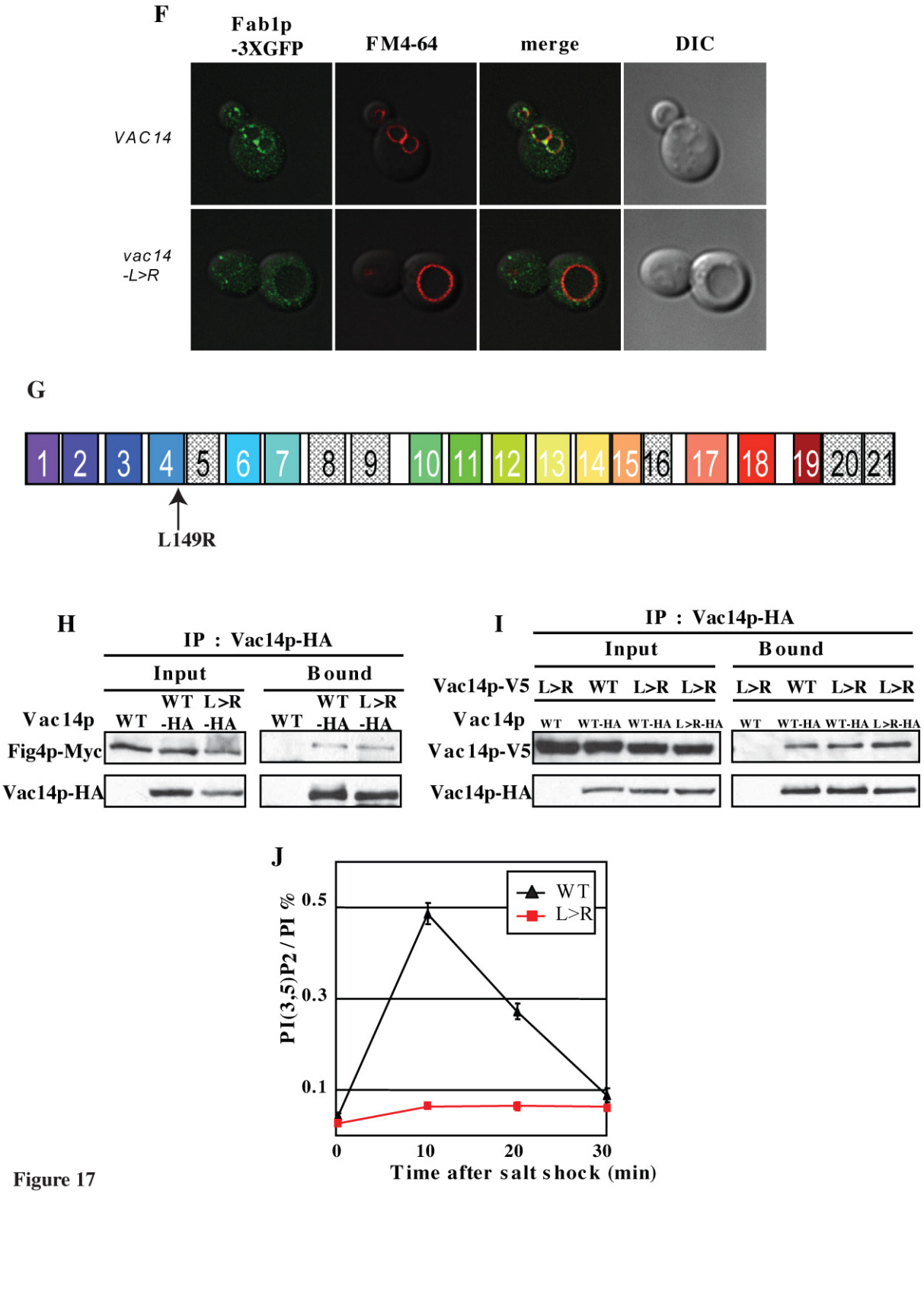
F
Fab1p
-3XGFP
FM4-64
merge
DIC
VAC14
vac14
-L>R
G
1 2 3 4 5 6 7 8 9 10 11 12 13 14 15 16 17 18 19 20 21
L149R
H
IP : Vac14p-HA
Input
Bound
Vac14p
WT
WT -HA
L>R -HA
Fig4p-Myc
Vac14p-HA
I
IP : Vac14p-HA
Input
Bound
Vac14p-V5
L>R WT L>R L>R
L>R WT L>R L>R
Vac14p
WT WT-HA WT-HA L>R-HA
WT WT-HA WT-HA L>R-HA
Vac14p-V5
Vac14p-HA
J
PI(3,5)P2 / PI %
0.5
0.3
0.1
WT
L>R
0 10 20 30
Time after salt shock (min)

Figure 17

Figure 17. *ingls*/*vac14-L149R* mutation disrupts the interaction bertween Fab1 kinase and the Vac14 complex, in yeast and mouse.

(A) The ingls mutation disrupts the interaction between Vac14 and Fab1.
Yeast two-hybrid test of human Vac14 with either Fab1,
Fig4 or itself. Full-length human Vac14 or vac14-L156R *(ingls)* was fused
with the GAL4-activation domain (AD). Residues 346-1134 of human Fab1, full-length human Fig4,
full-length human Vac14 or vac14-L156R was fused with the GAL4-binding domain (BD).
Plasmids were cotransformed into the yeast cells and transformants were plated onto
the SC-LEU-TRP plate and replica-plated onto SC-LEU-TRP (control) or
SC-LEU-TRP-ADE-HIS plate (test). Plates incubated 24ºC, 10 days.
Growth on the test plate indicates protein-protein interaction.
(B) vac14-L149R protein is stable. Cell lysates from a *vac14*Δ strain expressed pRS413-VAC14-HA or
pRS413-vac14-L149R-HA (L>R) were analyzed by western blot.
Vac14p detected with anti-HA antibody. Loading control; Pgk1.
(C) Vacuoles in the vac14-L149R mutant are intermediate in size between *vac14*Δ and wildtype vacuoles.
Vacuoles visualized with FM4-64 (red). *vac14*Δ strain ecpressed pRS413-VAC14,
pRS413-vac14-L149R (vac14-L>R), or pRS413 (vector).
(D) The equivalent yeast mutant of *ingls*, vac14-L149R, disrupts the interaction between Vac14p and Fab1p,
Vac7p or Atg18p.
Yeast two-hybrid test of Vac14p or vac14-L149R with either Fab1p, Fig4p, Vac7p, Atg18p or Vac14p.
Full-length Vac14p or vac14-L149R was fused with the GAL4-activation domain (AD).
Residues 538-1085 of Fab1, full-length Fig4, residue 394-918 of Vac7 or full-length Atg18 was fused
with the GAL4-binding domain (BD). Plasmids were cotransformed into the yeast cells and transformants were
plated onto the SC-LEU-TRP plate and replica-plated onto SC-LEU-TRP (control) or
SC-LEU-TRP-ADE-HIS+3AT plate (test). Plates incubated 24ºC, 7 days. Growth on the test plate indicates
protein-protein interaction.
(E) Pull-down of Fab1p-TAP coprecipitates Vac14p, but not vac14p-L149R.
*vac14*Δ or *vac14*Δ / *FAB1-TAP* cells expressed pRS413-VAC14-HA (WT), or pRS413-vac14-L149R-HA (L>R).
(F) Fab1p localization is defective in the vac14p-L149R mutant.
*vac14*Δ / *FAB1-3XGFP* cells expressed pRS413-VAC14 or pRS413-vac14-L149R (vac14-L>R) were used.
Cells were labeled with FM4-64 (red) for visualizing the vacuole membrane.
(G) Schematic of the vac14-L149R mutant. Black arrow shows L149R mutation site.
(H)-(I) vac14-L149R mutant retains the partial function in the interaction with Fig4p and itself *in vivo*.
(H) vac14-L149R coprecipitated Fig4p-Myc. *vac14*Δ / *fig4*Δ cells expressed pRS415-FIG4-Myc and
pRS413-VAC14-HA or pRS413-vac14-L149R(L>R)-HA were used.
(I) vac14-L149R coprecipitated Vac14p or itself.
*vac14*Δ cells expressed pRS413-VAC14-HA or pRS413-vac14-L149R (L>R)-HA and pRS416-VAC14-V5 or
pRS416-vac14-L149R (L>R) -V5 were used.
(J) In the vac14-L149R mutant, the levels of PI(3,5)P2 is not elevated in response to hyperosmotic stress.
*vac14*Δ cells expressed pRS413-VAC14 (WT) or pRS413-vac14-L149R (L>R) labeled with [3H]inositol, 16 h
and exposed to 0.9 M NaCl for times indicated.
Values are the percent of total extracted [3H]PI. Error bars; SD (n=3).

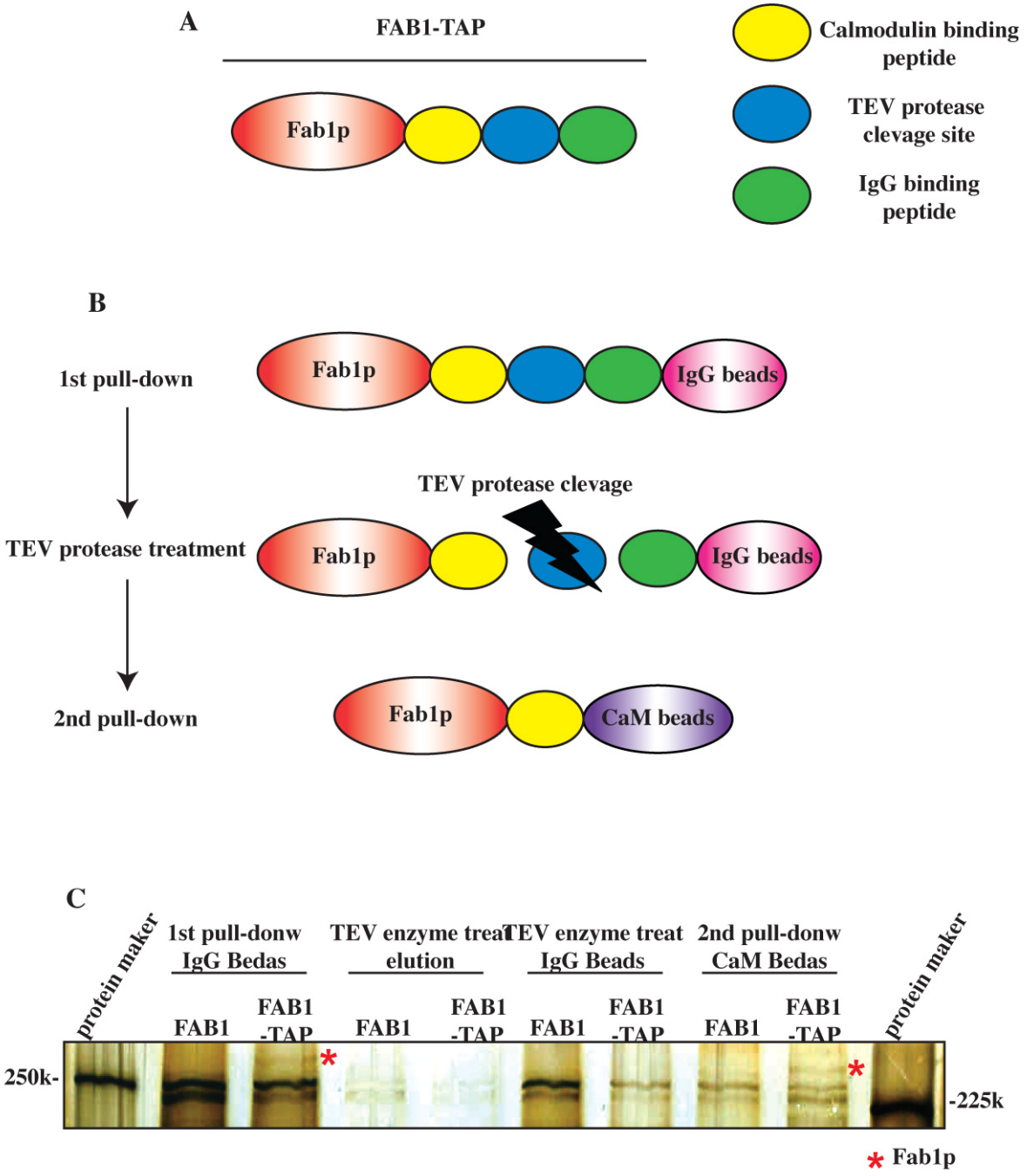
A
FAB1-TAP
Fab1p
Calmodulin binding peptide
TEV protease clevage site
IgG binding peptide
B
1st pull-down
Fab1p
IgG beads
TEV protease clevage
TEV protease treatment
Fab1p
IgG beads
2nd pull-down
Fab1p
CaM beads
C
protein maker
1st pull-donw IgG Bedas
TEV enzyme treat elution
TEV enzyme treat IgG Beads
2nd pull-donw CaM Bedas
FAB1
FAB1 -TAP
FAB1
FAB1 -TAP
FAB1
FAB1 -TAP
FAB1
FAB1 -TAP
protein maker
250k-
-225k
* Fab1p

Figure 18

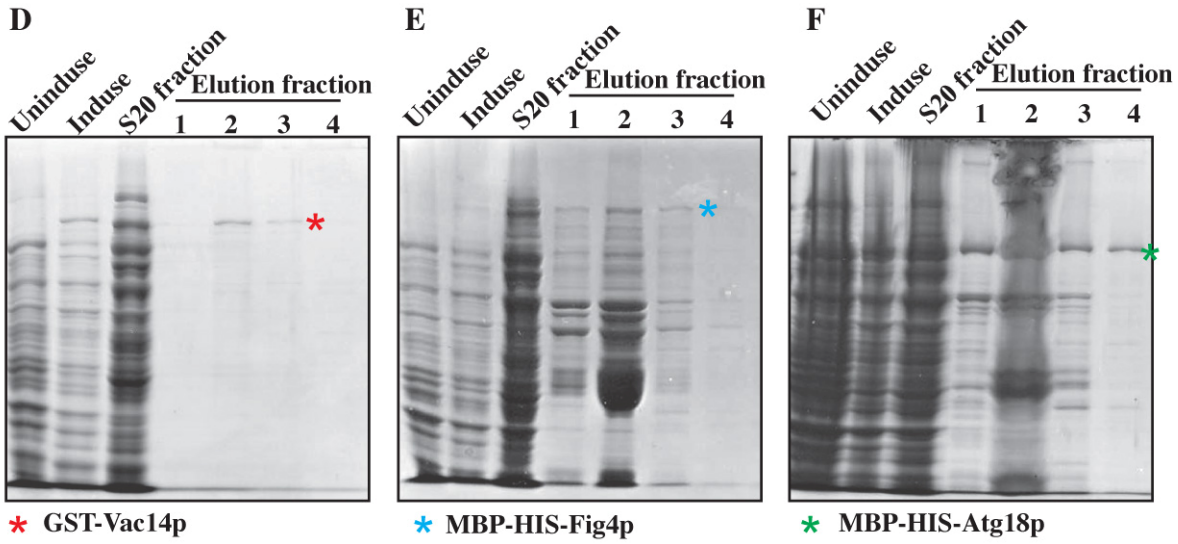

Figure 18. Full-length Fab1p, Vac14p, Fig4p and Atg18p were purified from yeast or *E.coli*.
(A) Schematic of FAb1p-TAP. (B) Schematic of Tandem affinity purification (TAP) method.
(C) The silver stainig image of a purified Fab1p-TAP protein by TAP mathod.
(E)-(F) The coomassie stainig image of a purified GST-Vac14p, MBP-HIS-Fig4p or MBP-HIS-Atg18p.
GST-Vac14p was indused using 1mM IPTG and eluted using 20mM Glutathione in (B).
MBP-HIS-Fig4p or Atg18p was indused using 1mM IPTG and eluted using 150mM imidazole in (C) and (D).

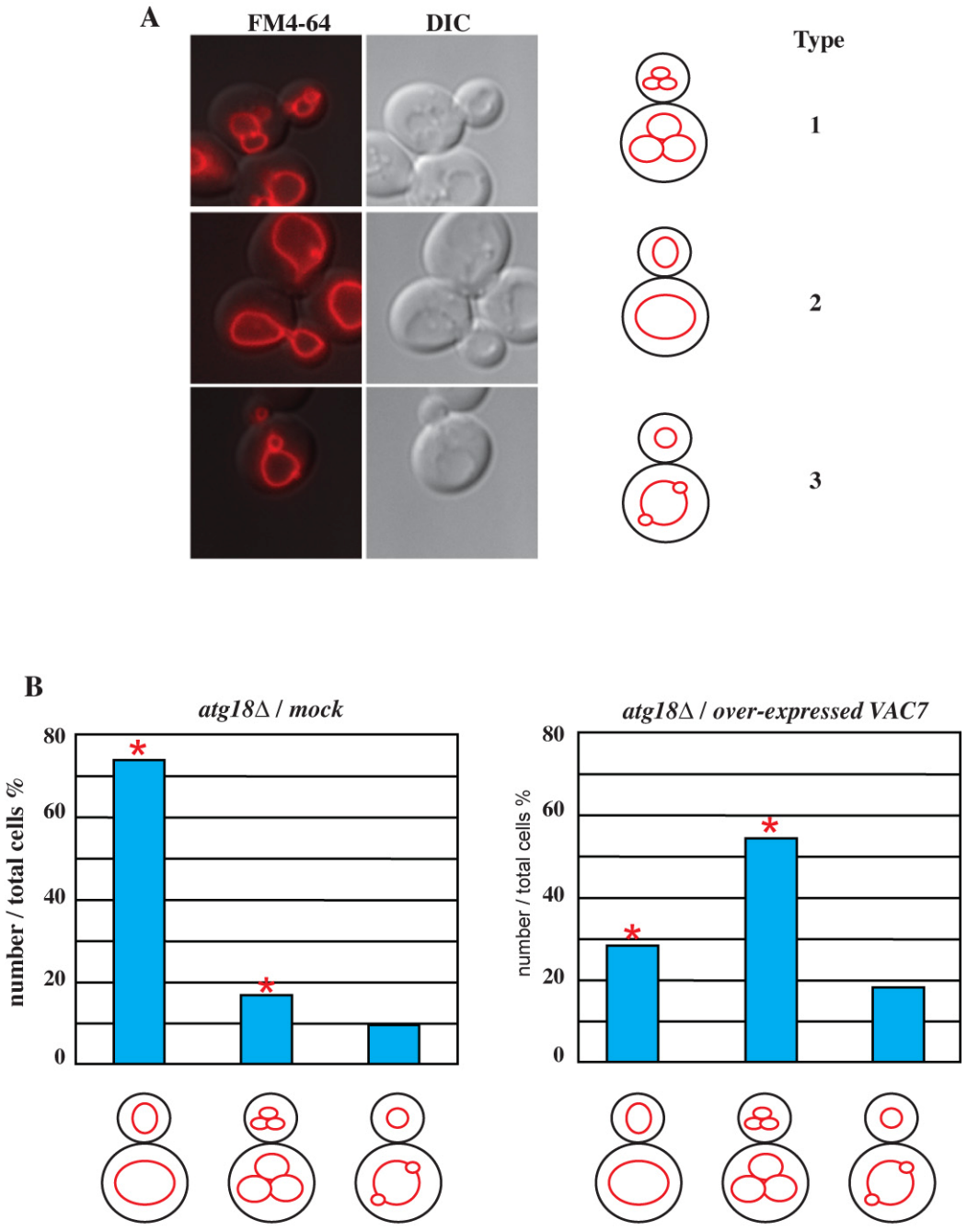
A
FM4-64
DIC
Type
1
2
3
B
atg18Δ / mock
atg18Δ / over-expressed VAC7
number / total cells %
80
60
40
20
0

Figure 19

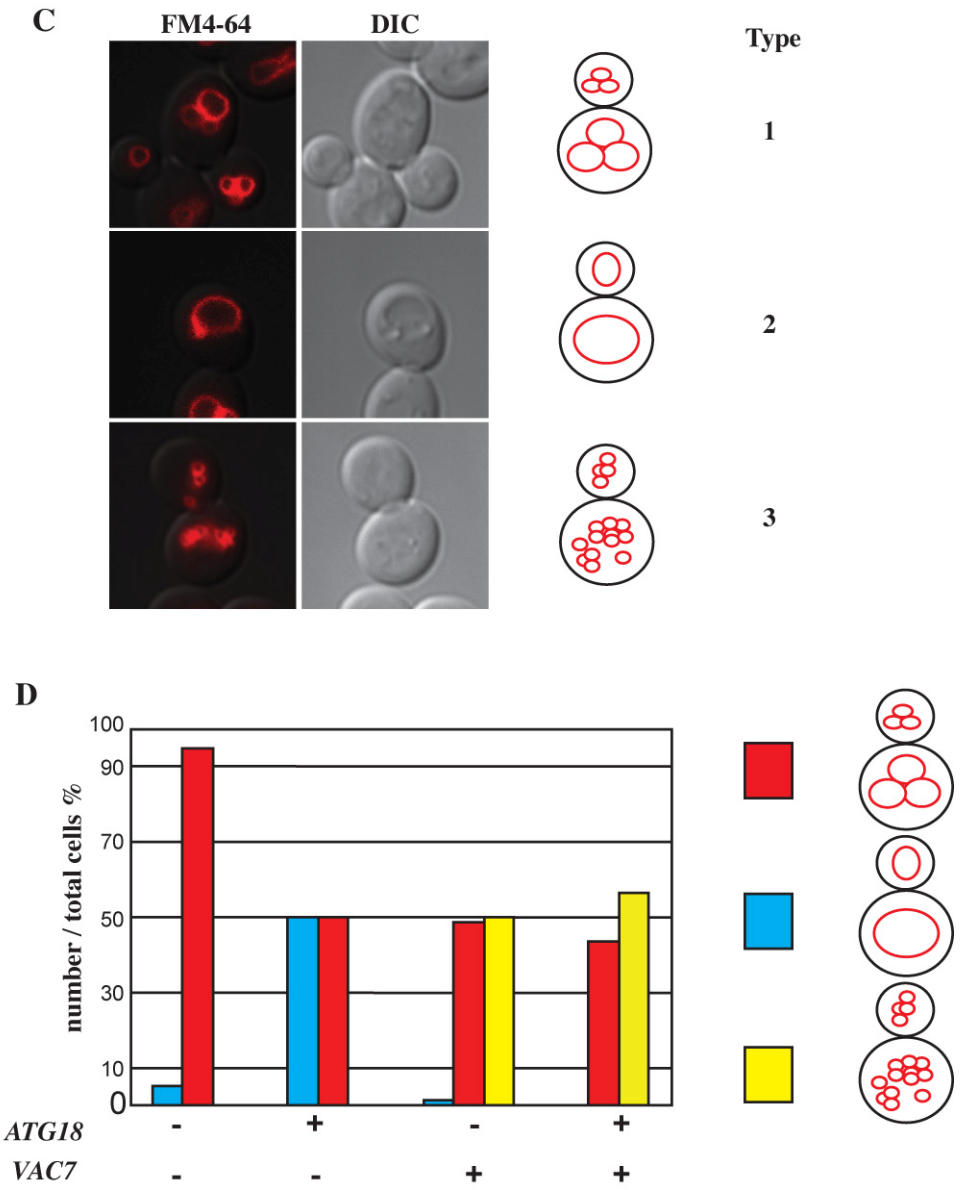
C
FM4-64
DIC
Type
1
2
3
D
number / total cells %
100
90
70
50
30
10
0
ATG18
VAC7
E
ATG18
VAC7
Vac7p
Atg18p
Pgk1p

Figure 19

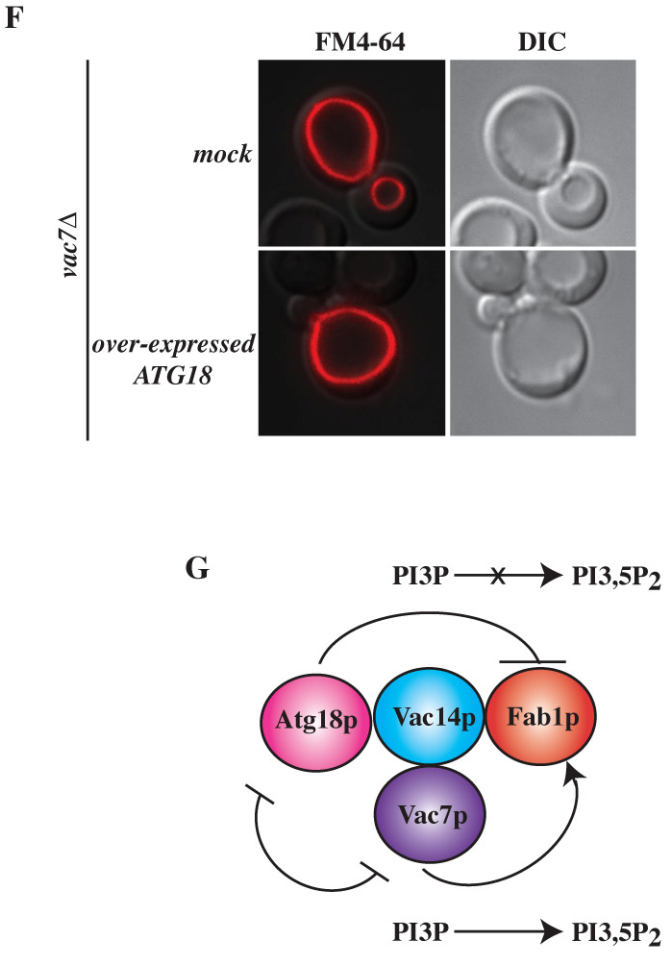

Figure 19. Vac7p and Atg18p compete each other in the regulation of vacuole morphology.
(A) *atg18*Δ cells were classified into 3 types in the vacuole morphology.
Cells were labeled by FM4-64 (red) for visializing vacuole membranes.
(B) Over-expressed Vac7p was supressed the vacuole morphology in *atg18*Δ cells.
In left panel: pRS426 (mock) and in right panel; pRS426-VAC7 was expressed in *atg18*Δ cell.
(C) When Atg18p or Vac7p was over-expressed in wild type cells, cells were classified into 3 types in the vacuole morphology. Cells were labeled by FM4-64 (red) for visualising vacuole mebranes.
(D) Over-expressed Vac7p was supressed the vacuole morphology of over-expressed Atg18p.
pRS426/pRS, pRS426/pRS425-ATG18, pRS425/pRS426-VAC7 or pRS426-VAC7/pRS425-Atg18 was expressed in wild-type cell.
(E) Western blot analisis. Vac7p and Atg18p were over-expressed.
(F) Over-expressed Atg18p was not supressed the vacuole morphology of *vac7*Δ cell.
(G) Vac7p and Atg18p compete each other through the binding witrh Vac14p,
in the regulation of Fab1 kinase activity.

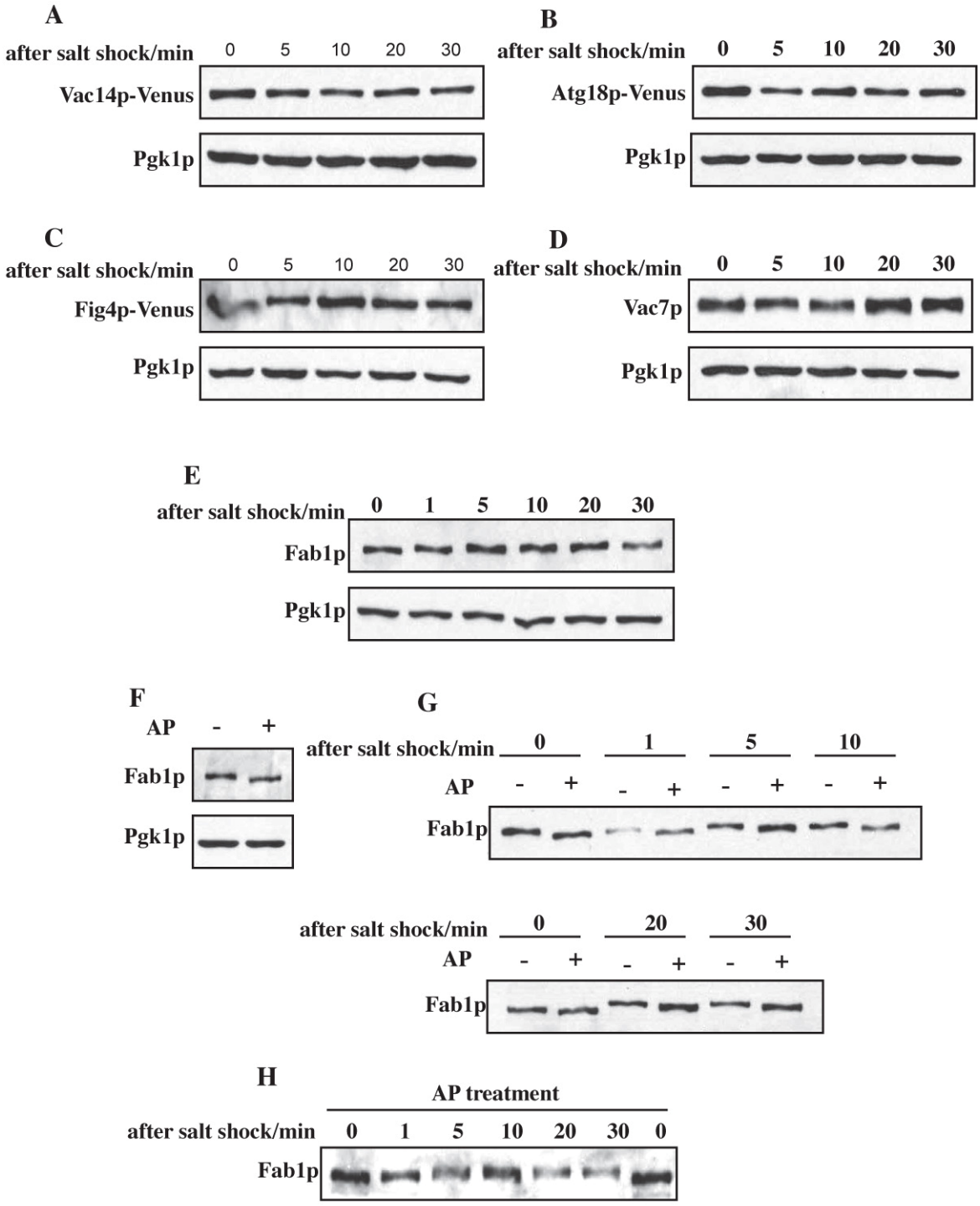
A
after salt shock/min 0 5 10 20 30
Vac14p-Venus
Pgk1p
B
after salt shock/min 0 5 10 20 30
Atg18p-Venus
Pgk1p
C
after salt shock/min 0 5 10 20 30
Fig4p-Venus
Pgk1p
D
after salt shock/min 0 5 10 20 30
Vac7p
Pgk1p
E
after salt shock/min 0 1 5 10 20 30
Fab1p
Pgk1p
F
AP - +
Fab1p
Pgk1p
G
after salt shock/min 0 1 5 10
AP - + - + - + - +
Fab1p
after salt shock/min 0 20 30
AP - + - + - +
Fab1p
H
AP treatment
after salt shock/min 0 1 5 10 20 30 0
Fab1p

Figure 20

Figure 20. Post-translatinal modification of a lipid kinase of Fab1.
(A)-(E) The expression levels of Fab1p and its regulators are not changed before and after osmotic stress. *VAC14-Venus, ATG18-Venus, FIG4-Venus*, wild-type cell were used.
(F) Fab1p was phosphorylated ay basal condition. Cells were lysed, precipitated by TCA and treat Alkaline phosphatase (AP).
(G) Fab1p was phosphorylated before or after hyperosmotic stress.
(H) Fab1p was post-tranlationally modified. After treating by 0.9M NaCl, cells were lysed, precipitated by TCA and treat AP (G) and (H). (F)-(H) Wild-typs cell was used.

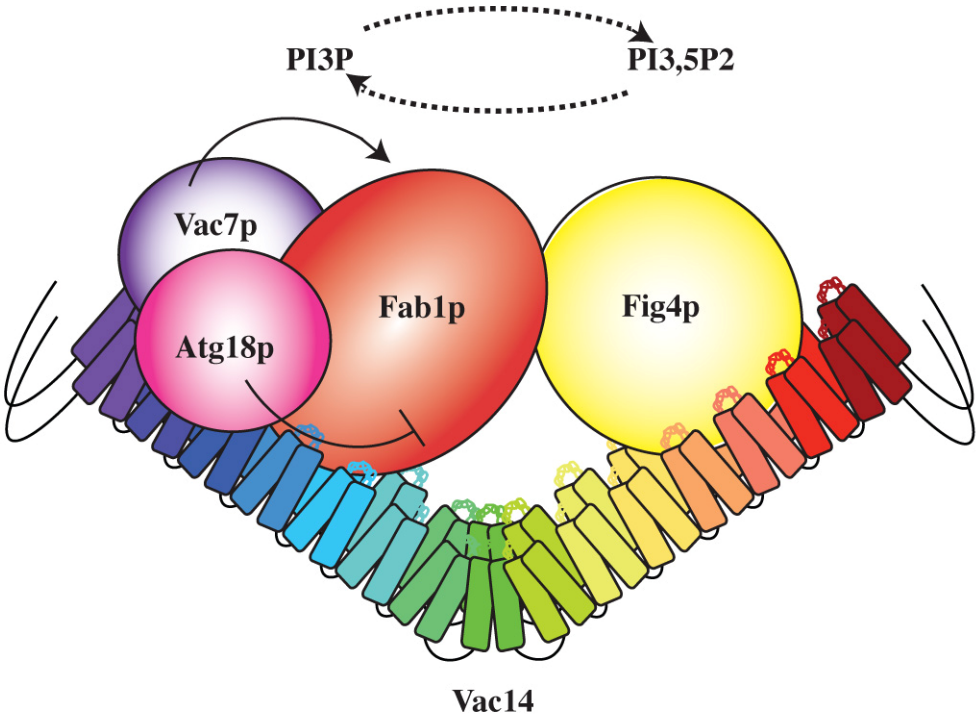

Figure 21. The model of Vac14 complex.
Vac14p binds to both Fab1p and Fig4p and may undergo a conformational change that brings Fab1p into contact with Fig4p. Fig4p functions both as an activator of Fab1p, and as a PI(3,5)P2 5-phosphatase. Fig4p and Fab1p bind to distinct regions on Vac14p.
Vac7p regulates Fab1 kinase activity, positivelly and ATg18p regulate negtatively in this complex.
Also Vac7p and Atg18p cmpete each other through the binding with Vac14p,
may be HEAT repeat 2 and 3 of Vac14.

Table I. **Strains used in this thesis**

Strains	Genotype	Source
PJ69-4A	*MATa,leu2,3-112, ura3-5, his-Δ200, trp1-901, gal4Δ, gal80Δ, GAL2-ADE2,met::GAL7-lacZ*	James *et al*., 1996
LWY7235	*MATa, leu2,3-112, ura3-52, his-Δ200, trp1-Δ901, lys2-801, suc2-Δ9*	Bonangelino *et al*., 1997
LWY2055	*MATa, leu2,3-112, ura3-52, his-Δ200, trp1-Δ901, lys2-801, suc2-Δ9, fab1Δ::LEU2*	Bonangelino *et al*., 2002
LWY5177	*MATa, leu2,3-112, ura3-52, his-Δ200, trp1-Δ901, lys2-801, suc2-Δ9,vac14Δ::TRP1*	Bonangelino *et al*., 2002
LWY6474	*MATa, leu2,3-112, ura3-52, his-Δ200, trp1-Δ901, lys2-801, suc2-Δ9, fig4Δ::TRP1*	Duex *et al*., 2006a
LWY6538	*MATa, leu2,3-112, ura3-52, his-Δ200, trp1-Δ901, lys2-801, suc2-Δ9, fig4Δ::TRP1, vac14Δ::TRP1*	Duex *et al*., 2006b
LWY8792	*MATa, leu2,3-112, ura3-52, his-Δ200, trp1-Δ901, lys2-801, suc2-Δ9, FIG4-3xGFP::KAN*	This study
LWY8014	*MATa, leu2,3-112, ura3-52, his-Δ200, trp1-Δ901, lys2-801, suc2-Δ9, VAC14-Venus::KAN*	This study
LWY8953	*MATa, leu2,3-112, ura3-52, his-Δ200, trp1-Δ901, lys2-801, suc2-Δ9, FAB1-Tdtomato::HIS3, VAC14-Venus::KAN*	This study
LWY8251	*MATα, leu2,3-112, ura3-52, his-Δ200, trp1-Δ901, lys2-801, suc2-Δ9, vac14Δ::TRP1, fig4Δ::TRP1, ATG18-Venus::KAN*	This study
LWY8429	*MATa, leu2,3-112, ura3-52, his-Δ200, trp1-Δ901, lys2-801, suc2-Δ9, vac14Δ::TRP1, FAB1-TAP::KAN*	This study
LWY8436	*MATa, leu2,3-112, ura3-52, his-Δ200, trp1-Δ901, lys2-801, suc2-Δ9, fig4Δ::TRP1, FAB1-TAP::KAN*	This study
LWY8789	*MATa, leu2,3-112, ura3-52, his-Δ200, trp1-Δ901, lys2-801, suc2-Δ9, vac14Δ::TRP1, FAB1-3xGFP::KAN*	This study
LWY8798	*MATa, leu2,3-112, ura3-52, his-Δ200, trp1-Δ901, lys2-801, suc2-Δ, vac14Δ::TRP1, FIG4-3xGFP::KAN*	This study
LWY8812	*MATα, leu2,3-112, ura3-52, his-Δ200, trp1-Δ901, lys2-801, suc2-Δ9, fig4Δ::TRP1, FAB1-3xGFP::KAN*	This study
LWY8640	*MATa, leu2,3-112, ura3-52, his-Δ200, trp1-Δ901, lys2-801, suc2-Δ9, fig4Δ::TRP1, VAC14-Venus::KAN*	This study
LWY8818	*LWY2055, FIG4-3xGFP::KAN*	This study
LWY8257	*LWY2055, VAC14-Venus::KAN*	This study
LWY8958	*MATa, leu2,3-112, ura3-52, his-Δ200, trp1-Δ901, lys2-801, suc2-Δ9, FAB1-TAP::KAN, VAC14-Venus::KAN*	This study
LWY8964	*MATa, leu2,3-112, ura3-52, his-Δ200, trp1-Δ901, lys2-801, suc2-Δ9, fig4Δ::TRP1, FAB1-TAP::KAN, VAC14-Venus::KAN*	This study
LWY8966	*MATa, leu2,3-112, ura3-52, his-Δ200, trp1-Δ901, lys2-801,*	This study

	suc2-Δ9, FAB1-TAP::KAN, FIG4-Venus::KAN	
LWY8967	*MATα, leu2,3-112, ura3-52, his-Δ200, trp1-Δ901, lys2-801, suc2-Δ9, FAB1-Tap::KAN, FIG4-Venus::KAN, vac14Δ::TRP1*	This study
LWY8274	*MATa, leu2,3-112, ura3-52, his-Δ200, trp1-Δ901, lys2-801, suc2-Δ9, VAC14-Mcherry::HIS3, FIG4-Venus::KAN*	This study
LWY8538	*MATa, leu2,3-112, ura3-52, his-Δ200, trp1-Δ901, lys2-801, suc2-Δ9, VAC14-Mcherry::HIS3, vac7Δ::KAN*	This study
LWY8279	*MATa, leu2,3-112, ura3-52, his-Δ200, trp1-Δ901, lys2-801, suc2-Δ9, VAC14-Mcherry::HIS3, ATG18-Venus::KAN*	This study
LWY8816	*MATa, leu2,3-112, ura3-52, his-Δ200, trp1-Δ901, lys2-801, suc2-Δ9, VAC14-Venus::KAN, vac7Δ::KAN*	This study
LWY8923	*MATa, leu2,3-112, ura3-52, his-Δ200, trp1-Δ901, lys2-801, suc2-Δ9, FAB1-3xGFP::KAN, vac7Δ::KAN*	This study
LWY8834	*MATα, leu2,3-112, ura3-52, his-Δ200, trp1-Δ901, lys2-801, suc2-Δ9, FIG4-4xGFP::KAN, vac7Δ::KAN*	This study
LWY8287	*MATa, leu2,3-112, ura3-52, his-Δ200, trp1-Δ901, lys2-801, suc2-Δ9, vac14Δ::TRP1, vac7Δ::KAN*	This study

Table II. **Yeast mutant vac14-ingls, fab1-2 and vac14-2 are defective in hyper-osmotic shock induced synthesis and turnover of PtdIns(3,5)P_2.**

PtdIns(3,5)P_2/ PtdIns3P %				
		After hyper-osmotic shock		
	Basal	10min	20min	30min
WT	0.043±0.006	0.49±0.023	0.27±0.018	0.089±0.016
vac14-ingls	0.026±0.0009	0.064±0.0053	0.064±0.0091	0.063±0.0025

PtdIns(3,5)P_2/ PtdIns3P %				
		After hyper-osmotic shock		
	Basal	10min	20min	30min
WT	0.056±0.0038	1.15±0.086	0.32±0.034	0.11±0.0031
fab1-2	0.033±0.0064	0.076±0.0049	0.035±0.0036	0.023±0.0049

PtdIns(3,5)P_2/ PtdIns3P %				
		After hyper-osmotic shock		
	Basal	10min	20min	30min
WT	0.046±0.0016	0.38±0.0011	0.13±0.0056	0.041±0.0093
vac14-2	0.11±0.0051	0.19±0.0012	0.15±0.0051	0.085±0.010